ANALYSIS OF THE NAMIB AND KALAHARI DUNE SAND DEPOSITS IN NAMIBIA AND THEIR APPLICATION IN POTASSIUM SILICATE SYNTHESIS

A THESIS SUBMITTED IN FULFILMENT

OF THE REQUIREMENTS FOR THE DEGREE OF

MASTER OF SCIENCE IN CHEMISTRY

OF

THE UNIVERSITY OF NAMIBIA

BY

WILHELM PENDUKENI NUUMBEMBE

200824651

AUGUST 2016

Main Supervisor: Prof Fred Kamona

Co-supervisors: Dr Veikko Uahengo & Dr Heike Wanke

ABSTRACT

Silica sand is a main component in the synthesis of potassium silicates that are commonly used as binding, coating, and adhesives agents. Physical and chemical properties of the sand particles such as grain size, mineralogical and geochemical compositions, determine the viability of sand in the synthesis of potassium silicates. This study analysed sand samples from dunes in the Namib and Kalahari deserts in order to 1) evaluate their suitability in potassium silicate synthesis as well as to 2) synthesize potassium silicate and characterize microstructural and chemical properties of the potassium silicate. Sand grains were analysed and characterized using the following techniques: mechanical sieves, ICP-EOS/MS spectrometry, and X-ray diffractometry. Synthesized potassium silicate was characterized using techniques of XRD, ICP-OES, and SEM-EDX. The dunes sand grain sizes range from 45 – 2000 µm, with 98 % of the Namib dune sand are distributed in the grain size range 63 – 500 µm and only 60% of the Kalahari dune sand are distributed in the similar grain size range, while the other 20 % is confined in the 45 -63 µm grain size range and the other 20 % confined in the grain size 500 - 2000 µm. Quartz is the dominant mineral in all sand samples and feldspar minerals were observed only in the Namib dune sand samples. High SiO_2 contents 93-99 % and 85-88 % were observed in the Kalahari dune sands and in the Namib dune sands, respectively. In contrast, oxides (Al_2O_3+Fe_2O_3+K_2O+Na_2O) contents are relatively high in the Namib dune sands (9-11%) compare to the Kalahari dune sands (0.9-2%). Similarly, trace elements and REE such as Rb, Sr, Ba, Y, Zr, La, V, Cr, Ce, and Nd are present in higher contents in the Namib dune sands compare to the Kalahari dune sands. Chemical index of alteration (CIA) values are high in Kalahari dune sands (76-82 %), compare to values in the Namib dune sands (58-59%). Finer and well-sorted grains, geochemical and mineralogical compositions of the Kalahari dune sands are attributed to long distance aeolian transportation, intense weathering and sediment recycling processes,

whereas for the Namib dune sand, coarser and well-sorted grains and the presence of feldspars are ascribed to fluvial transportation by the Orange River as well as marine, and short aeolian transportation and a moderate degree of weathering.

An amorphous potassium silicate glass with a 4.24 SiO_2/K_2O molar ratio and a dense, uniform surface morphology based on ESEM micrographs is reported in this study. SiO_2/K_2O molar ratio correlates with the concentrations of Si, K, and Al recorded by EDX point analysis. The concentrations of SiO_2, K_2O and Al_2O_3 were determined as 71.67±0.21 wt.%, 26.56±1.75 wt.% and 1.76±0.01 wt. %, respectively, resulting in a silicate glass composition of $K_2Si_2O_5$.

In view of specification and requirements of silica sand as raw material in the synthesis of potassium silicate such as high SiO_2, low contents of Al_2O_3, K_2O, Fe_2O_3 and Na_2O, low contents of refractory and heavy minerals, it is recommended that Kalahari sand deposits are suitable for exploitation in the development of silicate glasses. In contrast, the Namib dune sands with high contents of Al_2O_3, K_2O, and Na_2O can be considered in the processing and manufacturing of other sand type products such as refractory sand, foundry sand, coal-washing sand and metallurgical sand.

Keywords: Kalahari and Namib Dune sands, grain size parameters, major elements, trace elements, REE, Potassium silicate, SiO_2/K_2O molar ratio.

Table of Contents

List of Tables.

List of figures.

LISTS OF ABBREVIATIONS AND SYMBOLS

BSE	Back-Scattered Electron
EDAX	Energy Dispersive X-ray
ESEM	Environmental Scanning Electron Microscope
GmbH	Gesellschaft mit beschränkter Haftung
ICP-OES/MS	Inductive Coupled Plasma-Optical Emission Spectroscopy /Mass Spectroscopy
Ka	Thousand years
Kasil	Potassium silicate
KeV	Kilo electron volts
KS	Kalahari Sand
KWG-5	Potassium silicate water glass
KWG-com-5	Potassium silicate water glass commercial
NASA	National Aeronautics and Space Administration
NS	Namib Sand
NSP	National Silicate Product
NOX	Nitrogen Oxides
OECDSIDS	Organisation for Economic Cooperation and Development Screening Information Dataset
REE	Rare Earth Elements
SEM	Scanning Electron Microscope
SO	Sorting Index
VOC	Volatile Organic Compounds
µm	micro meter
λ	Wavelength
wt.	Weight

ACKNOWLEDGMENTS

First of all, let me thank the Almighty God my creator for the strength, wisdom, and determination throughout the entire course of this study and for all the knowledge acquired in this study**.**

Let me also express my appreciation and gratitude to the following people:

My supervisor, Professor Fred Kamona for his highly esteemed and constant supervision of this study.

The NamiBind team: Dr. Erold Naomab, Dr. Ingrid Wiess, Dr Bernd Reihard,Dr Mirko Bukwoski Dr Uehango Veikko, Dr Heike Wanke, Dr. Stefan Louw, Dr. Martha Kalili, Nicole Schiff, Angela Rutz, Hannelie Naris and Bianca Nawases.

Let me also extend my gratitude to Dr. Marcus Koch for the XRD and ESEM-EDX analysis, Ms Andrea Jung for ICP-OES analysis at INM and the Ministry of Mines and Energy-Geochemistry and laboratories department for the XRD scans.

I would again sincerely like to thank the Gentes family for accommodating us during our two stays in Saarbrucken.

I would like to thank Dr. Erold Naomab again for his tireless coordination of the NamiBind project here in Namibia, under which this study falls.

Let me thank Professor Edet Archibong for encouraging me to do this study and for his mentorship throughout my entire undergraduate and postgraduate studies.

Let me also thank all my friends and my families for the love, support, encouragements, and patience throughout the entire course of this study.

Let me thank the University of Namibia and Leibniz Institute of New Material for collaborating and allowing this study.

Lastly, and most importantly, let me express my outmost gratitude to the Bundesministerium fűr Bildung und Forschung (BMBF) for fully funding this study.

To my late father Tomas Shikongo Nuumbembe (1962-2004)

And to

My mother Hendrina Nuukelo Angula and my grand-mother Magdalena Tomas

DECLARATIONS

I, **Wilhelm Pendukeni Nuumbembe**, declare hereby that this study is a true reflection of my own research, and that this work, or part thereof has not been submitted for a degree in any other institution of higher education.

…….

CHAPTER 1: INTRODUCTION

1.1 General introduction

In recent efforts to explore, evaluate, and determine the viability of the readily available natural resources i.e. silica (SiO_2) sand, through sustainable technological developments and eventually valorize them, the Institute of New Materials (INM) and the University of Namibia under the NAMIBIND Project (Natural and Mineral–based Binder for Ecological Building Industries), are currently investigating the physical and chemical properties of the Kalahari and Namib dune sands in order to determine exploitation potential of the sands as raw materials in the synthesis of potassium silicates that are commonly used as adhesive, binding and coating agents (Weiss, 2013).

Ascertaining the viability of the Kalahari and Namib Dune sand deposits as silica sources in the synthesis/manufacturing of potassium silicate can be done through determining and evaluating geochemical and mineralogical compositions, and grain size parameters of the dune sands and subsequently compare them to sand compositions and grain sizes standard specifications and requirements such as (>99.4% SiO_2, <0.03% Fe_2O_3 and <0.2% Al_2O_3) used by Ash Associates (1996) and the study by Cuesta Consultant Limited (2015) of silica sand (SiO_2 > 99%, < 0.5% Fe_2O_3 and <0.01% Al_2O_3)) and sand grains with (0 % coarser than 1mm, >90% between 125µm and 500 µm and >7% finer than 125µm) (Cuesta Consultants limited, 2015).

The Kalahari sand sea covers most of eastern and northern Namibia. The sand fills the three basins namely Owambo Basin, Omaheke Basin and Aranos Basin (Dierks, 1994; Miller, 2008). The Namib sand sea covers an area of approximately 34,000 km^2, which extends from Luderitz to Kuiseb River (Miller, 2008; Livingstone, 2012). Kalahari sands are naturally siliceous (high in SiO_2) (Mbangira, 2007; Strohbach, B, Strohbach, Kutuahuripa, & Mouton,

2008,). Namib sands on the other hand are dominated by quartz grains, with minor contents of feldspars and heavy minerals (Garzanti, Andò, Vezzoli, Lustrino, Boni, & Vermeesch, 2012). The sand deposits are compositionally and textually controlled by physical and chemical processes such as wind actions, marine and fluvial weathering processes (Muhs, 2004; Kasper-Zubillaga and Zollezzi-Ruiz, 2007; Garzanti et al., 2012). Given such a highly quartz-dominated mineralogy and high SiO_2 chemical compositions, these sand deposits provide very important reserves of siliceous sands.

Namib sands deposits are reserved as National Heritage Sites (UNESCO Heritage List, 2013), while Kalahari sands deposits uses are currently limited to a domestic scale, as they are only used in the construction of roads and buildings (Dierks,1994), leaving them unexploited for their valuable silica (SiO_2) content. The low utilization of these sand deposits may be attributed to the lack of detailed studies on the suitability of exploiting these silica sands for other technological product and applications such as potassium silicate synthesis.

Besides, the provision of raw materials, the potential use of natural and readily available resources in the synthesize potassium silicate could be more economic than the use of industrial based raw materials that are synthesized using silane precursors from silicon industry and nano sized SiO_2-particles via sol-gel technology. Moreover, knowledge such as geochemical, mineralogy and physical properties of Namibian dune sands from this study can be useful in future research studies that seek to explore alternative uses of silica sands, other than silicates synthesis and add an economic mineral value to the dune sand deposits.

Quartz sand with a high silica content and very low levels of alumina, iron oxides, refractory minerals, heavy minerals and other contaminants is the most valued raw material of most glass and silicate manufacturing industries (Ash Associates, 1996; GWP consultants, 2010; McLaws, 1971). The quartz sand usually makes up ca.75% or more of the manufacturing

batches (PQ Corporation, 2004; Vail, 1975). Chemical and mineralogical compositions, and grain size parameters of the silica sand must conform to very closely defined requirements and specifications in order to manufacture quality potassium silicate (Ash Associates, 1996; Cuesta Consultant Limited, 2015).

Potassium silicates (also known as potassium silicon oxide) are water soluble and glass-forming silicate salts that are formed by fusion of precisely measured proportion of silica sand (SiO_2) and Potassium carbonate (K_2CO_3) in hearth furnace at temperature around 1100-1200 °C (Masaro 2011; Otterstedt & Brandreth, 2013; PQ corporation, 2004; Rabbi, 2001). They are characterized by properties such as: non- toxic and odourless, non-flammable, resistance to high temperature and bondable to fibrous materials (CEES, 2013). With these versatile properties, ability to undergo various reactions such as hybridization and low cost in their productions, potassium silicates have found a wide range of applications as adhesives, coating and binding agents. Iron ore, silica, detergents and roofing granules are a few examples of materials that have used silicate based binders and coatings for decades (McDonald & Thompson, 2006). PQ corporations are currently formulating heavy duty potassium silicate detergents that are preferred over sodium silicate detergent because of their solubility and compatibility with other ingredients.

Recent studies (Le Bras, Wilkie, & Bourbigot, 2005; Pandey & Mishra, 2011; Skirona & Tikhomirova, 2012; Weiss, 2013) have shown that composite materials (binder, adhesive and coatings) with potassium silicates are mostly characterized by superior properties such as high-mechanical strength, fire-resistances, thermal and chemical stability. Moreover, potassium silicate based binders have traditionally been favored over organic and resin based binders, because they do not face the handling, safety and environmental issues associated with resin based binders (Vail, 1975). In addition, the pricing of soluble silicates is not

subject to the same market fluctuations as petroleum based or sugar based binders (Thompson, 2012).

In this study, the geochemical and mineralogical compositions, and grain size parameters of the Kalahari and Namib Dune sand deposits have been determined. The study has also synthesized potassium silicate glass, characterized its microstructural features, and determined its chemical composition. The suitability of the Kalahari and Namib dune sands in the synthesis and manufacturing of potassium silicate is also discussed.

CHAPTER TWO: LITERATURE REVIEW

The next section has reviewed the history and the current industry of potassium silicates. The section has also discussed the chemistry, physio-chemical properties, production processes, uses and application of potassium silicates. The section has also briefly reviewed some studies on synthesis and microstructural characterizations, and the effect of SiO_2/K_2O molar ratios on their solubility and intumescences behaviours of potassium silicates.

The section has further reviewed some researches and studies focusing on the general properties of silica sand and the sand processing techniques required, in order to conform with some physical and chemical specification and requirements in the manufacturing of potassium silicates. Investigation and bench-scale tests of different silica sand deposits with various physical and chemical composition and features on their viability as silica source in the synthesis of soluble alkali silicates have been briefly reviewed as well.

Finally, the section has reviewed some studies on the formation process, grain size parameters, mineralogy and geochemical signatures of the both Kalahari and Namib dune sand deposits

2.1 Potassium silicate.

2.1.1Potassium silicate history and industry.

It has been known since the 17^{th} century that sand and sodium or potassium carbonate reacts at red heat to form a water-soluble glass called “water glass”. Water glass was defined in Von Wagner's Manual of Chemical Technology (1892 translation) as any of the soluble alkaline silicates, first observed by Van Helmont in 1640 as a fluid substance made by melting sand with excess alkali. Glauber made what he termed "fluid silica" in 1648 from potash and silica (Wills,1982). Von Fuchs, in 1825, obtained what is now known as water glass by treating

silicic acid with an alkali, the result being soluble in water, "but not affected by atmospheric changes". Von Wagner distinguished soda, potash, double (soda and potash), and fixing as types of water glass. The fixing type was "a mixture of silica well saturated with potash water glass and a sodium silicate" used to stabilize inorganic water colour pigments on cement work for outdoor signs and murals (Will, 1982; Mishra, 2013).

As noted by Vail (1975), Johann Nepomuk von Fuchs was the first to investigate alkali silicate systemically. He proposed that their solution could be used as adhesive, cements, and fire-proof paints. By 1855 water glass was being made commercially, both in Europe and America.

Manufacturing has generally been carried out in large open-hearth furnaces above 1300 °C by the following reactions:

$$3\ SiO_2 + Na_2SO_4 + ½\ C \rightarrow ½\ C + SO_2 + 3SiO_2\ Na_2O. \qquad \textit{Eq. 1}$$

$$3SiO_2 + Na_2CO_3 \rightarrow CO_2 + 3SiO_2\ Na_2O. \qquad \textit{Eq. 2}$$

Much reference is made to the Philadelphia Quartz Co. (PQ Co.) - now the PQ Corporation, because this company has been a major contributing factor throughout the whole period and because it has been able to make much more early data available (Vail,1975).

Soluble silicates as an adhesive had long been used in small amounts when in the 1890's there began an intensive and continuing effort to produce paper boxes to compete with the wooden packaging then in general use. Paperboard with a corrugated ply between two sheets and complex machines were developed (Will, 1982).

In 1970, PQ Corporation reported a research by NASA, where potassium silicate was mixed with silica hydrogel and zinc powder to develop coatings for space-related applications. Potassium silicate's molar ratio was specified to be in a range of 4.8 to 5.3 with solids in the range of 19-22 %.

The Woellner GmbH & Co. KG, with its own research and development department produces alkali silicates. Its products are used in the building chemistry, paint and plaster, and paper industries, among others. Its range of alkali silicates and related products include:

• Lithium Silicates, marketed as Woellner Betolin™ Li series

• Potassium Silicates, marketed as Woellner Betolin™ K and P series

• Sodium Silicates, marketed as Woellner Betol™ series

• Silicate Powder, marketed as Woellner Sikalon™ series

PQ Corporation and National Silicate Products (NSP) use their own brand names for their potassium silicate solid and liquid products, such as Kasil® Potassium Silicate, Kasil®SS Potassium Silicate, Kasil® SS Anhydrous Potassium Silicate Powder, Kasil® 2.5 Flake Glass, Kasil® Potassium Silicate Flakes, Kasil® 2.5 Powder Potassium Silicate, AgSil® l6H Potassium Silicate, AgSil® 25F Potassium Silicate, AgSil® 25A Potassium Silicate, AgSil® 25H Silicate, Kasolv®16 , AgSil®6HHydrous Potassium Silicate Powder and EcoDrill® Potassium silicate (Masaro, 2011; McDonald & Thompson, 2006; Otterstedt & Brandreth, 2013). From these products, PQ Corporation have developed a potassium silicate solution as a bonding and coating agent that is bondable to metals, particles (e.g. refractory materials), fibrous materials (e.g. paper, fiberglass, glass, ceramics) (Thompson, 2012).

Zalcon LLC (2014) recently reported a potassium silicate product called Zalcon E-200 potassium silicate, an ultra-pure aqueous solution developed specifically for the electronic industry. It is characterized by low level of metals such as nickel, copper, iron and sodium. Due to its high purity, E-200 potassium silicate is ideal for use as a display or projection phosphor binder, photolithographic applications, high temperature coatings, and fuel cell binders.

2.1.2 Potassium silicate chemistry.

Potassium silicates are usually represented with molecular formula: $K_2O.nSiO_2$ or K_2SiO_3. Their basic structural units are silicon-oxide tetramers (tetra-potassium orthosilicate) (Fig.1). At molecular level, these fundamental building blocks of silicate species are silica tetrahedrons consisting of the silicon atom at a center of an oxygen cornered pyramid. The negative charge of the unshared oxygen atom is balanced by potassium cations which are randomly spaced in the interstices (Chemspider, 2013; Thompson, 2012). Tetra-potassium orthosilicate have a molecular weight of 248.44 and molar ratio of 0.5.

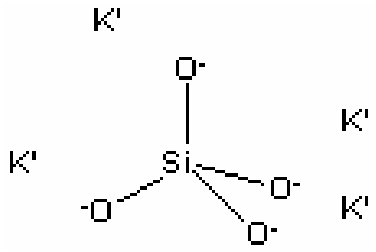

Figure 1. Tetra potassium ortho-silicate unit showing relative positions of Si, K, and O atoms.

At low concentrations, aqueous potassium silicate is monomeric; however, as the concentration increases and the pH decreases, potassium silicate becomes increasingly polymeric. The basic building block in the polymerization is the monomer; mono silicic acid (this tetrahedral unit) carries four negative charges (Fig.1) and is written as (SiO_4^{4-}). Mono-silicic acid ($Si(OH)_4$) is an unstable compound and has the property of polymerization involving sharing of OH^- groups between Si atoms (equation 3). This results in the formation of siloxane (Si-O-Si) bonds and the elimination of water (OECD SIDS, 2004).

$$Si(OH)_4 \rightarrow (OH)_3–Si–O–Si(OH)_3 + H_2O. \qquad \textit{Eq. 3}$$

The polymer species are not of uniform size; they may be linear or cyclic (Fig. 2). They can be characterized by the number of oxygen bridges to other silicon atoms.

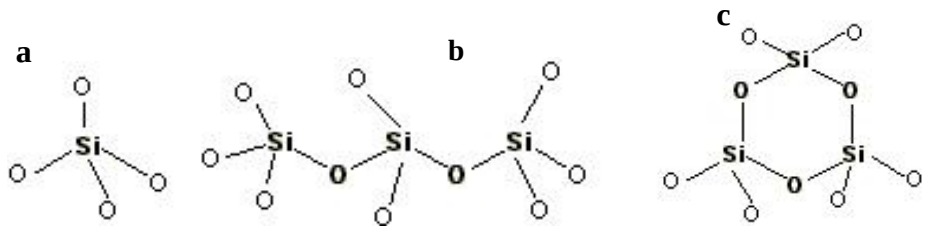

Figure 2. Silicate polymers species: a) tetramer, b) linear, c) cyclic.

Poly-silicate ions have been identified with up to 12 Si atoms. These polymeric species are in thermodynamic equilibrium. There are two main factors which influence the distribution of silicate anion types, which are the ratio of silica to alkali and the concentration of the silicate solution (Vickers, van Riessen & Rickard, 2015).

Figure 3 shows the distribution and qualitative interpretation of silicate anion species as the modulus increases at constant concentration. Moving from left to right (reducing alkali content) shows a shift from high monomer ("monosilicate") to more complex structures and polymers via a series of growing chains and rings. The distribution of anionic species can be altered by the addition of alkali or dilution with water, known as respeciation, which causes the solution to change to the species distribution appropriate to the new modulus (McDonald & Thompson, 2006; Vickers et al., 2015).

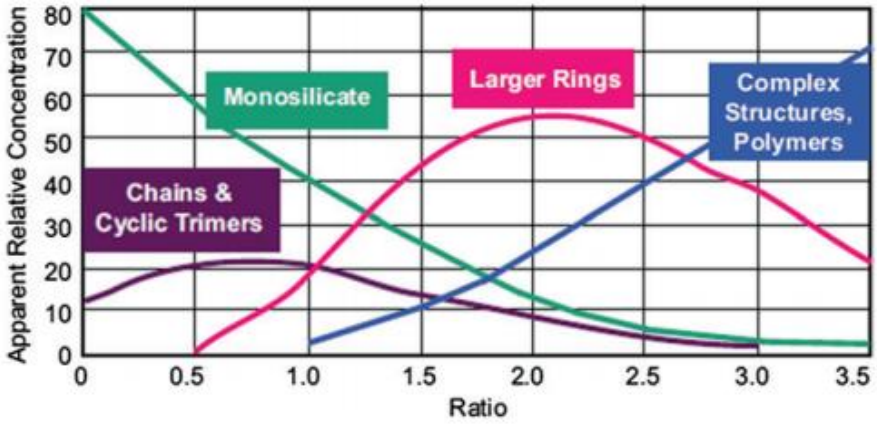

Figure 3. Silicate anion structure equilibria (1M solutions) Silicate ratio vs. Molecular weight distribution (Vickers et al., 2015).

Solutions having a ratio of 2 or less will tend to be nearer to true solutions containing monomeric SiO_4^{4+} and $Si_2O_5^{2-}$ ions usually in a hydrated form. However, at higher concentration, larger polysilicate anions prevails and when solutions are diluted there is an instant partial de-polymerization and re-arrangement (PQ Europe, 2004).

The common way to characterize the composition of potassium silicate is to use the ratio of silica to alkali by weight. The silica refers to the SiO_2 content of the material, and the alkali to K_2O content. This characteristic value is called the modulus (OECD SIDS, 2004; Vickers et al, 2015). The molar ratio of a potassium silicate is defined as molar (SiO_2 / K_2O). The weight ratio is defined as wt.% (SiO_2 / K_2O). For potassium silicates, the molar ratio is 1.57 times the weight ratio. Commercially available potassium silicates have molar ratios between 1.5 to 5.0, and more commonly 3.3 (OECD SIDS, 2004; PQ Europe, 2004).

Potassium silicate solid is alkaline and is commonly manufactured at a molar ratio of 1.5 to 3.0 relating to SiO_2 and K_2O contents. The silicate solid is slightly hydroscopic and may be a transparent or cloudy glass-like substance when not dissolved in liquid (Chemspider, 2013).

Potassium silicate solid that has interacted with air usually appears to be covered with a chalky white powder (Masaro, 2011; PQ Europe, 2004).

According to McDonald and Thompson (2006), soluble silicates are also moderately strong buffers and can be involved in four basic types of chemical reactions such as gelation, hydration/dehydration, metal ion reaction/precipitation, and surface charge modification, each of which can play a role in binder applications.

Potassium silicate solid is considered to be a (qausi)-speciality chemical and a commodity in most markets globally. As a commercial binders' raw material, the pricing of soluble silicates is not subject to the same market fluctuations as petroleum based or sugar based binders (McDonald and Thompson, 2006).

2.1.3 Physio-chemical properties.

Most of the physical and chemical properties of potassium silicates are controlled by the SiO_2/K_2O molar ratios (OECD SIDS, 2004; PQ Corporation, 2004).

Melting point: Solid crystalline silicates have discrete melting points which depend on the content of crystallization water. Amorphous silicate glasses do not have discrete melt points but rather flow points. They reversibly solidify and soften within a broad temperature range depending on their molar ratio. Potassium silicate lumps start to soften at 700 °C and reach the flow point at 900°C (OECD SIDS, 2004).

Solubility and stability in water: Solid silicates of molar ratios below 2 are hygroscopic and they dissolve fairly well in water. Anhydrous solid dissolves extremely slowly at ambient conditions; they can be solubilised only at elevated temperature and pressure (ca.150 °C and ≥ 5 bar). However, solutions are infinitely miscible with water and spray-dried solutions readily dissolve in water (PQ Corporation, 2004).

The degree of polymerisation of the silicate anions increases with increasing concentration and increasing SiO_2/K_2O ratio of the solution. On the other hand, pH is also strongly influencing the polymerisation-depolymerisation equilibrium: above a pH of 11 - 12 stable solutions of monomeric and polymeric silicate ions exist and no insoluble amorphous silica is present. Acidification below pH 11 - 12 leads to increasing precipitation of amorphous silica which is characterised by the loss of interstitial alkali ions from the three-dimensional network. The soluble content rapidly decreases when the pH is lowered to 9. At pH values below 9 only a low but constant amount remains in solution as monomeric silicate ions (OECD SIDS, 2004).

Alkalinity and buffering capacity: The pH of silicate solutions is dependent on concentration and silica to alkali ratio. The pH of silicate solutions is inversely correlated with the silica to alkali ratio ad ranges from pH of 10-13 (OECD SIDS, 2004; Vail, 1975). Electrometric titration with acid and dilution reduces the pH, but high pH is maintained until the alkali is almost neutralized this is due to the buffering action of the silicate which increases with increasing proportions of soluble silica. However, even the pH of a 1 wt. % solution is lowered by only about 1 unit compared to the concentrated solution (OECD SIDS, 2004). The buffering capacity (the ability of a solution to resists change in pH) increases with increasing proportions of soluble silica. However, even dilute silicate solutions will maintain a relatively constant pH despite the addition of acid (PQ Europe, 2004).

Specific gravity: The specific gravity or density of silicate solution depends on the concentration (solid content), temperature, and silica to alkali ratio. At a given solids content the density will increase with the decreasing ratio. Commercial silicate solutions have densities ranging from ca. 1.2-1.7 g/cm^3 at 20 °C (Falcone, 1997).

Viscosity: The viscosity of a sodium silicate solution is a function of concentration, density, ratio and temperature as indicated in most silicate manufacturing companies' technical reports and hand books (Le Bras at el., 2005; PQ Corporation, 2004). Soluble silicates can range in viscosity from fluid, slightly sticky consistencies to thick substance. Viscosity strongly increases with increasing ratio and decreases with rising temperature. High ratio solutions will increase in viscosity until they become semisolid. An increase in the viscosity of the silicate will decrease the wetting coefficient, the amount of water absorbed and rate of absorption. Aside from adding water, the viscosity of potassium silicate can be decreased by the addition of a small amount of potassium hydroxide or by gently warming the silicate (McDonald & Thompson, 2006; OECD SIDS, 2004)

2.1.4 Production Process

It has been well documented in most hand books, technical reports and other forms of literature that fusion of highly pure silica sand or quartz with potassium carbonate in varying proportions at elevated temperature results in synthesis of potassium silicates of varying silica to alkali molar ratios e.g. (Masaro, 2011; Otterstedt & Brandreth, 2013; PQ Corporation, 2004; Vail, 1975). As indicated by various studies (Masaro, 2011) and silicate production companies (PQ Corporation, 2004; PQ Europe, 2004), the common process by which potassium silicate solid is produced is essentially the same for all manufacturers in the world. The most common process used in the manufacture of potassium silicate solid involves 4 (four) phases: (1) batch preparation, (2) fusing, melting measured ingredients/chemicals in a furnace; (3) hardening/forming the molten liquid into a solid; and (4) breaking solid potassium silicate into smaller pieces. In the case of potassium silicate powder, an additional process of milling or grinding from glass pieces to a powder takes place or other further manufacturing steps.

The batch preparation step involves measuring quantities of (1) potassium carbonate (manufactured as a derivative product of potash) and (2) high quality silica sand depending on the desired ratio composition. The measured quantities are moved to the high temperature furnace.

Potassium silicate is manufactured by fusing in a high temperature furnace (usually electric arc or natural gas) potassium carbonate and high quality silica sand to form a melt or molten substance according to equation 4 and synthesis route shown in Fig.8

$$K_2CO_3 + xSiO_2 \rightarrow K_2O.xSiO_2 + CO_2. \qquad \textit{Eq. 4}$$

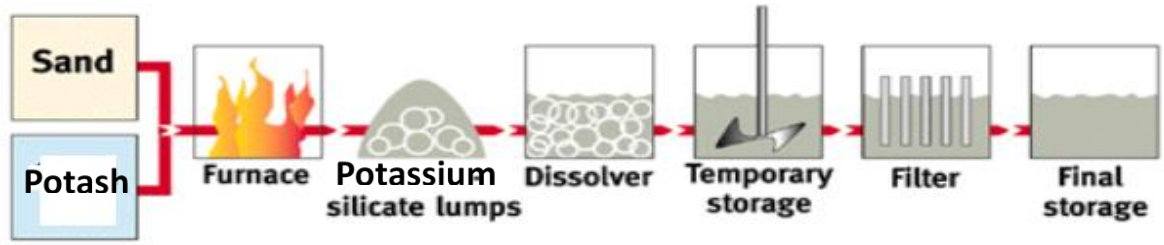

Figure 4. Schematic diagram of furnace route synthesis (PQ Corporation, 2004).

The molten potassium silicate is emptied from the furnace (often on a continuous conveyor system) and spreads to the width of the moving conveyor system. The molten potassium silicate cools quickly and hardens to form potassium silicate solids. Along the conveyor system, at a point where the potassium silicate is partially or fully hardened, it is rolled to cause the potassium silicate to form smaller pieces or to facilitate the breaking of the cooled potassium silicate solid into smaller pieces. The solid potassium silicate resembles chunks, flakes, pieces, granules of clear to cloudy glass. However, for greater certainty, potassium silicate flake generally resembles a broken window pane of flat glass and is not like soap flakes. It is possible (but unusual) to manufacture very small pieces (Masaro, 2011; McDonald & Thompson, 2012).

Solutions of soluble silicate of lower molar ratios can also be synthesized through a hydrothermal route. However, this production process is less common as it's only used to synthesis silicate with certain qualities (OECD SIDS, 2004; PQ Corporation, 2004). In here reactive silica sources (mainly silica sand) are dissolved in their respective alkaline hydroxide solutions (NaOH or KOH) at temperatures around 200 °C and under high autoclave pressure (20 bar), according to the following equation:

$$2MOH + xSiO_2 \rightarrow M_2O.xSiO_2 + H_2O. \qquad \textit{Eq. 5}$$

2.1.5 Uses and applications of potassium silicate.

Sodium and potassium silicates have many useful properties that are not shared by other alkaline salts. These varied properties and functional characteristics can be utilized to efficiently and economically solve many problems that arise in chemical and industrial processes (PQ Corporation, 2004).

Potassium silicate of various grades has versatile properties which are used in a wide variety of industrial and consumer applications. The more alkaline silicates are used in the manufacturing of detergent and soup whereas the higher ratio products are used to produce various silicate derivatives, e.g. zeolite and miscellaneous crystalline and amorphous products. These two broad categories use up roughly 75% of the volume consumed (Spencer, Reifsynder, & Falcone, 2013). In other uses potassium silicate is used either as coating, binders, adhesive, soil scouts or cements. These uses and applications however, are manifold and can only be illustrated by selected important examples illustrated in various studies (Masaro, 2011; McDonald& Thompson, 2006; Otterstedt & Brandreth, 2013; PQ corporation, 2004).

Standard Grades

Welding Rods: Potassium silicate is preferred for the clay and fluxing materials used in welding rod applications. Potassium silicates produce a smoother, quieter burning arc for stable welding than sodium silicates. This is particularly important for stainless steel and AC welding. Potassium silicates combined with sodium silicates are used when a controlled amount of arc sputtering is acceptable (McDonald & Thompson, 2006).

Protective and Decorative Coatings: Potassium silicate coatings do not form white carbonate films; they do not hide pigments. As a result, potassium silicates yield clear, rich colours with a soft quality perfect for decorative pigments that are applied to stone, concrete, stucco, brick, and metal surfaces. Potassium silicate can be used to create zinc rich protective coatings. Zinc dust is mixed with the silicate component, yielding a coating that resists water, rain, condensation, and corrosion upon curing (Otterstedt & Brandreth, 2013).

Soaps and Detergents: Liquid potassium silicates provide increased solubility and phosphate reversion resistance in detergent and hard surface cleaner formulations. As a source of K_2O, they enhance liquid detergents with acid soil neutralization, oil saponification, and anti-redeposition benefits (PQ Corporation, 2004). In phosphate-built hard surface cleaners, sand K_2O stabilize poly- and pyro-phosphates.

When liquid potassium silicates are used in place of sodium alkali sources, high-solid liquid detergent formulations can be produced without stability problems. In fact, only potassium silicates provide the benefits of K_2O solubility, alkalinity, and silicate corrosion inhibition in a single, raw material (PQ potassium silicate, 2004).

Refractory Cements: Potassium silicate solid is also used as an ingredient in refractory brick and mortar. Refractory bricks and mortar are used to line furnace, oven, reactor, and vessels where the furnace, the oven, the reactor or the vessel must withstand very high temperatures or highly acidic conditions. Potassium silicate solid is used because it improves the ability of

the refractory bricks and mortar to withstand certain types of chemicals (e.g. corrosive acids) (PQ potassium silicate, 2004).

Silica Gels: Potassium silicates are ideal for use in special catalysts when the presence of the sodium ion is undesirable. These gels can also be used as culture media in connection with plant physiology, mycology, etc. (Rawlyk & McDonald, 2001).

Antifreeze: Potassium silicates have a strong tolerance for glycol, they are preferred over other forms of silicate for ethylene glycol automotive antifreeze formulations (PQ Corporation, 2012).

Binder: Potassium silicate liquid is used as a binder in refractories and as a flux binder in welding electrodes or rods. Potassium silicate is specifically recommended as a binder for consumable electrodes ("stick rods") which are used with alternating current welding machines. Along with binding properties, potassium silicate serves as a fluxing component and produces a steady hot arc voltage. Potassium silicate is used as a binder in welding rods for mild, low hydrogen and stainless steel. Potassium silicate is also used to bind vanadium pentoxide catalysts for sulfuric acid manufacture and in acid-resistant cements (PQ Corporation, 2004).

Waste treatment: Potassium silicate solid is also used as an ingredient in potassium silicate liquid for use in waste treatment. Many waste treatment operations require a neutralizing, suspending or stabilizing agent to remove or fix the hazardous substances present in the water or soil being treated. Potassium silicate contains potassium and is especially compatible with soil applications. Potassium silicate is a multi-functional safe chemical capable of sequestering waste (e.g., heavy metals) and acidity in waste streams stress (Spencer et al., 2013).

Hydroponics/Plant Health: Potassium silicates are a convenient source of potassium – a primary nutrient for good plant health. More recently potassium silicate is being considered

as a binder for fertilizer applications. In this case, the more soluble potassium silicate can strengthen prills or pellets but then dissolve in use to release the nutrients of the fertilizer while providing additional potassium and silicon for plants. Potassium is a primary plant nutrient, and silicon has gained significant recognition as a beneficial plant nutrient that helps to physically strengthen plant tissue as well as improve nutrient uptake and alleviate salt and drought (PQ potassium silicate, 2004).

Electronic Grades

Monitors and Screens: Low levels of iron, copper, and sodium in electronic-grade potassium silicate products make them compatible with phosphor compounds and perfect as settling agents for use in CRT manufacturing of computer monitors, oscilloscopes, radar screens, and automated teller machine (ATM) monitors. The absence of magnetic metals in potassium silicates helps ensure that no "pinholing" or clumping occurs on the inside surface of screens, leaving a smooth, continuous layer of phosphor particles for consistent colour reproduction (Otterstedt & Brandreth,2013; Zalcon LLC,2014).

Adhesive Coatings: As an adhesive, potassium silicates bond the phosphor to the glass in screen/monitor applications. The lower-ratio potassium silicate also helps to etch the glass surface more easily. The higher-ratio potassium silicate, however, offers more silicate for binding (Zalcon LLC, 2014).

2.1.6 Potassium silicate microstructural characterization.

Alkali silicate glasses are X-ray amorphous. In amorphous state, diffraction of x-rays results in a broad diffuse halo rather than sharp diffraction peaks. An XRD analysis by Sooksaen, Boonmee, Witpathomwong, and Likhitlert (2010) on a silicate based glasses have revealed that glasses of various weight ratios of K_2O to SiO_2 are characterized by a broad XRD peak at 2θ range of 20° to 35°. The most important reflection peaks from sodium potassium disilicate phase are at 2θ = 21.920 - 22.482° and at 2θ = 30.916 - 32.053°. A study by Skorina and Tikhomirova (2012) on sodium silicate binder has also reported a broad halo peak registered between 2θ = 16° and 2θ = 30°, and it was attributed to silicate xerogel, lacking long-range order. Another Alkali-silicate gel XRD analysis by Tambelli, Schneider, Hasparyk, and Monteiro (2006) have also observed a strong reflection at 2θ = 26° for all silicate gel with various K_2O contents.

Yunsheng, Wie, and Zingjin (2008) microstructural study of K-geo-polymer constituting K_2O and SiO_2, observed a XRD spectra with a large halo peak approximately at 2 θ =20 ° to 40 °, which indicates the amorphous characteristic K-polymers, consisting of randomly arranged Si-O-Al poly-tetrahedra with lack of periodically repeating Si-O-Al atomic ordering. Further corroborating results appeared in an XRD patterns of alkali activated blast furnace slag of various (% K) studied by Qureshi and Ghosh (2013). This slag and another studied by Puligilla (2011) were characterized as amorphous glass with small amount of crystalline of ankermanite, genlenite, mullite, and Quartz.

However, a study by Langille, Nguyen, Bernt, Veinot, and Murthy (1991) of potassium silicates samples heated at 450°C, noted a quite noisy signal of a distinctly crystalline component ($KHSi_2O_5$) in an amorphous polysilicate matrix.

Sharp peaks were also observed in X-ray diffractrogram of sodium silicate binder studied by Skirona and Tikhomirova (2012) and they were ascribed to the presents of crystalline components in the binder i.e. Malladrite and Villiaumite stemming from setting agents in the binder synthesis. High temperature processing of silicates leads to formation of silicate polymers characterized with some crystalline phases (Simonsen, Sønderby, & Søgaard, 2009).

Qureshi and Gosh (2013) performed a Scanning Electron Microscopy (SEM) and Energy Dispersion Spectroscopy (EDX) analysis on an alkali activated slag pasted with K_2O contents of 4%, 6%, 8% and 10 %. Their SEM micrograph showed a microstructure that is less uniform with high porosity level when the K_2O content is 4% and 6%. However, at 8% and 10% K_2O contents, a dense, gel structure with few micro-cracks and refined pores structures were observed.

Skorina and Tikhormirova (2012) also analysed the microstructure of alkali silicate binders with water glasses of various SiO_2: M_2O (M =Na, K) molar ratio. The SEM micrograph produced from water glass with low molar ratio exhibit a compact globular microstructure, whereas a study of water glass with higher molar ratio observed a more branched xerogel. Silicate and silica gel materials with meso-porous structures under SEM microscope were also observed by Sdiri et al. (2014).

2.1.7 Solubility and intumescence behaviour of potassium silicate.

Numerous experimental works have indicated that SiO_2/K_2O molar ratio, water content, and strength of bonding in the silicate network determine the degree of solubility and intumescence (Langille et al, 1991 & Le Bras et al., 2005).

Literature has evidenced that water contained in silicates as ionic water has a drastic effect on their volume expansion upon exposure to flame. This intumescence results from the rapid

liberation of water vapour upon to high temperature. An intumescence test by Langille et al, (1991) on potassium silicates observed an increase in degree of intumescence with an increase in SiO_2/K_2O molar ratio from 2.55 to 3.92. An increase in molar ratio higher than 3. 92 resulted in silicates with lower degree of intumescence.

Further intumescence investigations done on dried commercial Kasil#6 from PQ Corporation and sodium trisilicate solution from Reidel-de-Haen, incorporated with fumed silica to increase the molar ratio to 3. 9. The silicates were cured at 100°C. The study noted a higher degree of intumescence in sodium- based silicates than in potassium-based silicates.

A mass loss of 30% was recorded after intumescent test at 100°C for both silicates. However, intumescence test at 400°C lead to a mass loss of 10% and 3% recorded for sodium based silicate and potassium silicate respectively (Le Bras et al., 2005).

A lixiviation or solubility test was done using same Kasil#6 potassium silicate and sodium trisilicate both dried at 100 °C for 24 hours. The silicate samples were powdered and immersed in distilled water at ambient temperature for an hour. The samples were filtered and allowed dried overnight before weighed to determine the mass loss. It was found that potassium silicate has a high water resistant whereas sodium silicate dissolves faster.

Another solubility test study by Langille et al. (1991) on potassium silicate systems of molar ratios: 2.55, 2.75, 3.00, 3.64, 4.00, 4.35, and 4.72, has revealed that the degree of solubility trend decrease as the molar ratio increases. The study has also observed that potassium silicate systems with molar ratio above 4.00 are insoluble in distilled water at temperature of 22°C.

2.2. Silica sand

The term “sand” is applied to loose granular materials falling within a specific grain size range from ~63 μm to 1000 μm (Blott & Pye, 2011). As such sand has a strictly textural connotation, because the constituent particles can be composed of a variety of artificial and natural substance. A study by Pachauri, Singla, Satsangi, Lakhani, Kumari (2013) has described the diameter of silica particles to be in a range from 10–30 μm and these particles have tubular structure.

However, the conventional use of term “sand” without qualification implies a granular material composed of natural mineral particles, among which quartz (SiO_2) is an abundant, if not the dominant constituent (GWP consultants, 2010; Mclaws, 1971). Silica sand or quartz sand or industrial sand is defined as sand which contains more than 90% silica; the most common mineral form is quartz (SiO_2) with minor amounts of other minerals or organic constituents such as feldspar, carbonate, iron oxide, mica, clay and coal (Carrigy, 1970; Edem, Malu, & Iita, 2014; Malu, Edem & Iita, 2015). Silica sand is one of the most common minerals in Earth’s crust and they are found in almost every rock type (igneous, metamorphic and sedimentary rocks), from which they had broken down into small granules over years through the action of water and wind (weathering processes).

Silica exists in nine different crystalline forms or polymorphs, but the three main forms are: quartz (which is by far the most common), tridymite and cristobalite (Fig. 5). Fibrous forms have the general name chalcedony and include semi-precious stone versions such as agate, onyx and carnelian. Granular varieties include jasper and flint. There are also anhydrous forms - diatomite and opal. The silica in the sand will normally be in the crystalline form of

quartz (Malu et al., 2015; Sundararajan, Ramaswampy, & Ranghavan, 2009).

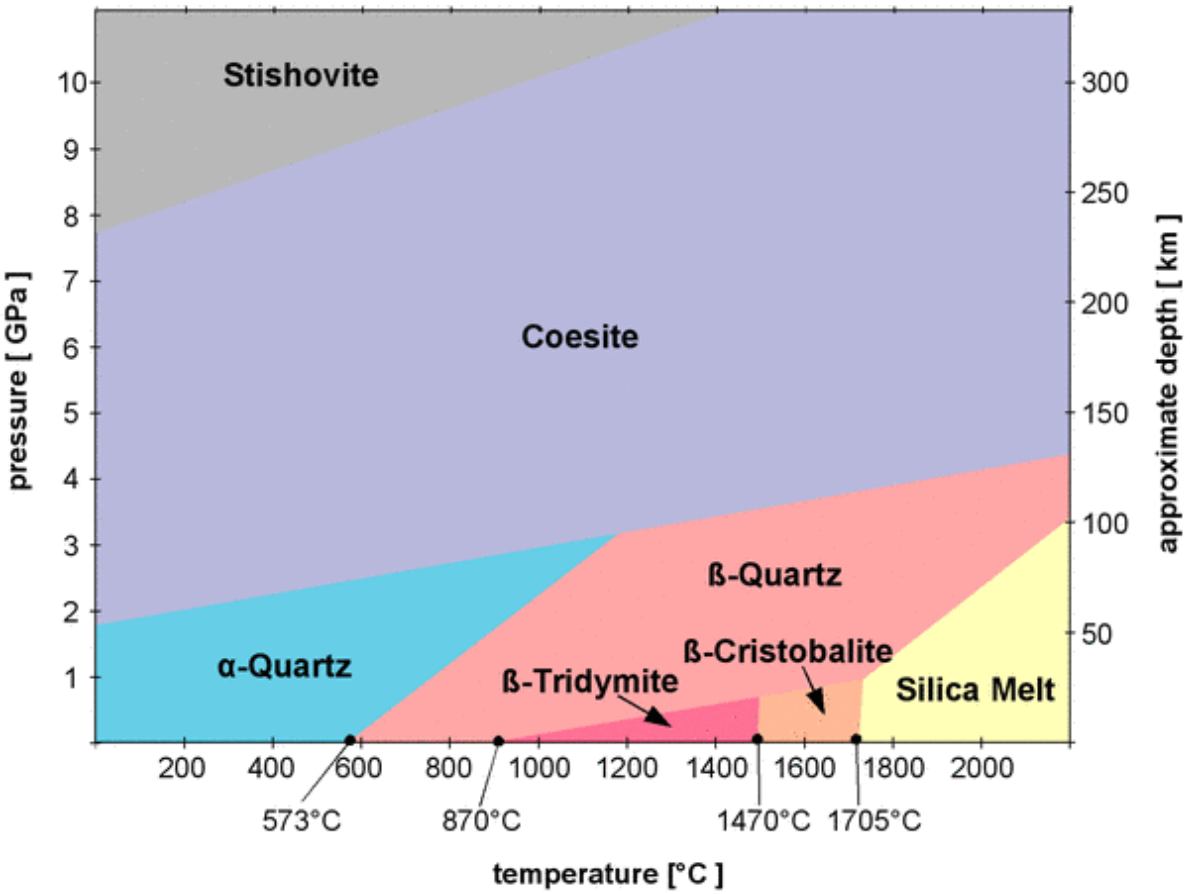

Figure 5. Some of the existing silica polymorphs (Sundararajan et al., 2009).

Silica sand granules can be used for different purposes and it is found deposited in most non tropical region of the world. In Africa, silica sand deposits are mostly found deposited particularly in riverine, estuaries and beaches, where they are commonly surface mined in open pit operation and dredging (Malu et al., 2015).

Pure quartz sands (those composed entirely of SiO_2) are unknown while sand containing 98-99% SiO_2 are extremely rare and are eagerly sought for the manufacture of glass (Carrigy, 1970). However, a study by Muhs (2004) has revealed that sands with more than 90 -99% quartz were reported in the Jafurah sand sea of Saudi Arabia, while in the northern part of the Great Sand of Desert (Canning Basin) area of north-western Australia, quartz contents are

generally 95% and as high as 99%. In North America, some dunes of Moenkopi Plateau in northern Arizona are up to 100% quartz and sand in the Monahans dune field of south-western Texas is 98-99% quartz (Muhs, 2004).

2.2.1 Silica sand processing and beneficiation techniques

Nature separates and purifies silica sand to a great degree through fluvial and aeolian weathering processes, but further processing is needed to produce sufficiently pure silica sand (Edem et al., 2014). Current processing techniques with a focus on silica content beneficiation, can upgrade sand deposits that are not naturally pure enough for uses such as glass manufacturing.

Studies by Carrigy (1970), Mclaws (1971), and Edem et al., (2014) have reported that chemical purity and particle size are the most important parameters. These studies have further revealed that in most sand deposits the main contaminants are iron (Fe_2O_3), alumina (Al_2O_3), and titanium Oxide (TiO_3). Others include lime (CaO), soda (Na_2O) and potash (K_2O).

Iron is a strong colorant and must be carefully controlled. Alumina affects the viscosity and density of glass. Alkalis affect melting temperatures; certain refractory heavy minerals (usually silicates or oxides) in parts per million levels are counted as number of grains. Therefore, raw materials are usually processed to remove minerals that contain contaminants. Edem et al., (2014) have pointed out that rare heavy minerals can be deleterious even when present in only very low levels.

In the processing of silica sand, the processing methods employed are usually a combination of size screening, attrition scrubbing, washing, filtering and drying, followed by magnetic separation and/or froth flotation.

Sizing of large grains is done by screening to remove oversized >1 mm grains assuming that most grains are about 0.5 µm. Size separation (screening) techniques are also used to remove heavy minerals, as they tend to be concentrated in the 0.15 to 0.21 mm sieve fraction (Carrigy, 1970; Sundararajan et al., 2009).

Brown & Redeker (1980) and Ash Associates (1996) have described attrition scrubbing as a processing technique that loosens and disperses coating of iron oxides, clay minerals, and other cementing and flotation-affecting materials from the sand grain surface. Attrition also prepares fresh surface on the detrimental non-quartz minerals for reagent attachment in the subsequent flotation condition step.

In silica sand washing processing, water is added to the sand then the slurry is pumped to a cyclone separator. Movement of slurry and grain-to-grain rubbing loosen clays and fine contaminants, however cyclone separator are used if clay are low (<3%) and hydrosizers using kindred settling techniques are efficient if clay contents are > 74 % (Chang, 2002).

Strong rare-earth magnets or electromagnetic cells removes certain slightly magnetic minerals such as magnetite and certain minerals can be separated based on their electrical charges by turboelectric methods (Carrigy, 1970; Chang, 2002; Schurlz and Kohl, 1991; Sundarrajan et al., 2009). Flotation is another technique in which a liquid with a specific gravity of 2.9 sinks and remove undesirable minerals including micas.

Heavy minerals and iron oxide can be removed by gravity separation using separators in which lighter particles are pushed to the outside of spiral pans (Chang, 2002; Edem et al.,2014; Goldman, 1994). A study by Khalifa, Hajji, and Ezzaouia (2012) have revealed that, surface iron staining removal technique can be subsequently used after heavy mineral separation techniques, by acid leaching technique in acid mixture of $HF/HCl/H_2O$ to remove surface and cracks iron stains. Carrigy (1970) and Ash Associates (1996) have further

discovered that, treatments such as sand boiling in 1 percent hydrochloric acid can be used to remove surface iron coating and inclusions. A study by Haddon (2005) removed oxide coating from the sand grains by using hot hydrochloric acid and revealed that the surfaces of the rounded (larger) grains are generally frosted whereas the angular grains are generally glassy.

2.2.2 Silica sand as glass sand

Silica sand is a major raw material for almost all commercial glasses; comprising 70 to 75 weight percentage of the furnace batch, thus its chemical quality is of paramount importance (Carrigy, 1970; Mclaws, 1971). The quality of the sand required in the glasses manufacturing depends largely on the type of glass e.g. optical, container, sheet, fiberglass etc. for better grades of glass the sand must have extremely high silica content (99% or more) and be essentially free of inclusion, stains, coatings, or accessory detrital heavy minerals.

Various research works by Carrigy, (1970), Mclaws, (1971), Brown & Redeker, (1980) and GWP consultants, (2010), Cuesta Consultants Limited (2015) have discussed criteria for evaluating glass sand, which are mostly chemical and physical specifications below:

Silica (SiO_2): Glass sand requires high silica content, ideally 99 to 100% and any departure from this absolute purity is undesirable.

Iron Oxide (Fe_2O_3): Iron oxide in ferric state of oxidation is the most common and most troublesome impurity of this kind glass industry incurs expense to obtain silica sand with sufficiently low Fe_2O_3. The permissible total iron content, commonly reported as Fe_2O_3 is mostly lowest for optical glass. In bottles, plate glass, window glass, amber and green bottles and colored wares, successively large amount of total iron (0.20%) are allowed. Sand for

making optical glasses generally have less than 0.008%; for colorless milk bottles have less than 0.04%; and for window glass less have than 0.15%.

Alumina (Al_2O_3): Alumina was formally considered an objectionable glass sand impurity, but it is now intentionally added to some glass batch. It gives chemical durability, lower coefficient of expansion and a greater degree of devitrification. Too much alumina increases the viscosity of glass and decrease the transparency of the glass. Alumina should exceed 0.1% for best grade of flint glass, but for some type of amber glass up to 4 percent maybe be allowed. The form in which alumina is present in the sand is of great importance. If the alumina is present in a clay form, is not readily soluble; if in the form of feldspar, however, it is easily dissolved.

Lime (CaO): Sand containing lime in a form of calcite ($CaCO_3$) and dolomite [$CaMg(CO_3)_2$] are to be avoided, although lime is an important ingredient for most commercial glasses. The calcareous materials present in sand are erratic in distribution.

Magnesia (MgO): Magnesia which is generally present in small quantities in the sand can cause trouble in glass making. An excess amount (1 percent or high) raises the fusion point glass batch, necessitating the use of extra fuel or energy requirements. MgO however, is added to some batches to improve resistance to detrivification.

Titanium dioxide (TiO_2): Titanium dioxide content in glass sand should be below 0.03 percent. It colors glass and is difficult to neutralize compare to iron oxide. However, high TiO_2 is allowed in special glasses that are used in glass beads that are in high way reflective paint because of their high refractive index.

Minor contaminants: Most of the detrital heavy mineral are undesirable and must be removed or at least reduced to extremely lower levels, in order for the sand to qualify for glass making.

Minerals such as magnetite (Fe_2O_3) and ilmenite ($FeTiO_3$) are objectionable because of their iron oxide content. Highly refractory minerals such alumina silicates (andalusite, silliminite and kyanite) and spinel groups (spinel, magnetite and chromite) are detrimental because they survive melting, giving rise to unsightly "stones" in the product. The sand should be mica free as well, as they cause spots and holes in the product.

Secondary mineral coatings and stains on the sand grains are also objectionable for example manganese oxide often associated with trace amounts of cobalt, a powerful blue colorant. As little as 0.002%, cobalt produces a distinct tint in the glass.

Physical specification: Silica sand to be used in the glass making generally should pass a 20-mesh sieve (0.83mm) and 95 percent or more be retained on a 100-mesh (0.15 mm). Excessive fines in the sand are undesirable because they tend to carry impurities that cause dusting, and they also cause foaming in the glass making tank. Fines can also contribute to small but persistent seed or blisters in the glass melt. On the other hand, excessively coarse grains survive melting causing formation of harmful scums, stones, and cords. Coarse grains are also difficult to fuse and decrease the out-put of the furnace.

Based on the above specification and requirements, a study by Sdiri, Higashi, Bouaziz, and Benzina (2014) investigated the suitability of Albian sand (Tunisia) in synthesis of sodium silicate used as a precursor in the synthesis of silica gel. Ash Associate (1996) performed a bench-scale test with silica sand from Manitoba (Canada) in the synthesis of sodium silicate. Cuesta consultant Limited (2015) investigated the soft and silica sand of Folkestone Formation, South Down east Hampshire for Sodium silicate manufacturing.

2.2.3 Other uses of silica sand

Silica sand with other various chemical and physical specifications can be classified and used in other applications as abrasive sand, hydraulic fracturing sand, refractory sand, chemical sands, building sand etc. (Cuesta Consultant Limited ,2015; GWP consultants, 2010; Mclaws, 1971).

2.3 Namib dune sands

2.3.1 Dune sand formation

The Namib sand sea, also known in its geological context as Sossus Sand Formation is made up of unconsolidated aeolian sands. The most extensive area that this cover is between Lüderitz and Kuiseb River which is approximately 34,000 km^2 (Miller, 2008; Gehring, Riahi, Kind, Almqvist, & Weidler, 2014). The sand sea is dominated by large linear dunes, with areas of star dunes on its eastern margin and a belt of simple and compound transverse and barchan dunes along the coast as shown in Figure 6 (Livingstone, 2012). Linear dunes are younger (~5.7 ka) than big star dunes (43 ± 10 ka) (Bristow, Duller, & Lancaster, 2007; Garzanti et al., 2012; Livingstone, 2012).

The Orange River is the predominant ultimate source of sand for the Namib Desert dunes after long-distance fluvial transport (3000 km). At the coast Orange River sand is washed by ocean waves and dragged northwards by vigorous long-shore currents. Southerly winds blew the sand inland and carried it farther north to accumulate in the Namib Sand Sea (Namib erg) (Fig.7) about 34000 km^2 (Garzanti et al., 2012; Gehring et al., 2014).

Garzanti et al. (2012), on the Namib dune sand's provenance analysis has revealed that there is a strict compositional resemblance between Orange River sand. This proves that most of the Namib sand is derived from the Orange River. In their study, the overall abundance and relative percentages of feldspar, volcanic-rock-fragment, and heavy-mineral species are virtually identical in Orange and coastal Namib sands. They have argued that, common mafic volcanic detritus and rich clino-pyroxene-dominated suites with minor epidote and amphibole are signatures that characterise no hinterland river draining into the Namib erg, and are even more extreme in coastal Namib dunes than in the modern Orange River itself. The estimated rate of sand input to the Namib Sand Sea is ~ 400,000 m^3/a (Lancaster, 1989).

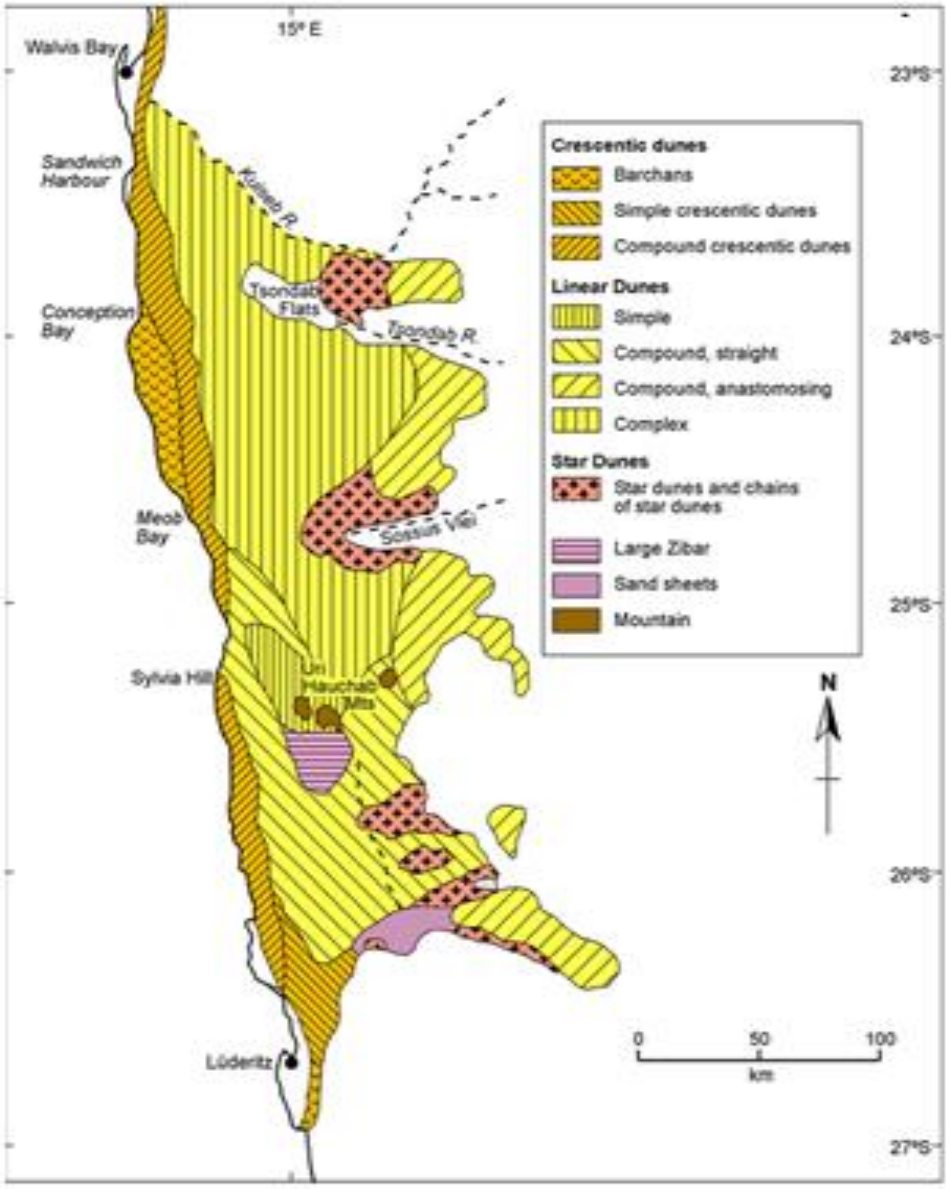

Figure 6. Types of dunes in the Namib sand sea (Livingstone, 2012).

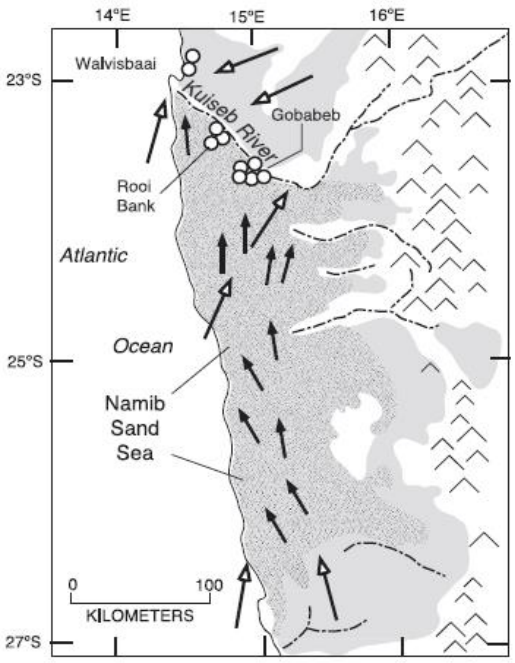

Figure 7. Aeolian sand input processes in Namib sand sea (Muhs, 2004).

2.3.2 Dune sand mineralogy and geochemistry.

Mineralogical studies by Garzanti et al. (2012) and Garzanti, Vermeesch, Padoan, Resentini, Vezzoli, and Andò (2014) have revealed that dune sands in the coastal Namib are invariably feldspar-quartz volcanoclastic, with a homogeneous composition from Lüderitz to Walvis Bay. Plagioclase prevails over K-feldspar and mafic volcanic rock fragments predominate over granitoid, sedimentary, and metamorphic grains and micas are absent. Rich heavy-mineral assemblages are clino-pyroxene-dominated, with subordinate opaque Fe-Ti-Cr oxides, garnets, epidote, and amphibole.

Sand grains from eastern Namib dunes are mainly composed of feldspar and quartz, with less volcanic rock fragments, while K-feldspar prevails over plagioclase. The mineral assemblage of the north east Namib corner dunes includes epidote, Fe–Ti–Cr oxides, garnet, clino-pyroxene, amphibole, minor titanite, tourmaline, rutile, staurolite, andalusite, and apatite

(Miller, 2008 & Garzanti et al., 2012). A study by Miller (2008) has further reported that heavy minerals constitute 1% from the average of mineralogical composition of Namib dunes sands and are represented by iron oxide, tourmaline, muscovite, garnet and pyroxene.

Namib dune sands are mostly composed of 81–87% of SiO_2 and 7–10% of (K_2O+Na_2O+Al_2O_3) contents (Muhs, 2004).

2.3.3 Dune sand-grain size

Namib dunes sand are mainly medium-grained, well-sorted, and symmetrical with mesokutic distribution (Garzanti et al., 2012). A study by Muhs (2004) has found the sand particles near Rooi bank and Gobabeb to be coarse to medium in particle size. However, the grain size tends to decrease, whereas sorting increase in eastern Namib dunes (Lancaster, 1989; Livingstone, 2012).

2.4 Kalahari dune sand

2.4.1 Dune sand formation

The upper most unit of unconsolidated sands of the Kalahari Group cover an area of over 2.5 million km^2, stretching from the Orange River in the south as far north as the Democratic Republic of Congo, and are thought to form the largest continuous sand body on earth (Baillieul, 1978; Haddon,2005; Thomas & Shaw, 1990). The thickness of the unconsolidated sands varies across the basin, from a few centimetres to over 200m in the north of Namibia in an area adjacent to Etosha Pan. The dominant landform associated with the sands is the dune fields (Miller, 1983). Dune sediments have in filled the uplifted basin with mainly sands inter-bedded with calcrete and silcrete. Areas within the basin have also shown to comprise of weathered material (Haddon, 2000; Wang, D'Odoricoa, Ringroseb, Coetzee, Macko, 2007).

The Namibia Kalahari dune fields are divided into three sections according to their geomorphology (Fig.8). The Northern Kalahari dune field is composed of linear, fossil now vegetated -dunes, while the central dune field is composed of crescent and lunette dunes and the south eastern section of the field is made-up of simple, un-vegetated linear dunes (Lancaster, 2007).

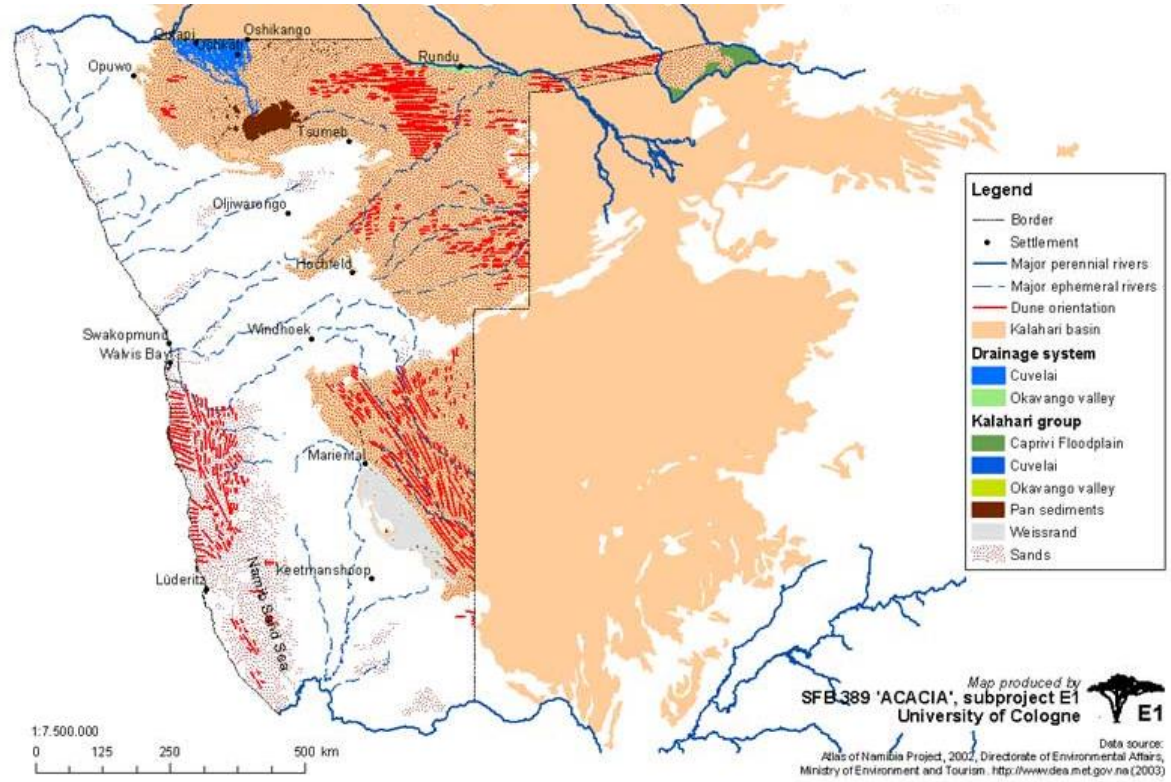

Figure 8. Namibian Kalahari dune fields and sand deposits (indicated in light brown colour). (http://www.uni-koeln.de/sfb389/e/e1/download/atlas_namibia/pics/physical/kalahari-group.jpg).

The Kalahari sand dunes are of the late Pleistocene to recent geological time scale (Pye & Tsoar, 1990). They are a result of aeolian reworking of the uppermost aggradational deposition of sand in the Kalahari Basin. The dune's sediments were supplied by the downwind direction as well as from local sources. The linear dunes have been derived from the near underlying Kalahari sands and calcretes, whereas the lunette dunes materials have

been derived from the adjoining pans or dry river bed and sand transported across the pan or river bed (Miller, 2008).

2.4.2 Dune sand mineralogy

A particle characterization study of sand particles form Kalahari deposits by Mbangira (2007) have revealed three sand types in the Kalahari sand sea and these are:

1)Pure quartz sand with red skin around the particles. These sand particles of the fossil sand dunes in the northern section of the Namibian Kalahari are made up of pure quartz particles that are iron oxide-coated (Strohbach et al., 2008).

2) Combination of two distinct sands; an aeolian component of quartz grains and a finer feldspathic type derived from the underlying sandstones. A study by Strohbach et al., 2008 has also revealed that these sand particles from Omaheke Basin are coated with goethite and hematite, with a presence of feldspar and plagioclase in varying quantities. Miller (2008) has added that the dune field has a kyanite, staurolite and the epidote-dominated assemblage.

3) Aeolian component of pure quartz without the feldspathic component. These sand particles in the Aranos Basin of south Namibian Kalahari consists of aeolian quartz particles, with epidote and zoisite; while amphibole and garnet are the dominant components of the heavy mineral suite in the linear dunes (Mbangira, 2007; Miller, 2008).

2.4.3 Dune sand grain size

A grain size analysis study by Bailliel (1978) has characterized Kalahari sands as generally fine material with almost 99 % of the material finer than 2 mm. The mean grain size of the sands falls in the interval ranging from 1.74 ϕ to 2.61 ϕ. Sorting values range between 0.44 ϕ to 2.53 ϕ on the ϕ -scale with bimodal grain size distribution (Mbangira, 2007; Miller, 2008). A sedimentology analysis by Thomas (1986) has also characterized Kalahari sands as sediments that fall in the fine sand fractions.

CHAPTER 3: METHODOLOGY

3.1 Sample collection and preparations

A total of thirteen (13) sand samples were collected from four (4) main dune-fields in Namibia at thirteen (13) various locations indicated in the Fig. 9 and Table 1, during the period of November 2014 until April 2015. The samples were collected at depth of 10 cm of the sand deposit's surface. The samples were sealed in plastic bags and transported to the University of Namibia Geology Department for storage and some analyses. All sand samples were dried at 105 °C for 24 hours and further preparations were done according to the analysis techniques below.

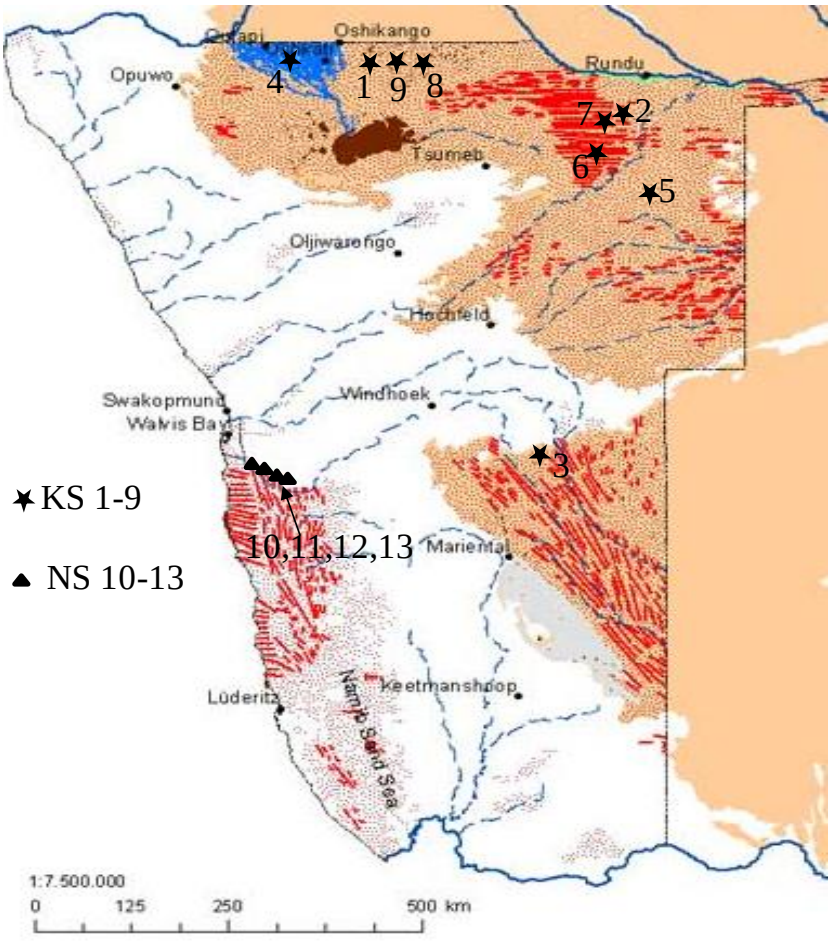

Figure 9. Locations of sampling sites from Kalahari sand dunes (KS1-9) and Namib sand dunes (NS10-13).

Table 1. Sample identification and locations.

Sample laboratory identification	Samples field identification
KS 1	Kalahari-Deposit 3
KS 2	Kalahari-Mururani2
KS3	Kalahari-Kuzikuzu
KS 4	Kalahari-Onampira
KS5	Kalahari-Anker
KS6	Kalahari-Die End
KS7	Kalahari-Mururani1
KS8	Kalahari-Deposit1
KS9	Kalahari- Deposit 2
NS 10	Namib-Rooi Bank 1A
NS11	Namib- Rooi Bank 1E
NS12	Namib-Rooi Bank 2A
NS 13	Namib-Rooi Bank 2E

3.2 Grain size determination

The grain-size analysis was carried out to determine the percentage ideal fraction of the sand samples using a mechanical set of sieves (from 40-2000 μm). The sieve analysis allows particles whose shortest diameters will fit through a square aperture of a designated size to pass (Livingstone, Bullard, Wiggs, & Thomas, 1999).

250 g of each dried sand sample was dry-sieved by electrical agitation of mechanical sieve for three (3) minutes and the grain size percentage retention of each sample on each sieve fraction was calculated, from which the grain size distribution and cumulative frequency curves were plotted and grain size parameters such as mean and sorting index were calculated as follows.

The graphic mean of each sand sample were calculated using a graphical method: $(\phi_{16} + \phi_{50} + \phi_{84})/3$, where ϕ_{84}, ϕ_{50}, and ϕ_{16} represent the value (in ϕ) at 84%, 50%, and 16%, respectively, on the grain size cumulative frequency curves (Folk & Ward, 1957). The sorting index was determined by equation $\sigma_1 = ((\phi_{84} - \phi_{16})/4) + ((\phi_{95} - \phi_{15})/6.6)$ where ϕ_{95} and ϕ_{15} represents the

grain-size corresponding to cumulative contents of 95% and 15 %, respectively (Folk &Ward, 1957).

3.3 Mineral identification

The bulk mineralogy of the samples was determined using a Bruker D8 ADVANCE, X-Ray Diffractometer (at Ministry of Mines and Energy Geochemistry laboratories in Windhoek) equipped with a dual goniometer of Cuα (λ=1.5406 μm) at acceleration voltage of 40 kV. The diffraction angle was scanned from 5° to 55° 2θ range. Using a computer software program, the observed peaks positions were matched against the International Centre for Diffraction Data (ICDD) Joint Committee on Powder Diffraction System (JPDS) card database. The height of a mineral's primary 100-percent peak relative to the total counts-per-second value of the raw data scan was used to provide a semi-quantitative analysis of the mineral components in the samples.

3.4 Geochemical analysis.

The geochemical analyses of the sand samples were done at the Activation laboratory, Toronto, Canada. The samples were pulverised to smaller than -75μm. Aliquot of 0.2 g of each sand sample was analysed for bulk chemical composition. The samples were mixed with a flux of lithium metaborate and lithium tetraborate and fused in an induction furnace to form a molten bead. The molten bead was then poured into 5% nitric acid solution containing internal standards and continuously mixed until the bead have completely dissolved.

The resultant solutions were analysed for major oxides using a combination simultaneous/sequential Thermo Jarrel-Ash ENVIRO II ICP-OES or Varian Vista 735 ICP-OES. Then the percentage composition of the major oxides was determined. The samples were also analysed for trace elements and rare earth elements (REE) using a Perkin Elmer Sciex ELAN 6000 ICP-MS and their concentrations in ppm were determined.

3.5 Potassium silicate synthesis and characterization

Potassium silicate glass lumps were synthesized at (Institute of New Material (INM) Leibniz, Saarbrucken, Germany) by fusing 2 parts (166.7 g) of (sand sample 4) silica sand, 1 part (83.3 g) of reagent grade potassium carbonate and 0.2 (0.098 g) parts of furnace grade carbon. The mixture was fused using a platinum crucible using in an electrical-fired furnace at 1200 °C for 8 hours and a heating rate of 10°C/min. The melt was left to cool and solidify in the crucible. Due to some silicate synthesis process-related complications and technicalities such as removal of potassium silicate from crucible (owing to silicate-crucible interaction) and the size of the crucible used for fusion, the study only managed to synthesize few grams of one potassium silicate system, that were only enough for microstructural and chemical composition analysis.

XRD patterns of the synthesized potassium silicate (KWG-5) with 4.24 SiO_2/K_2O molar ratio and a 2.90 SiO_2/K_2O molar ratio-commercial (KWG-com-5) potassium silicate (from van Baerle Silicates, Worms, Germany) were determined using a Brucker AXS D8 Advance, equipped with dual goniometer of Cuα, at acceleration voltage of 40 kV. The diffraction angles were scanned from 5° to 145° 2θ range.

Synthesized potassium silicates (KWG-5) and commercial potassium silicate lumps (KWG-com) were further characterized, using the following technique:

An ESEM-FEI Quanta 400 FEG working in low vacuum mode, at acceleration voltage of 15 kV and 10.2 mm working distance. The chamber pressure was set to 100.0 Pa. A gaseous secondary electron detector (GSED-Large Field Detector) was used for ESEM image formation. Backscattered electron (BSE) images were obtained to determine point to point difference in average atomic number of the samples. Cation concentrations in the silicate glass were determined by energy dispersive X-ray (EDX) using an EDAX Genesis V6.04

equipped with an energy solution of 127 eV. Due to the nature of the potassium silicate, sample coating was not necessary.

3.6 Elemental composition determination.

Elemental composition of the synthesized potassium silicate was also done at INM. About 24. 43 mg of potassium silicate glass lumps (KWG-5) were weighed in digestive vessels and digested using aqua regia method (1 ml of KNO_3, followed by 3ml of HCl, and 2 ml of ultra-pure water). The mixture was digested in a microwave system, cooled down to room temperature, the resultant solution was topped up with ultra-pure water to 100 ml.

The elemental composition (K, Al, and Si) in mg/l of the synthesized potassium silicate (KWG-5) was analysed and determined using Horiba Jobin Yvon Ultima2, ICP-OES instrument. The mg/l were converted to K wt.% and Si wt. %, from which K_2O wt. % and SiO_2 wt. % were calculated by multiplying wt.% K and wt. % Si by oxide conversion factor of 1.20458 and by oxide 2.13932, respectively.

CHAPTER 4: RESULTS

4.1 Sand grain size distribution

The two main grain size distribution parameters (mean grain size and sorting index) for Kalahari sand samples (KS1-9) and Namib sand samples (NS10-13) are shown in Table 2.

Table 2. Grain size distribution parameters of the Kalahari and Namib dune sand samples.

Sample Identity	**Mean size (ϕ)**	**Sorting index(σ_1)**
KS1	2.91	0.95
KS2	2.49	0.64
KS3	2.58	1.20
KS4	2.58	1.20
KS5	2.49	0.45
KS6	2.49	0.64
KS7	2.49	0.64
KS8	2.49	0.64
KS9	2.91	0.95
NS10	2.00	0.11
NS11	2.00	0.11
NS12	2.49	0.30
NS13	2.49	0.30

From Table 2, the mean grain size of the Kalahari dune sand samples ranges from 2.49 ϕ to 2.91 ϕ, with sorting index (σ_1) ranging from 0.45 to 1.20, whereas the mean grain size of Namib dune sand samples ranges from 2.00 ϕ to 2.49 ϕ and the sorting index ranges from 0.11 to 0.30.

The mean grain size ranges of the studied sand samples (Table 2) show that both Kalahari (2.49 ϕ to 2.91 ϕ) and Namib (2.00 ϕ to 2.49 ϕ) dune sand samples are mainly medium to fine grained. According to Folk & Ward (1957) classification scale for sorting, both Kalahari and Namib dune sands are well sorted.

The particle size distribution illustrated in Fig.10 shows a unimodal frequency distribution of sand grains in a grain size range of 45 µm to 2000 µm. The graph indicates that 98% of the Namib sand grains were retained in grain size range of 63 µm to 500 µm and only 60% of the Kalahari sand grains were retained in the same grain size range.

The grain size distribution frequency curves shown in Fig. 11 indicate that 99% of the Kalahari sand samples (KS1-KS9) are finer than 1000µm, whereas 100% sand samples NS 10-NS 13 were fine than 1000 µm.

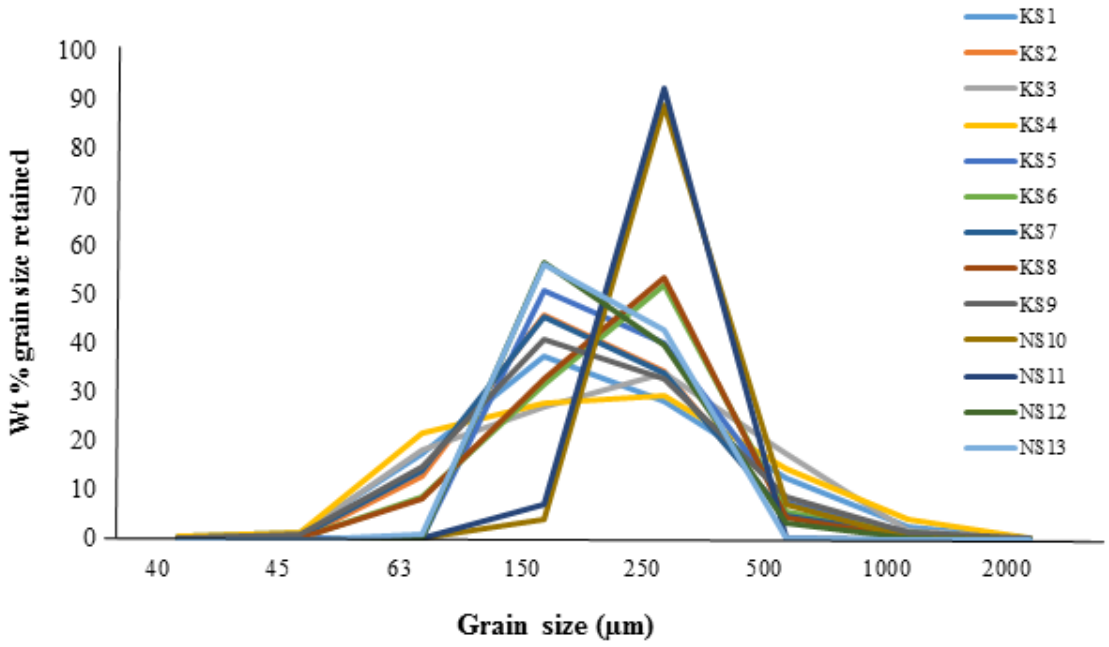

Figure 10. Sand particles grains size distribution of Kalahari sand samples (KS1-9) and Namib sand samples (NS10-13).

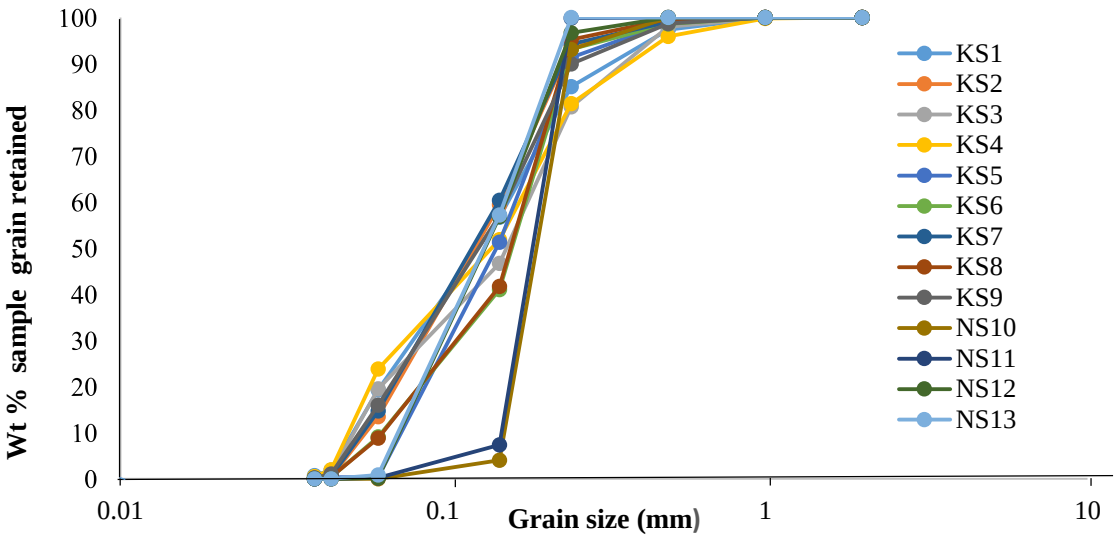

Figure 11. Cumulative frequency grain size distribution curves of Kalahari sand samples (KS 1-19) and Namib sand samples (NS10-13).

4.2 Bulk mineralogical composition of dune sands.

The mineralogical compositions of the dune sands were calculated based on the semi-quantitative XRD results of minerals in the Kalahari and Namib dune sand deposit as shown Table 3. The XRD scans for all sand samples analysed are shown in Appendix A (1-13).

Table 3.Mineral compositions of dune sands.

Sample ID	Quartz %	K-feldspars %	Albite %	Total
KS 1	100	n.d	n.d	100
KS 2	100	n.d	n.d	100
KS 3	100	n.d	n.d	100
KS 4	100	n.d	n.d	100
KS 5	100	n.d	n.d	100
KS 6	100	n.d	n.d	100
KS 7	100	n.d	n.d	100
KS 8	100	n.d	n.d	100
KS 9	100	n.d	n.d	100
NS 10	93	2.46	4.54	100
NS 11	92.33	4.00	3.66	100
NS 12	93.63	2.18	4.19	100
NS 13	93.78	4.34	1.88	100

Quartz is the only mineral detected by XRD analysis in the Kalahari dune sands due to the siliceous nature of the sands. However, the Namib dune sands contain an average of 93.19 %quartz, 3.24 % K-feldspars (orthoclase and microcline), and 3.56 % albite due to the quart-feldspathic mineralogy composition of the sands.

The XRD patterns of sand from Kalahari dunes system indicates one family of peaks that are characteristic to quartz of primitive Bravais lattice (Appendix A_{1-9}), with a prevailing peak at $2\theta = 27°$ of miller indices (110) of and other peaks appearing at $2\theta = 21°$ (100), 36.5° (111), 40° (200), 46° (210), 50° (212) and 55 ° (220) are also characteristics pattern of quartz.

XRD patterns of sand samples from Namib dunes deposits have also indicated one family of peaks characteristic to quartz at $2\theta = 21°$, 27°, 36.5 °, 46°, 50 °, and 55° of a primitive Bravais lattice (Appendix A_{10-13}).Further peaks at 2θ ranging from 20°-35°, were also reflected in XRD patterns of sample NS10 and NS13 which are characteristic to crystals of microcline and albite (both of base-centered-C-1), while peaks characteristic to orthoclase and albite are reflected in X-ray patterns of sample NS11 and NS12. Significant peaks of K-feldspars (microcline and orthoclase of base-centered-C-1 lattice) appearing at $2\theta = 27.4°$ and albites appearing at $2\theta = 27.8°$.

4.3 Geochemical composition.

Geochemical results for major oxides, trace and REE concentrations of the sand samples analysed by ICP-OES are depicted in Table 4, Table 5, Table 6, and some relevant ternary plots in Figures 13, 14 and 15. Further results are also shown in normalized plot in figure 12, 16, and 17. The Chemical Index of Alteration (CIA) was determined as [Al_2O_3/ (Al_2O_3 + CaO + Na_2O +K_2O)] ×100 (Nesbitt & Young, 1982). Only the trace elements appearing in significant amounts are indicated in Table 5. The complete results are in Appendix B, including elements below detection limits. All ternary plots from this study are in Appendix $C_{1\text{-}3}$.

Major element compositions of the Kalahari sand and Namib sand samples:

The Kalahari dune sands have relatively higher SiO_2 (93.4.3-99.6%, with an average of 97.7% SiO_2 compared to the Namib dune sands (85.2 – 88.1%), with an average of 86.4% SiO_2.

In Kalahari dune sand samples, Al_2O_3 ranges from 0.34 to 2.55% with an average 0.66%; Fe_2O_3 ranges from 0.55 to 1.25% with an average 0.80%; K_2O range 0.02 to 0.77% with an average 0.14%; Na_2O ranges from 0.01 to 0.09 % with an average 0.02%; CaO ranges from 0.01 to 0.04 % with an average 0.03%; LOI ranges from 0.2 to 1.1% with an average 0.6 %

In the Namib dune sand samples, Al_2O_3 ranges from 1.7 to 2.68% with an average 2.24%. Fe_2O_3 ranges from 5.33 to 6.18 % with an average 5.84%; K_2O ranges from 1.46 to 1.65% with an average 1.55%; Na_2O ranges from 1.11 to 1.27%; average 1.2; CaO ranges from 1.112 to 1.51% with average 1.36%; LOI ranges from 0.6 to 0.7% with an average 0.6%.

Table 4. Major elements composition of the Kalahari and Namib dune sands (values in %).

Sample ID.	Locality	SiO_2	Al_2O_3	$Fe_2O_3^{(T)}$	MnO	MgO	CaO	Na_2O	K_2O	TiO_2	P_2O_5	LOI	Total
KS 1	Kalahari	97.7	1.16	0.77	0.01	0.04	0.02	<0.01	0.06	0.11	< 0.01	0.8	101
KS 2	Kalahari	98.4	0.77	0.86	0.01	0.03	0.02	<0.01	0.07	0.08	0.02	0.4	101
KS 3	Kalahari	93.4	2.55	1.25	0.01	0.07	0.04	0.09	0.77	0.28	0.03	1.1	99.5
KS 4	Kalahari	99.1	0.34	0.55	0.01	0.01	0.01	<0.01	0.05	0.09	0.01	0.2	100
KS 5	Kalahari	97.5	0.86	0.87	0.01	0.04	0.02	<0.01	0.06	0.1	0.01	0.7	100
KS 6	Kalahari	97.1	1.19	0.87	0.01	0.05	0.04	0.01	0.11	0.11	< 0.01	0.8	100
KS 7	Kalahari	98.3	0.73	0.75	0.01	0.03	0.04	<0.01	0.06	0.09	0.03	0.4	101
KS 8	Kalahari	98.7	0.72	0.67	0.01	0.03	0.04	<0.01	0.03	0.08	<0.01	0.4	101
KS 9	Kalahari	99.6	0.36	0.57	0.01	0.03	0.01	<0.01	0.02	0.06	<0.01	0.2	101
NS 10	Namib	86.5	5.94	1.98	0.03	0.69	1.3	1.21	1.65	0.22	0.08	0.6	100
NS 11	Namib	86	5.91	2.61	0.05	0.9	1.5	1.22	1.53	0.31	0.08	0.7	101
NS 12	Namib	85.2	6.18	2.68	0.05	0.89	1.51	1.27	1.54	0.33	0.1	0.7	100
NS 13	Namib	88.1	5.33	1.7	0.03	0.55	1.12	1.11	1.46	0.19	0.08	0.6	100
Detection limits		0.01	0.01	0.01	0.001	0.01	0.01	0.01	0.01	0.001	0.01		

LOI: loss of ignition; <: values below detection limit.

Table 5.Some major oxides ratios and CIA values of Kalahari and Namib dune sands

Sample ID	K_2O/Al_2O_3	Al_2O_3/TiO_2	CIA
KS 1	0.052	10.27	92.80
KS 2	0.091	9.17	88.51
KS 3	0.302	9.14	75.67
KS 4	0.147	3.82	82.93
KS 5	0.070	8.27	90.53
KS 6	0.092	10.53	88.15
KS 7	0.082	8.30	86.90
KS 8	0.042	8.67	90.00
KS 9	0.056	6.32	90.00
NS 10	0.278	26.52	58.81
NS 11	0.259	18.82	58.17
NS 12	0.249	18.50	58.86
NS 13	0.274	28.05	59.09

CIA: Chemical Index of Alteration.

Table 6.Trace elements and REE analyses of Kalahari and Namib dune sands (values in ppm).

Sample ID	Locality	Rb	Sr	Ba	Y	Zr	La	V	Cr	Ce	Pr	Nd
KS1	Kalahari	6	4	32	7	121	2.2	16	< 20	5	0.47	1.9
KS2	Kalahari	4	4	26	8	79	3	12	< 20	5.2	0.58	2.2
KS3	Kalahari	27	15	172	10	119	5.2	21	30	9.1	1.13	4.4
KS4	Kalahari	2	2	35	7	149	1.7	5	< 20	3.3	0.36	1.4
KS5	Kalahari	4	3	24	9	114	3.7	13	< 20	6.6	0.78	2.9
KS6	Kalahari	8	5	33	9	109	4.1	13	< 20	7.8	0.84	3
KS7	Kalahari	4	5	30	9	89	2.6	11	< 20	4.9	0.54	2
KS8	Kalahari	4	3	28	10	109	2.1	10	< 20	4.2	0.43	1.5
KS9	Kalahari	2	3	22	7	76	1.7	9	< 20	2.9	0.3	1.2
NS10	Namib	64	87	322	16	96	11.3	40	50	19.1	2.5	9.8
NS11	Namib	56	85	303	18	179	11.8	54	70	20.7	2.66	10.4
NS12	Namib	60	90	307	21	138	15.8	53	90	27	3.51	12.7
NS13	Namib	55	78	294	15	69	11.5	32	30	19.5	2.51	9.6
Detection limits		2	2	3	2	4	0.1	5	20	0.1	0.05	0.1

In comparison with the values of the upper continental crust (UCC) of McLennan (2001), both Kalahari and Namib dune sands are enriched in SiO_2 and depleted in other major oxides

(Fig.12). Kalahari dune sand are highly depleted in Al_2O_3, K_2O, Na_2O, CaO and MgO than in the Namib dune sands indicating that Kalahari dune sand underwent more intense weathering and recycling processes compares to the Namib dune sand (Chakrabarti, Shome, Bauluz., & Sihna, 2009).

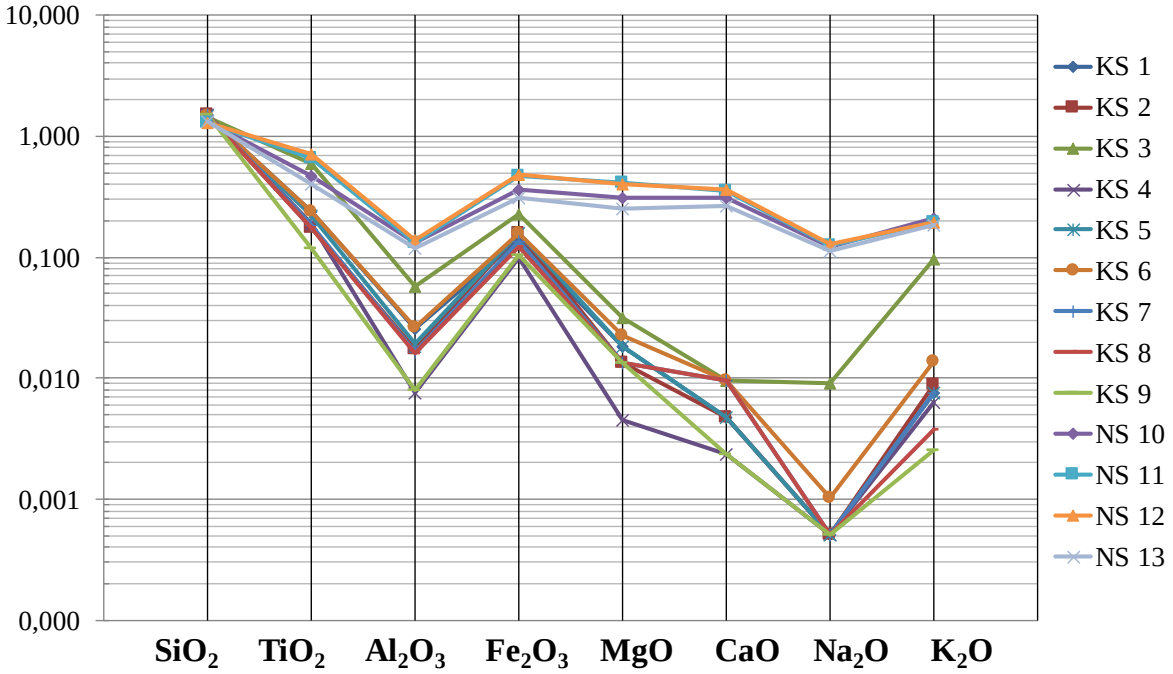

Figure 12. Major element Spider plots of the Kalahari and Namib dune sand samples normalised based to Upper continental crust (UCC) values of McLennan (2001).

A ternary plot with SiO_2-Al_2O_3+Na_2O+K_2O-Fe_2O_3+TiO_2+MgO poles is used to show relative abundance of quartz (SiO_2), feldspar (Al_2O_3+Na_2O+K_2O) and heavy mineral (Fe_2O_3 +TiO_2+MgO) content in the sand samples (Kasper-Zubillaga et al., 2007). Kalahari dune sands are plotting in 95-100% SiO_2 composition region, whereas Namib dune sand are dispersed in 85-90% SiO_2 composition region toward the SiO_2 apex of the ternary diagram (Fig.13). High SiO_2 content in the Kalahari dune sands indicates that they are more intensely weathered due to aeolian transportation than the Namib dune sands that have low content of

Al_2O_3, Na_2O, and K_2O which are associated with feldspar grains and heavy minerals (Kasper-Zubillaga et al., 2007).

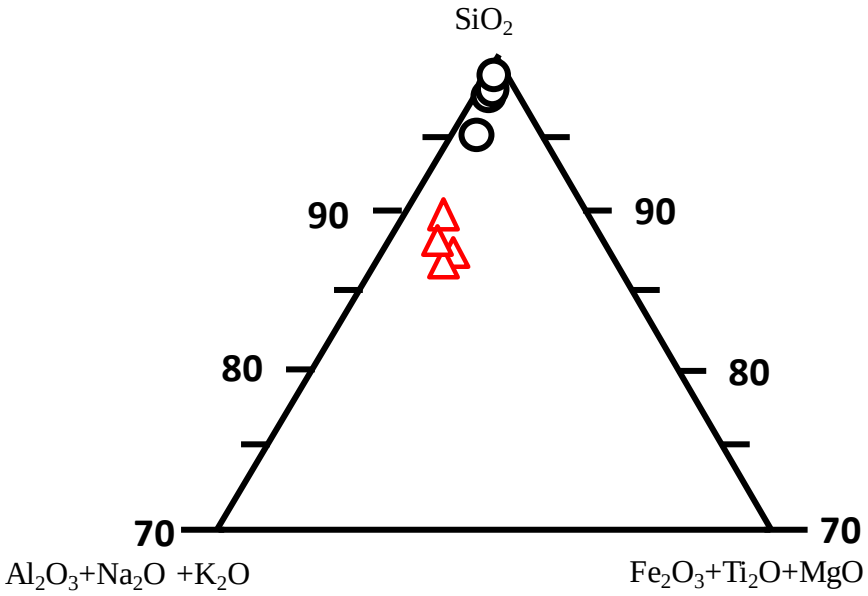

Figure 13. SiO_2 – Al_2O_3 + Na_2O + K_2O – Fe_2O_3 + TiO_2 + MgO ternary diagram with plots of Namib(**Δ**) and Kalahari dune sand(**o**) compositions.

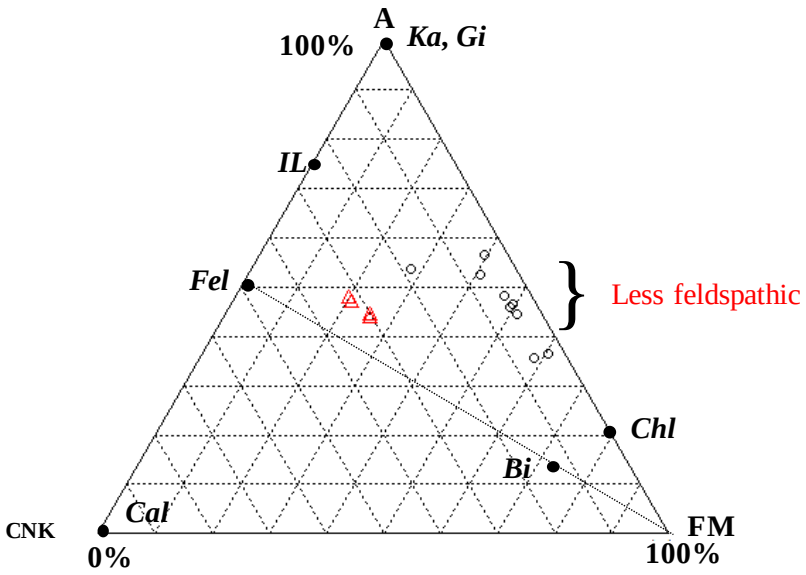

Figure 14. A-CNK-FM ternary diagram of the Kalahari (**o**) and Namib dune sands (**Δ**) with mineral compositions (filled dots) after Nesbitt et al. (1996). A = Al_2O_3, CNK = CaO* + Na + K_2O, FM = $Fe_2O_3^{(T)}$ + MgO. Ka = Kaolinite, Chl = Chlorite, Gi = Gibbsite, Il = Illite, Fel = Feldspar, Cal = calcite, Bi = Biotite.

In the Al_2O_3-CaO+K_2O+Na_2O-Fe_2O_3+MgO ternary plot (Appendix C_1), Kalahari dune sand are clustering at 50% Al_2O_3 and 50 % (Fe_2O_3+MgO) composition close to chlorite composition region and they are less feldspathic, while the Namib dunes sand are plotting toward Al_2O_3-

CaO+K_2O+Na_2O poles close to the feldspar composition region (Fig.14). Again, the Kalahari dune sands are less feldspathic due to intense weathering and recycling compare to the Namib dune sands (Chakrabarti et al., 2009). The clustering of Kalahari sands in the chlorite composition region indicates the presence of fine particles of iron-oxides and clay components, which could possibly have resulted from in situ weathering of felspathic and ferromagnesian minerals in the stable dunes as suggested by Dierks (1994) and Muhs (2004).

The calculated CIA values for the Kalahari dune sand ranged from 82.93 to 92.80%, while the average CIA value for Namib dune sands is lower as 58.73% (Table 5). In the A-CN-K ternary plot (Fig.15 & Appendix C_2), Kalahari dune sand data cluster is found near the A-K edge, along illite to chlorite and gibbsite compositions, indicating more intense weathering of the source rocks. Namib dune sand data are plotting just above the Plagioclase-K-feldspar line (Fig.15 and appendices C_7), that are less intensely weathered (Mishra & Sen 2012).

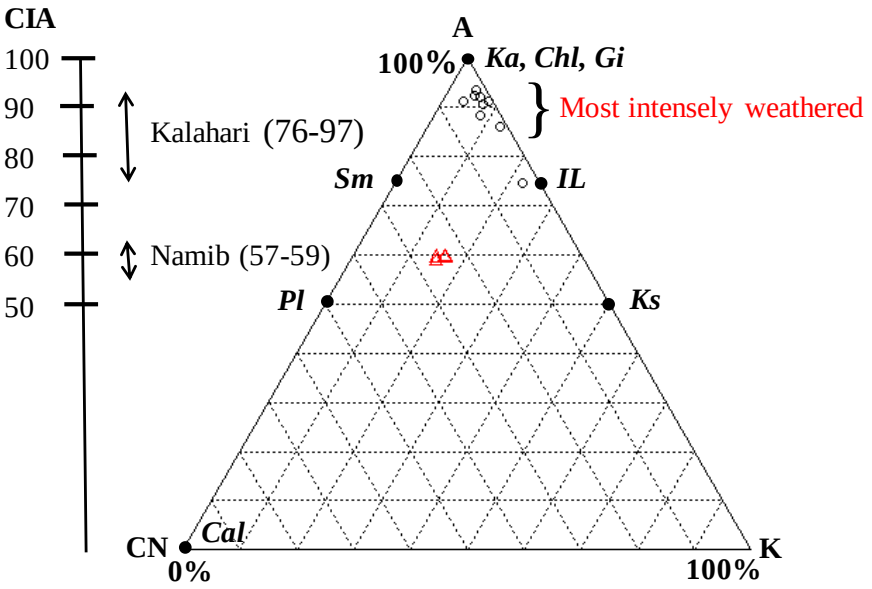

Figure 15. A-CN-K ternary diagram of the Kalahari (o) and Namib dune sands (Δ) with mineral compositions (filled dots) after Nesbitt et al. (1996). A = Al_2O_3, CN = CaO* + Na_2O, K = K_2O. Ka = Kaolinite, Chl = Chlorite, Gi = Gibbsite, Sm = Smectite, Il = Illite, Pl = Plagioclase, Ks = K-feldspar, Cal = calcite.

The K_2O/Al_2O_3 ratios of sediments can be used as an indicator of the original composition of ancient sediments. In the Kalahari dune sand samples, the K_2O/Al_2O_3 ratios are ranging from (0.046 to 0.302) (Table 5) and they are in the range of clay minerals, Low K_2O/Al_2O_3 ratios, indicates recycled nature of the dune sands (Chakrabarti et al., 2009); while in the Namib dune sand samples the ratios are ranging from (0.249 to 0.278) (Table 5) with K_2O/Al_2O_3< 0.3 indicating illite as the dominant clay mineral, since feldspars have higher K_2O/Al_2O_3 ratios (0.3 to 0.9) (Cox, Lowe, & Culleres, 1995).

The Al_2O_3/TiO_2 ratios of the Kalahari dune sand ranges between 3.8 -10.2 which indicates a mafic component in the source rocks, whereas the Namib dune sand on the other hand the ratios ranges between 18.5- 28.0, indicating a more felsic source rocks (Chakrabarti et al., 2009; Mishra & Sen ,2012).

There are higher values of trace elements like Ba, Zr, Rb, Cr, Sr, V, and Y for Namib dune sands compared to Kalahari dunes sand (Table 5). Th/Sc-Zr/Sc diagram (Fig.16) shows that the Namib dune sand are plotting close to the Post Archean Average Shale (PAAP), while Kalahari dune sand are Zr-enriched compare to the Archean Precambrian Granite (Fig.16). The considerable variation with little change accompanying in the Th/Sc ratio for Kalahari is typically displaced by more matured or recycled sediments which are associated with zircon addition as shown in Fig.16 (Kasper- Zubillaga et al., 2007; Mishra & Sen, 2012; Hu & Yang ,2016).

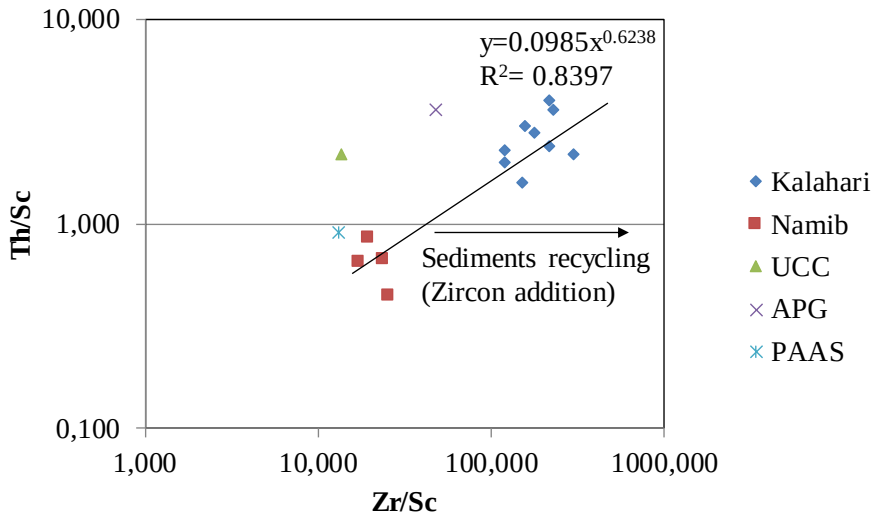

Figure 16. A Th/Sc vs Zr/Sc element ratio plot of the Kalahari and Namib dune sands in comparison to values of Post Archean Average Shale (PAAP), Average Precambrian Granite (APG) and the Upper Continental Crust (UCC) from Taylor and McLennan (1985), Condie (1993) and Rudnik & Gao (2003), respectively.

REE contents are less than 5 ppm except for La and Ce that have contents greater than 5 ppm in both Kalahari and Namib dune sand samples (Table 5). In the chondrite-normalized REE plots (Fig. 17), both Kalahari and Namib dune sands are depleted in REEs relative to Chondrite values of McDonough & Sun (1995), with the LREEs being more enriched than the HREEs and a more pronounced Eu negative anomaly in the Kalahari sands. Kalahari dune sands have lower REE concentrations indicating long aeolian transport distance,

whereas Namib dune sands have higher REE concentrations due to Orange River fluvial transport with short aeolian transport distance. (Garzanti et al., 2012; Kasper-Zubillaga, Acevedo-Vargas, B., Bermea, & Zamora, 2008).

The more pronounced Eu anomaly in the Kalahari sands is attributed to Eu depleted felsic igneous rocks in the source region (Mishra & Sen 2012).

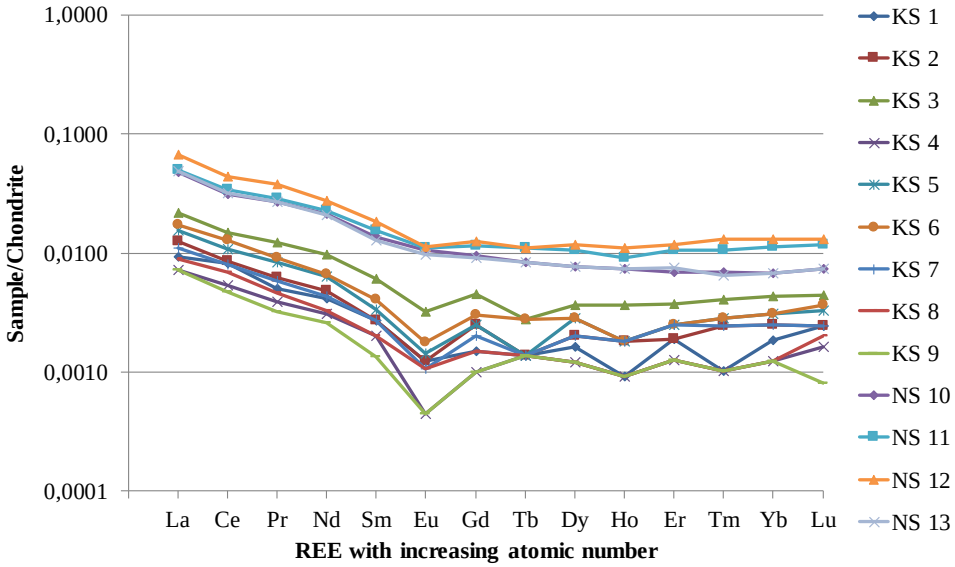

Figure 17. REE patterns for Kalahari and Namib dune sand samples normalised to the concentration Chondrite based on McDonough & Sun (1995).

4.4 XRD characterization of synthesized potassium silicate and commercial potassium silicate.

The XRD patterns of the synthesized and commercial potassium silicates are shown in Fig. 18 and Fig. 19, respectively. XRD patterns of (quartz sand and potassium silicate) mixture is depicted in Fig.20.Both X-ray patterns of the synthesized (Fig.18) and commercial potassium silicate glass (Fig.19) shows a characteristic broad diffuse peak at $2\theta = 20\text{-}35°$ due to their X-ray amorphous and complex structure of the silicates. The X-ray peak of the synthesized potassium silicate is shallow or short, while that of commercial silicate is steep or high due to low crystallinity of the synthesized (Sooksean et al., 2010). Furthermore, there are no crystalline phases' peaks in both XRD patterns due to the silicate compositions. However, crystalline phases peaks appeared in the XRD pattern of the ground mixture, owing to the quartz sand (SiO_2) at $2\theta = 21, 27, 43, 60°$ and Potassium carbonate components (K_2CO_3) at $2\theta = 32°$.

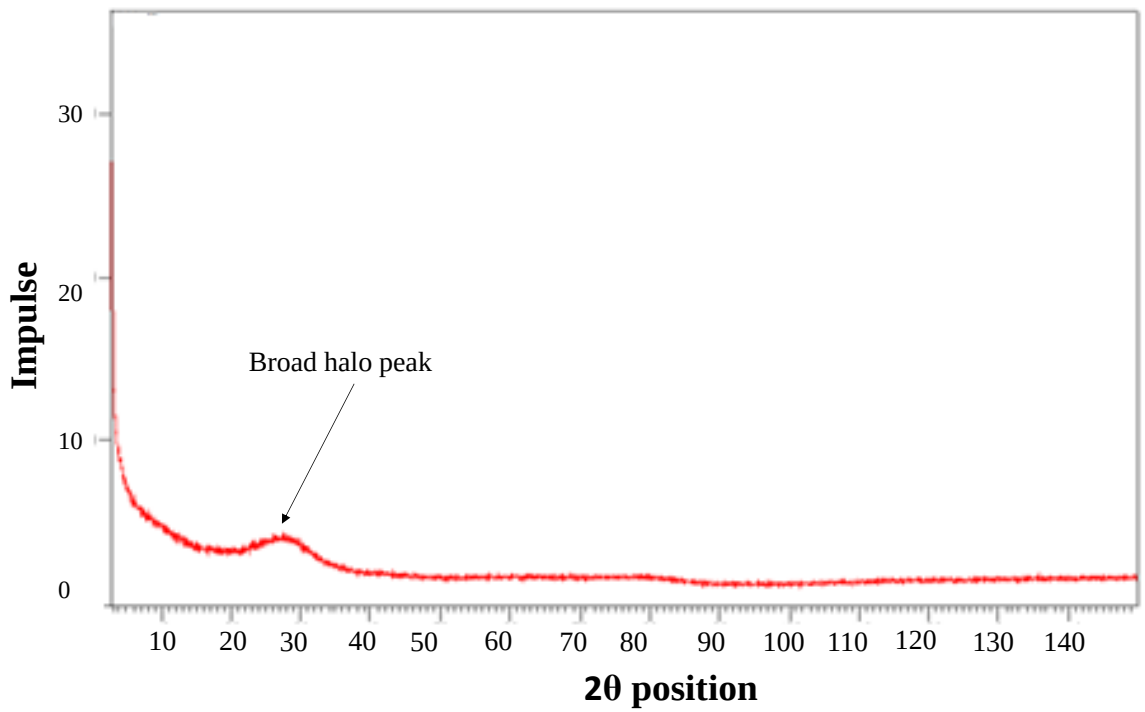

Figure 18. XRD patterns of synthesized potassium silicate (KWG-5).

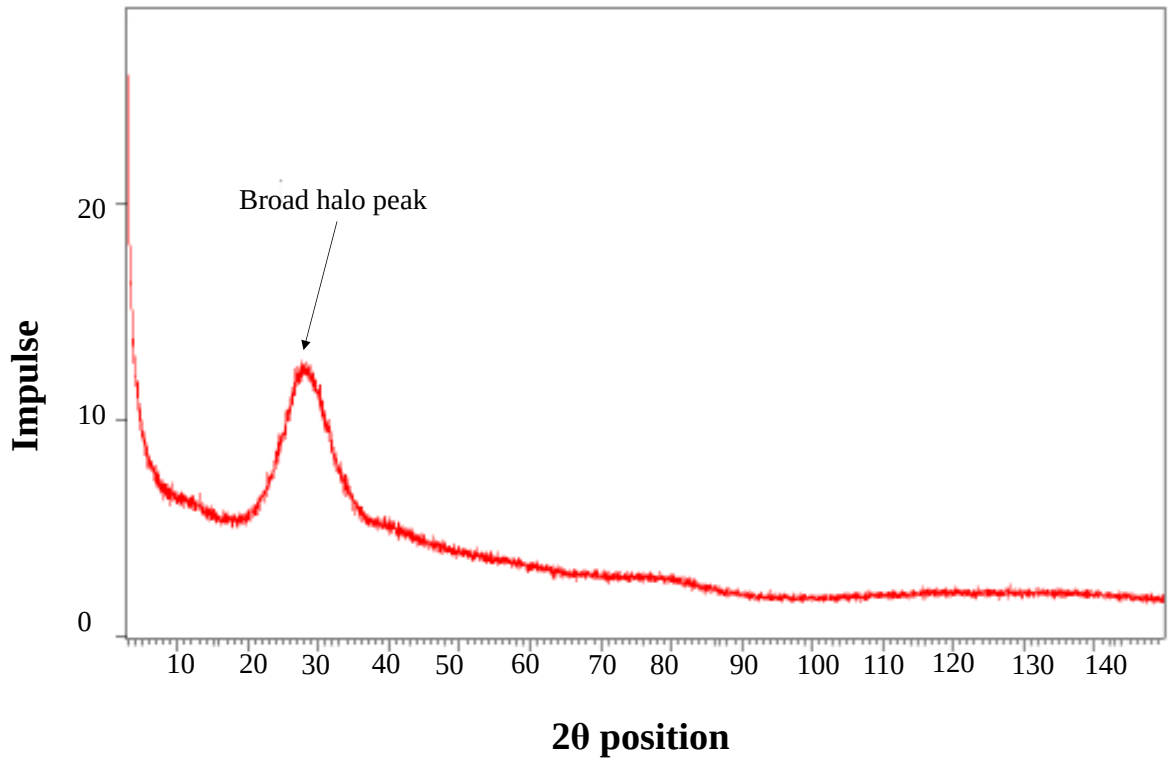

Figure 19. XRD patterns of commercial water glass (KWG-com-5

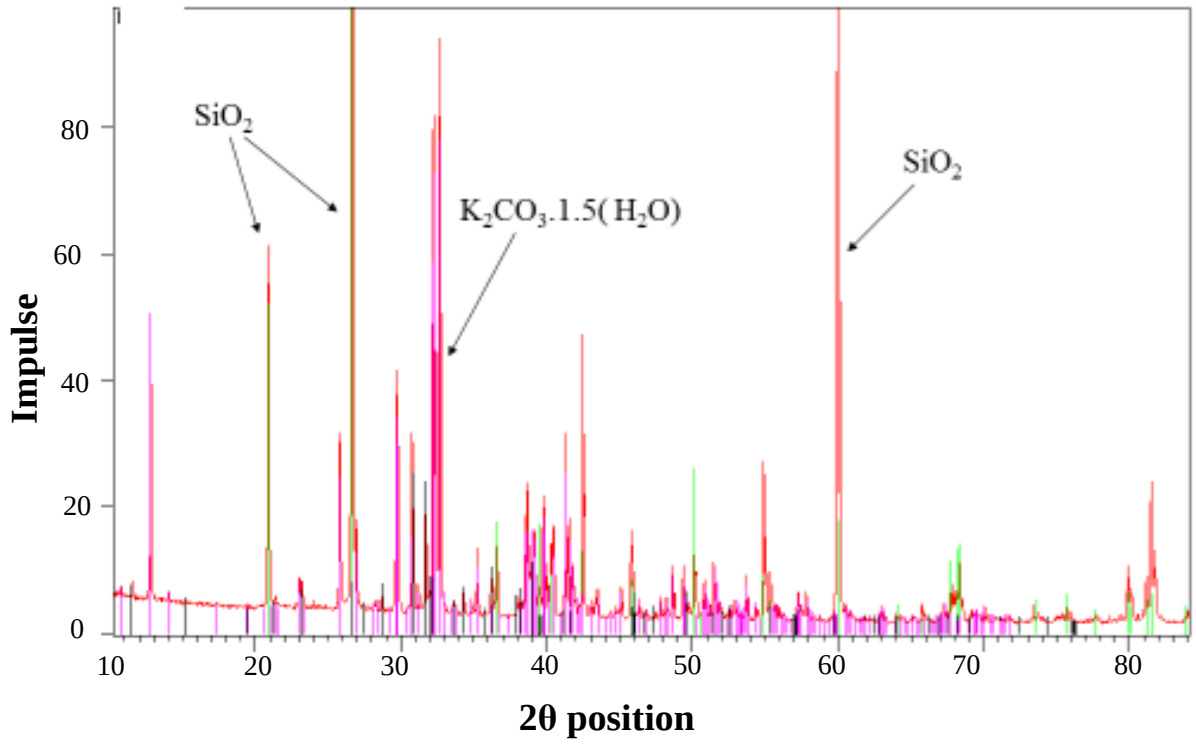

Figure 20. XRD pattern of ground mixture (2 parts of quartz sand, 1 part of potassium carbonate).

4.5 ESEM/EDX microstructural characterization of synthesized potassium silicate.

Figure 21(a & b), 22(a & b), and 23(a & b) show the ESEM microstructures and their corresponding EDX point analysis spectra taken at three various point of the synthesized

glass.

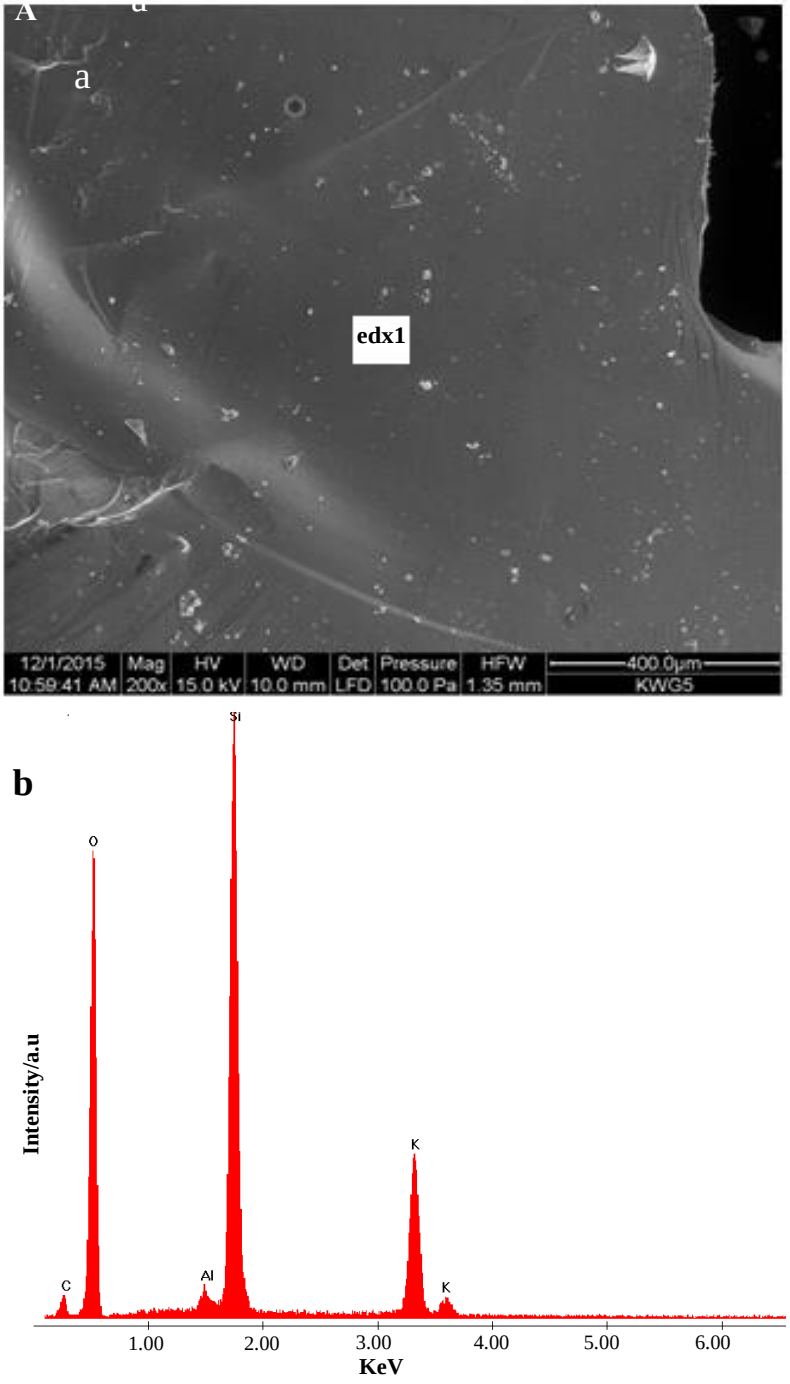

Figure 21. a) ESEM micrographs of synthesized potassium silicate (KWG-5) and b) a corresponding edx1 spectra. C - Carbon, O- Oxygen, Al-Aluminium, Si- Silicon and K- Potassium.

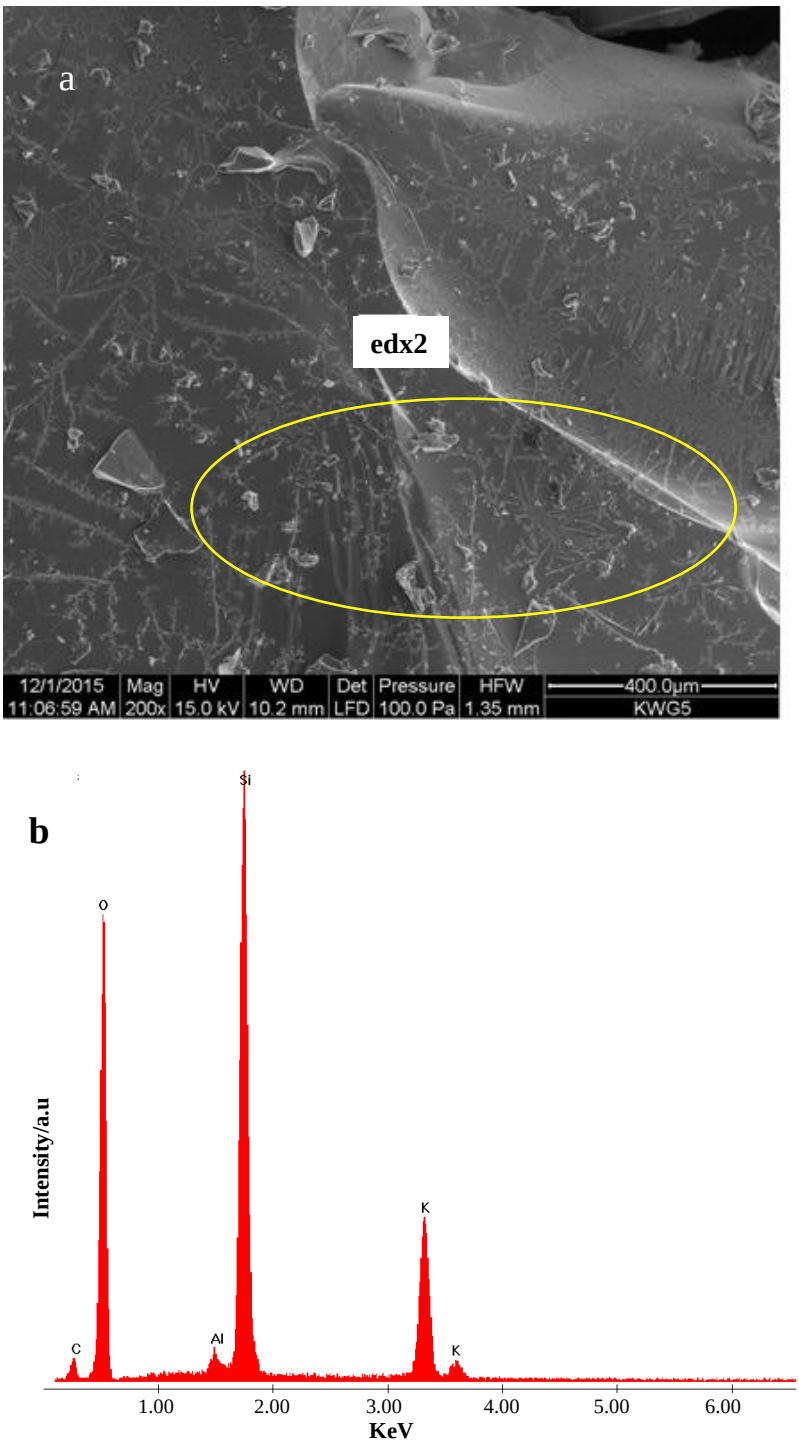

Figure 22. a) ESEM micrograph of synthesized potassium silicate (KWG-5) with dendritic surface chemical gardens growth (in circled) and b) a corresponding edx2 point analysis spectra. C - Carbon, O- Oxygen, Al-Aluminium, Si- Silicon and K- Potassium.

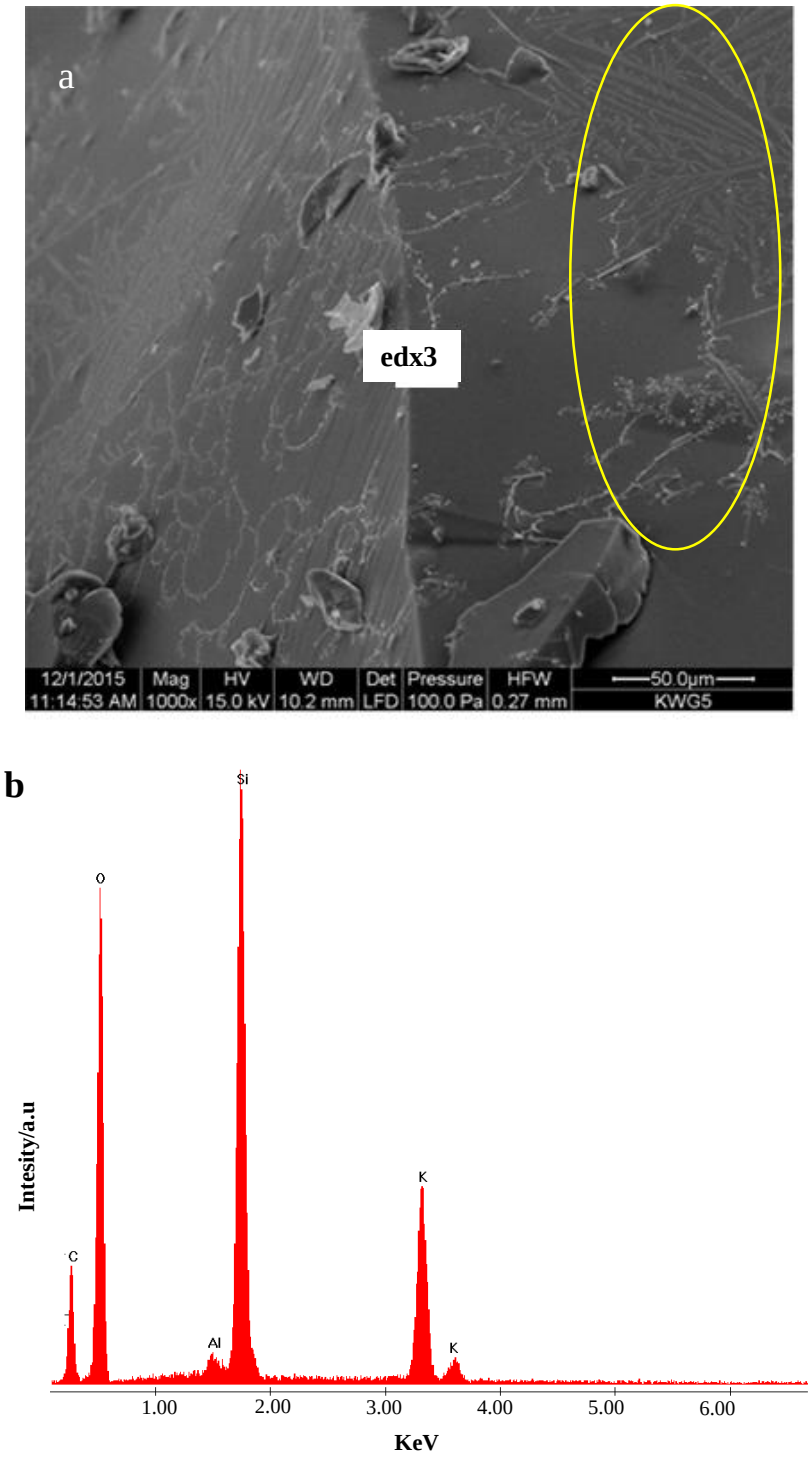

Figure 23. a) ESEM micrograph of synthesized potassium silicate (KWG-5) with dendritic surface chemical gardens growth (in circled) and b) corresponding edx3 point analysis spectra. C - Carbon, O- Oxygen, Al-Aluminium, Si- Silicon and K- Potassium.

The ESEM micrographs show the synthesized glass surface morphology characterised by a dense, fairly smooth surface morphology with no cracks. ESEM micrographs in figure 22 a & 23 a show the glass surface is further characterised by chemical gardens

The dendritic chemical gardens growth observed on the microstructure surfaces are possibly representing the narrow tubes of potassium ion-salt solution that might have flown from silicate glass and form precipitates on the glass surface during crystallization process (Julyan, Cartwright, Bruno Escribano, & Ignacio Sainz-Díaz, 2011).

The EDX spectra (21 a,22b,23c) for all elemental analysis points (edx1, edx2, and edx3) in the ESEM micrograph show the presence and intensities of the elements Si, K, Al, and C. It can be seen in all three EDX points analysis spectra that K, S, and Al are uniformly distributed across the bulk glass with an enrichment of Si at the surface of the silicate glass, with Si:K intensity ratios that are close to 3:1.

Figure 24, shows ESEM micrograph corresponding BSE image of the synthesized potassium silicate.

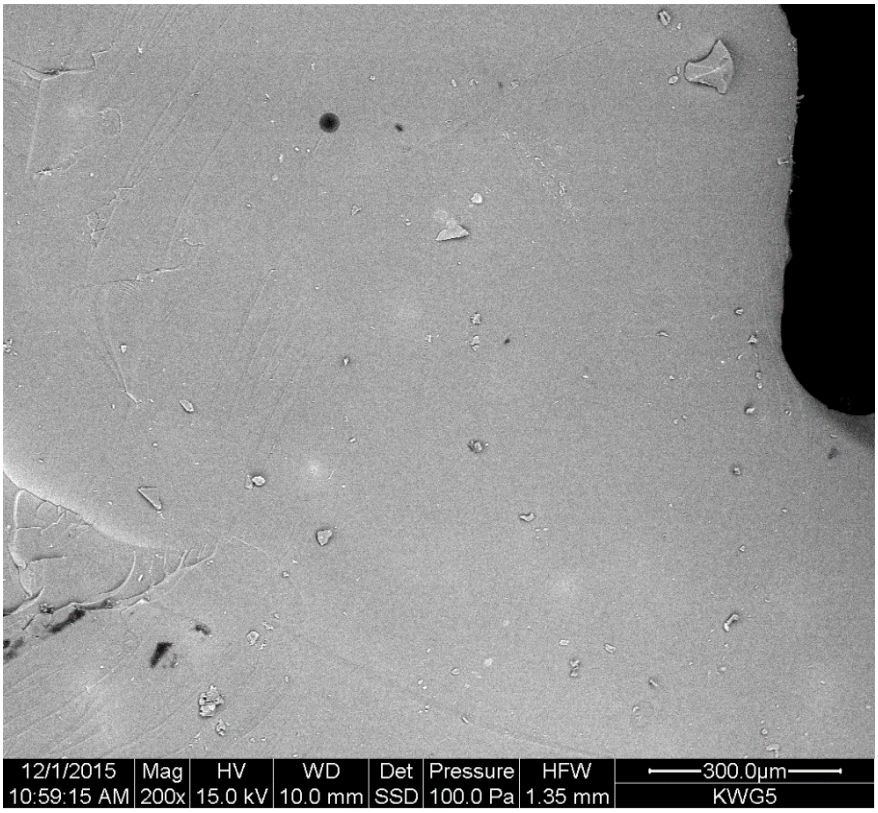

Figure 24.ESEM back scattered electron image of the synthesized potassium silicate (KWG-5).

The image shows a uniform back scattered electron image contrast throughout the entire micrograph. However, there are few pronounced dark spot which are probably entrapped Si-rich phase(s). Low contrast of BSE micrographs image indicates that the average atomic compositions of the entire silicate glass is almost homogenous, which again indicate a complete fusion of quartz sand and potassium carbonate.

4.6 Silica (SiO_2) and K_2O percentage composition of synthesized potassium silicate.

The SiO_2, K_2O, and Al_2O_3 percentage compositions of the synthesized potassium silicate are shown in Table 7. The results indicate that the % wt. SiO_2 is 2.7 times more than the % wt.K_2O and 40 times more than the % wt. Al_2O_3. The alkali and silica percentage ratio calculated suggests that the synthesized silicate is of 4.24 ±0.19 SiO_2/K_2O molar ratio.

Table 7. Si, K, Al, SiO_2, K_2O and Al_2O_3 % wt. composition and molar ratio of synthesized potassium silicate.

% wt. Si	% wt. K	% wt. Al	% wt. SiO_2	% wt. K_2O	% wt. Al_2O_3	Weight ratio SiO_2:K_2O	Molar ratio SiO_2:K_2O
33.50± 0.097	22.05± 1.45	0.933± 0.007	71.67± 0.21	26.56± 1.75	1.76± 0.01	2.70±0.12	4.24±0.19

The empirical formula of the synthesized silicate glass can be determined as follows:

% wt. of Si =33.50, thus no. of moles of Si= 33.50/28.085= 1.19 moles.

% wt. of K=22.05, thus no. of moles of K=22.05/39.098= 0.56 moles.

% wt. of Al =0.933, thus no. of moles of Al =0.933/26.981= 0.034 moles.

Using the % wt. SiO_2, K_2O, and Al_2O_3, moles of O in the silicate can be calculated as follows:

Moles of O in SiO_2 = 71.67/60.084=1.192 ×2= 2.384 moles.

Moles of O in K_2O = 26.56/94.196 =0.281 ×1= 0.281 moles.

Moles of O in Al_2O_3=1.76/101.961 =0.017×3 = 0.051 moles.

Total no of moles of O = 2.716 mole

Cation and Anion mole ratios:

Si	K	Al	O
1.19	0.56	0.034	2.716

Combining mole ratios of Al and Si, because of possible $Al^{+3} \leftrightarrow Si^{+4}$ substitution, then cation and anions ratio are then given as:

(Si, Al)	K	O
2.185	1	4.85

Alternatively, if Al oxides phases exist in the silicate glass as AlO_2 as it appears in most silicate geo-polymers, then the total O moles in the glass is 0.059, thus the anion ratio is 4.86.

Therefore, the likely synthesized glass's composition and empirical formula is:

$K\ (Al_{0.03}, Si_{2.185})\ O_{4.86} \approx KSi_2O_5$.

However, taking cations and anions charge balance into consideration, wt. % determination errors, and rounding off mole ratios to 2 decimal places the empirical formula is possibly, $K_2Si_2O_5$.

CHAPTER 5: DISCUSSION

5.1 Suitability of the Kalahari and Namib dune sands as silica sand in the potassium silicate synthesis.

From the mineralogical and chemical compositions, and grain size analysis of the thirteen (13) sand samples studied, the following aspects have been found about Kalahari and Namib dune sands as potential raw materials in the manufacturing of potassium silicate:

Kalahari sand samples with SiO_2 contents in a range of (93-99%) are ideal silica sand raw materials as they conform with requirements and specifications of silica sand for the manufacturing of silicates as discussed in studies by PQ corporation (2004) and Vail (1975).

However, with Al_2O_3 and Fe_2O_3 contents in the range of 0.34-0.72% and 0.55-0.67%, respectively (Table 4), these sands will require attrition scrubbing processing to enhance the SiO_2 content and reduce the undesirable Fe_2O_3 and Al_2O_3 contents (Brown & Redeker, 1980). Furthermore, this will enable the sands to conform with the closely monitored specifications (>99.4% SiO_2, <0.03% Fe_2O_3 and <0.2% Al_2O_3) used by Ash Associates (1996) in a bench scale study of sand and the study by Cuesta Consultant Limited (2015) of silica sand (SiO_2 > 99%, < 0.5% Fe_2O_3 and <0.01% Al_2O_3) for sodium silicate manufacturing. Additional processing of removing iron-oxide coatings from the sand grains with hot hydrochloric acid (Haddon, 2005), can lead to angular sand grains that are generally glassy and desirable in the fusion process of manufacturing potassium silicate glass.

Since the Kalahari dune sands do not possess heavy minerals, micas and spinel group minerals, which are often objectionable in the melting or fusion process, the synthesis of soluble silicates using Kalahari sand samples will result into silicate lumps with less or no holes, stones, or blisters (Vail, 1975).

From grain size analysis, it was found that more than 20 % of the sand grains of the samples from the Kalahari sand deposits (KS1-KS9) were retained in sieve size range 45 µm to 0.063 µm and less than 60 % of sand grains from were retained in the sieve size range 125 µm to 500 µm as shown in Figure 10. With that fine grain percentage, the sands will require a subtle physical processing particularly grain size screening, in order to meet key requirements and specifications for silica sand in the soluble silicate manufacturing (0 % coarser than 1mm, >90% between 125µm and 500 µm and >7% finer than 125µm) as discussed by Ash Associates (1996) and Cuesta Consultants Limited (2015).

Moreover, grain size screening removes finer particles that usually carry contaminants such as clay mineral phases, chlorite, gibbsite, goethite, and magnetic minerals (Vail ,1975 and Carrigy,1970). Thus, this processing technique will simultaneously eliminate these constituents that might affect the quality of the silicates. Evidently, this can be observed in the chemical composition of the synthesized potassium silicate glass of this study that contains 1.76% Al_2O_3 (Table 7), owing to the 0.34% Al_2O_3 contents of the unscreened sand sample used (KS4) in the silicate synthesis.

In contrast to the Kalahari sands, Namib dune sands (NS 10-13) with SiO_2 ranging from 85-88%, more than 5% Al_2O_3, 2% (CaO + MgO), and 2.5% Fe_2O_3 (Table 4) are less suitable in the synthesis of quality soluble silicates. Namib dune sands will require beneficiation techniques such as magnetic separation and flotation, cyclone separator that can deplete heavy and refractory minerals that are present as contaminants in mineral grain forms (Table 3) and further affect the fusion temperature (Carrigy,1970). According to Edem at el. (2014), these beneficiation techniques can enhance the SiO_2 content and improve the quality of the sands.

However, from the particulate analysis of Namib sand samples less than 1 % of the sand grains were retained in the same sieve size range (45 µm to 63 µm) and more than 90 % of the sand grains were retained in sieve size range (125 µm to 500 µm) (Fig.10). With such grain size percentage distribution, Namib sands conform well with the recent and closely monitored standard physical requirements and specifications of processed silica sand for silicate synthesis used in studies by Ash Associate (1996) and Cuesta Consultants Limited (2015).

5.2 Synthesis and characterization of the synthesized silicate glass.

Heating quartz sand and caustic potassium carbonate in an electrical fired- furnace have resulted into synthesis of chemically homogenous potassium silicate glass with envisaged characteristic and properties discussed below.

The synthesized potassium silicate (Fig.18) and commercial silicate (Fig.19) are both XRD amorphous. The inability to detect crystalline phases in the glasses by XRD scans as shown in XRD patterns further authenticate that the synthesized glass is X-ray amorphous or have a low crystallinity as it was discussed also by Sharafat (2009) and Langille et al. (1991). Furthermore, lack of other peaks in the X-ray spectra elucidate that reagents used (quartz sand and potassium carbonate) which are crystalline phases as seen in Fig. 20, have fully reacted and fused into a homogenous, amorphous silicate glass.

The X-ray pattern of synthesized potassium silicate observed indicates broad halo peak at 2θ =20-35°. Similar XRD patterns were also observed in alkali-silicates materials studied by Skorina and Tikhomirova (2012), Sooksaen et al. (2010), Tambelli et al. (2006), and Yusheng et al. (2008) and their broad peaks are also reflected at 2θ range =16 to 35º. The broad peaks of alkali silicate materials also indicate to the X-ray amorphous characteristic of the silicates (Langille at al.1991)

However, XRD patterns slightly different to those observed in the synthesized potassium silicate were observed by Skirona and Tikhomirova (2012) and Langille et al. (1991) in heated alkali silicates, where broad peaks in the same 2θ range are characterized further by other small sharp peaks on top, owing to crystalline phases induced by high temperature calcination (Lin, Ferreira & Roch, 2003).

The synthesized silicate glass has a high SiO_2/K_2O molar ratio (4.24) and therefore it is a complex silicate with higher degree of polymerization (PQ corporation, 2004). The suggested degree of polymerization of the synthesized silicate correlates with observed XRD patterns. Similar observation was also made in a study by Sooksaen et al. (2010), where the broad peak at 2θ=20 -35° was ascribed to presence of disilicates (Si_2O_5) in the polymer. Furthermore, PQ Corporation (2004) has noted that ortho-silicates or monomers are characterized by crystalline silicates, while polysilicates are characterized by amorphous silicates.

The ESEM microstructures (Fig.21a, 22a & 23a) have indicated less porous and compacted microstructural features which further substantiate the highly polymerized and complex structural nature of potassium silicate glass polymer, that are usually associated with higher SiO_2/K_2O molar ratio silicates (Vickers et al., 2015).

The intensity and Si/K ratios observed in EDX analysis spectra (Fig 21b, 22b & 23b) suggest a substantially high ratio of Si atoms relative to K atoms and this lead to formation Si-O-Si network with high cross-linked density, which in turn determine the ultimate microstructure of the silicate polymer (Langille et al., 1991; Skoriva & Tikhormirova, 2012).

The chemical composition of the synthesized potassium silicate (Table 7) shows minor wt. % of Al-oxide phases that possibly exist in the silicate glass as contaminants from the sand samples (KS4) used in the synthesis. Thus, by neglecting the Al cation in the synthesized glass composition the possible glass composition is $K_2Si_2O_5$ which gives an electrically

neutral and stable crystal structure. The proposed silicate glass composition and the calculated SiO_2/K_2O molar ratio (4.24) correlate with suggested the degree of polymerization. The high SiO_2/K_2O molar ratio indicates that wt. % of K cations are relatively low compare to wt. % of Si, which leads to more Si cations linking up with O anion and networks into O-Si-O chains and complex structures (Langille et al.,1991).

5.3 Weathering intensity- possible source rocks.

Kalahari dune sand with CIA values in the 82-90 % (Table 5) underwent intense weathering during long aeolian transportation and sediment recycling processes, while Namib dune sands with CIA values in the 58-59 % (Table 5) experienced a moderately weathering due to fluvial and short aeolian transportations. The high weathering intensities of the Kalahari sands are further established by their high CIA values in comparison to the CIA values in the range (46-56 %) of other fluvial and wind transported desert dune sands studied by Kasper-Zubillaga & Zollezi-Ruiz, 2007, Kasper-Zubillaga et al., 2007, Amini et al., 2012 and Hu & Yang, 2016. However, the CIA values of the Kalahari dune sands are rather close to those of fluvial transported, Upper Kaimur sandstones and shales, and Dhandraul sandstones of India (72-87 %) studied by Mishra and Sen (2012) and CIA values (70%) of the PAAS (Post-Archean Australia Average Shales) recorded by Taylor & McLennan (1985).

The difference in weathering degrees of the dune sediments has further indicated by high depletion of K_2O, Na_2O, Al_2O_3 and enrichment of SiO_2 in the Kalahari sand than in the Namib dunes sands (Fig. 12), that are slightly depleted in the same mobile elements, compare to the UCC composition values by McLennan (2001).

The A-CN-K ternary plot (Fig.15) demonstrates the intense weathering of mafic sediments to clay minerals such illite, gibbsite and chlorite, whereas less weathered sediments of the Namib dunes are feldspathic. Low K_2O/Al_2O_3 in the range (0.046 to 0.302) (Table 5)

observed in the Kalahari sands also confirm the recycled nature of the sands (Chakrabarti et al., 2009). Besides results from this study, the redness of the Kalahari dune sand was associated with the Kaolinite-haematite clay coating (Strohbach et al., 2008), which might have resulted from in-situ weathering of sand sized feldspar (as suggested by Goudie, Stokes, Livingstone, Bailiff, & Allison,1993). These also indicates long-dune stability after long distance transportation. Namib dunes on the other hand were found by Garzanti et al. (2012) to have a strict quartz-feldspathic mineralogical resemblance to that of the Orange river (sediments main source), which again corroborate the moderate weathering during marine to aeolian sequential transportation of the sediments from the source to the dune deposits.

Furthermore, the Fe_2O_3 contents (Table 4) and iron-oxides in the Kalahari dune sands are associated with haematite coatings formed during in-situ weathering processes as suggested by Muhs (2004) on the Great Sandy Desert of Australia.

The contrast in the weathering extents of sands from the two dune fields are also indicated by the presence of Rb and Ba trace elements which substitute for potassium in the lattice of K-bearing clay minerals such as illite and gibbsite of the intensely weathered Kalahari dune sands as suggested in the A-CN-K ternary plot (Fig. 15). Rb, Ba, and Sr are associated with the presence of K- feldspars, heavy minerals and possibly plagioclase in the moderately weathered Namib dunes sands as also discussed by Kasper-Zubillaga et al. (2007) and Muhs Reynolds, Been, & Skipp (2003). Ba abundances are also proxies for K-feldspars contents that overall are low for the desert sands compared to their SiO_2 contents (Kasper-Zubillaga and Zolezzi-Ruiz, 2007; Muhs et al., 2003). The Zr observed in the Kalahari dune sands can be attributed to zirconium-addition process as indicated in Figure 16, during recycling/reworking processes of the sediments (Kasper-Zubillaga et al.,2007; Mishra & Sen ,2012), whereas in the Namib dune sands it can be attributed to the presence of zircon minerals that forms part of the heavy mineral suite as suggested by Chakrabarti et al. (2009),

Kasper-Zubillaga et al. (2007) and Hu & Yang (2016). Again this indicates and substantiate the different in weathering degrees of the sands from the two dune fields.

REE are extremely depleted in both Kalahari and Namib dune sands (Fig.17) compared to the REE concentrations in other desert dune sands of the Altar desert in North America and Taklimakan desert in China (Kasper- Zubillaga et al., 2008). Furthermore, REE concentrations are also relatively low in both Kalahari and Namib dune sands compare to the PAAS and Proterozoic Sandstones (Chakrabarti et al., 2009; Mishra & Sen, 2012). The lower REE values of the Kalahari dune sands compare to Altar desert sand and Taklimakan desert sand are due to long aeolian distance transportation and recycling of sediments that increases the quartz dilution and depletion of REE concentration values (Kasper–Zubillaga et al., 2008; Mishra & Sen, 2012).

Kalahari dune sands are quartz-dominated as result of reworking quartz-rich bed rocks as discussed also by Miller (2008) and Muhs (2004), while Namib sand are quartz-feldspathic (Appendices C_1) which indicates that sediments resulted from weathering of continental crust felsic rocks. Studies by Garzanti et al. (2012) and Muhs (2004) have established that Namib Dunes are derived from sediments of Orange river which drains variety of felsic rocks types (sedimentary rocks, gneisses and granites) and basalts.

CHAPTER 6: CONCLUSIONS

This study was undertaken in order to investigate and determine the exploitation potential of the readily available Kalahari and Namib dune sand deposits for the synthesis of potassium silicates. This study has established that Kalahari dune sand with high silica (SiO_2) contents (>97%) makes them suitable for potassium silicate synthesis. The minor surface coatings of iron-oxides and clay minerals, resulting from intensely weathering and sedimentary recycling of the sand require treatments to remove these constituents. In addition, Kalahari sands requires grain size screening to remove fines less than 125µm.

Although the Namib dunes sands have grain sizes which fall well within the required grain size range for potassium silicates synthesis (where > 90% sand grains are between 125 µm and 500 µm), they are less suitable in the synthesis of potassium silicates, since they contain objectionable minerals such as feldspars and heavy minerals and refractory minerals resulting from moderate degree of weathering during transportation processes. Consequently, the Namib dune sands require beneficiation techniques in order to reduce the undesirable mineral constituents and enhance the SiO_2 contents.

The potassium silicate glass synthesis in this study is XRD amorphous, with a dense and smooth surface morphology. The glass is enriched in Si than K and Al and the average atomic composition is homogeneous throughout the entire glass. From these microstructural features, it is concluded that the starting materials (quartz sand and potassium carbonate) were completely and well fused into a pure potassium silicate glass in a high temperature electric arc furnace. It is therefore possible to fuse crystalline quartz sand and potassium carbonate into potassium silicate at a laboratory scale, as indicated by most hand books and technical reports. It is further established that, the synthesized glass has a Si_2O/K_2O molar ratio of 4.24 and the possible composition is $K_2Si_2O_5$. Given this high molar ratio and composition, it can be concluded that the synthesized silicate has a complex structure with a

high degree of polymerization. Due to its low solubility and low degree of dissolution, which are associated with high molar ratio and the high Al_2O_3 contents respectively, the synthesized potassium silicate is not suitable for the preparation of potassium silicate 'water glasses'.

Recommendations

The results of this study has established that Namibian sands, particularly the Kalahari sands can be potential raw materials in the silicates manufacturing industries and in other technological processes and products such as preparation silica gel absorbents for water treatment, heavy duty detergents formulation, silicate binders, and fire-resistance coatings. Thus, further bench-studies focusing on the qualities of the Kalahari sands as primary silica sources and their processing for silicates synthesis, will add more values to these deposits that currently have limited technological applications.

Furthermore, since potassium silicates of certain SiO_2/K_2O molar ratios range are characterized by a fire-resistance and mechanical strength properties, more studies focusing on synthesis of these potassium silicates can be considered and ultimately avail potassium silicates that can be incorporated in various technological and building materials.

REFERENCES

Ash Associates. (1996). Sodium silicate study- bench scale tests with silica sands of Manitoba.*An open file report.* Toronto, Ontario.

Amini, A., Moussavi-Harami, R., Lahijani., & Mahboubi. (2012). Sedimentological, geochemical and geomorphological factors in formation of coastal dunes and nebkha fields in Miankaleh coastal barrier system (Southeast of Caspian Sea, North Iran). *Geoscience Journal*, *16* (2), 139-152.

Baillieul, T.A. (1978). A reconnaissance survey of the cover of the Republic of Botswana. *Journal of sedimentary petrology*, *45*(2), 494-503.

Blott, S. J., & Pye, K. (2001). Gradistat: A grain size distribution and statistics package for the analysis of unconsolidated sediments. *Earth Surface Processes and Landforms, 26*, 1237–1248.

Bristow, C. S., Duller, G. A. T., & Lancaster, N. (2007). Age and dynamics of linear dunes in the Namib Desert. *Geology*, *35*(6), 555-558.

Brown, C. J., & Redeker, I. H. (1980). Processing Glass Grade Sand from Dune Sand. *MRL Rept*, 80-5.

Carrigy, M. A (1970). *Silica sand in the vicinity of Edmonton, Alberta*. Research Council of Alberta.

CEES. (2013). *Soluble silicate: Chemical, toxicological, ecological and legal aspects of production, transport, handling and application.* Retrieved from http://www.cees-silicates.eu.

Chakrabarti, G., Shome, D., Bauluz., B., & Sihna, S. (2009). Provenance and Weathering History of Mesoproterozoic Clastic Sedimentary Rocks from the Basal Gulcheru Formation, Cuddapah Basin. *Journal Geological Society of India*, *74*, 119-130.

Chang, L. L. Y. (2002). *Industrial mineralogy, materials, processes, and uses*. Upper Saddle River, NJ: Prentice Hall, 54-67.

Chemspider. (2013). Potassium Silicate, CSID:59585, Retrieved from http://www.chemspider.com/Chemical- Structure.59585.html.

Cox, R., Lowe, D.R. and Culleres, R.L. (1995). The influence of sediment recycling and basement composition on evolution of mud rock chemistry in the SW United States. *Geochem. Cosmochim. Acta, 59* (14), pp.2919-2940.

Cuesta Consultant Limited. (2015). Soft sand and silica sand study. Report to West Sussex County Council, pp 14-40.

Dierks, K. (1994). Road Building and geology in Namibia. Retrieved from www.klausdierks.com/Gelogy/index.htlm.

Edem, C. A., Malu, S. P., & Ita, B. I. (2014). Characterization and Beneficiation of the Glass Making Potentials of Silica Sand Deposit from River Benue North Central Nigeria. *Journal of Natural Sciences Research*, *4*(19), 49-58.

Falcone, J.S. (1997). Silicon compounds - Synthetic inorganic silicates. In: Kirk-Othmer *Encyclopedia of Chemical Technology*, 4th ed. Wiley, New York, USA. 22, 1-30.

Garzanti, E., Andò, S., Vezzoli, G., Lustrino, M., Boni, M., & Vermeesch, P. (2012). Petrology of the Namib sand sea: Long-distance transport and compositional variability in the wind-displaced Orange delta. *Earth-science Reviews*, 112, 173-189.

Garzanti, E., Vermeesch, P., Padoan, M., Resentini, A., Vezzoli, G., & Andò, S. (2014). Provenance of passive-margin sand (Southern Africa). *The Journal of Geology*, *122*(1), 17-42.

Gehring, A. U., Riahi, N., Kind, J., Almqvist, B. S., & Weidler, P. G. (2014). The formation of the Namib Sand Sea inferred from the spatial pattern of magnetic rock fragments. *Earth and Planetary Science Letters*, *395*, 168-172.

Goldman, H. B. (1994). Glass raw materials. In D. D. Carr (Eds.), *Industrial minerals and rocks*. Littleton: Society for Mining, Metallurgy, and Exploration, 869-877.

Goudie, A.S., Stokes, S., Livingstone, I., Bailiff, I.K., & Allison, R.J. (1993). Post-depositional modification of the linear sand ridges of the West Kimberley area of north-west *Australia. Geographical Journal*, *159*, 306– 317.

GWP consultants LLP. (2010). *A study of silica sand quality for Surrey and Kent final*. Surrey and Kent County councils.

Haddon, I.G. (2000). Kalahari Group sediments. In: Partridge, T.C. and Maud, R.M. (Eds) Cenozoic of Southern Africa. Oxford Monographs on Geology and Geophysics, 40, 173-181, Oxford University Press, New York, 173-181.

Haddon, I. G. (2005). *The sub-Kalahari geology and tectonic evolution of the Kalahari Basin, Southern Africa*. (Doctoral Thesis). University of the Witwatersrand, Johannesburg.

Hu, F. & Yang, X. (2016). Geochemical and geomorphological evidence for the provenance of Aeolian deposits in the Bandain Jaran Desert, north-western China. *Quaternary Science Reviews, 131*,179-192.

Julyan, H.E., Cartwright, J. H., Escribano, B., & Sainz-Díaz, C. I. (2011). Chemical-garden formation, morphology, and composition. I. Effect of the nature of the cations. *Langmuir*,*27*(7), 3286-3293.

Kasper-Zubillaga, J. J., Acevedo-Vargas, B., Bermea, O. M., & Zamora, G. O. (2008). Rare earth elements of the Altar Desert dune and coastal sands, North-western Mexico. *Chemie der Erde-Geochemistry*, *68* (1), 45-59.

Kasper-Zubillaga, J. J., Zolezzi-Ruiz, H., Carranza-Edward, A., Giron-Garcia, P., Ortiz-Zamora, G., & Palma, M. (2007). Sedimentology, modal analysis and geochemical

studies of desert and coastal dunes, Altar Desert, NW Mexico. *Earth surface processing landforms, 32,* 489-58.

Kasper-Zubillaga, J. J., & Zolezzi-Ruiz, H. (2007). Grain size, mineralogical and geochemical studies of coastal and inland dune sands from El Vizcaino Desert, Baja California Peninsula, Mexico. *Revista Mexicana de Ciencias Geologicas, 24,* 423-438.

Khalifa, M., Hajji, M., & Ezzaouia, H. (2012). Impurity removal process for high-purity silica production by acid leaching. In EPJ web of conference, 29, pp00014. EDP Sciences.

Lancaster, N. (2007). Development of linear dunes in the south-western Kalahari, southern Africa. *Journal of Arid Environments*, *14*(3), 233-244.

Lancaster, N. (1989). The Namib Sand Sea: dune forms, and sediments. Rotterdam, Balkema. 200 p.

Langille, K. B., Nguyen, D., Bernt, J. O., Veinot, D. E., & Murthy, M. K. (1991). Mechanism of dehydration and intumescence of soluble silicates. *Journal of materials science, 26 (3*), 695-703.

Lin, Z., Ferreira, A., & Roch, J. (2003). Synthesis and Characterization of novel tin and titanium potassium silicate $K_4M_2Si_6O_{18}$. *Journal of Solid State Chemistry*. *175*, 258–263.

Livingstone, I. (2012). Aeolian geomorphology of the Namib sand sea. *Journal of Arid Environments, 93,* 30-39.

Livingstone, I., Bullard, J. E., Wiggs, G. F., & Thomas, D. S. (1999). Grain-size variation on dunes in the Southwest Kalahari, Southern Africa. *Journal of sedimentary research, 69* (3).

Le Bras, M., Wilkie, C. A., & Bourbigot, S. (2005). *Fire retardancy of polymers: new applications of mineral fillers*. Royal Society of Chemistry.

Malu, S. P., Edem, C. A., & Ita, B. I. (2015). Chemical characterization of silica sand deposit from river Katsina-Ala, north central region of Nigeria. *Global Journal of Pure and Applied Chemistry Research*, *3*(1), 26-37.

Masaro, J. (2011). Complaint to Canada Border Service Agency on the dumping and subsidization of potassium silicate solids from Pakistan, Submitted by National Silicate Partnership, PQ Corporation Canada, Toronto, Ontario.

Mbangira, M. B. (2007). *Characterization of some particles properties of Kalahari sands*. CSIR Built Environment, South Africa: Pretoria.

McDonald, M., & Thompson, J. L. (2006). Sodium silicate a binder for the 21st century. *National silicates and PQ Corporation of Industrial Chemicals Division*.

McDonough, W. F., & Sun, S. S. (1995). The composition of the Earth. *Chem. Geol*. 120:223–253.

Miller, R. M. (2008). *The Geology of Namibia: Upper palaeozoic to Cenozoic*, *3*. Ministry of Mines and Energy Geological Survey of Namibia.

Mclaws, I.J. (1971). Uses and specification. *Research council of Albert Report*,*64*, 71-74.

McLennan, S.M., Hemming, S., McDanniel, D.K., Hanson, G.N. (1993). Geochemical approaches to sedimentation, provenance, and tectonics. In: Johnsson, M.J., Basu, A. (eds.). Processes Controlling the Composition of Clastic Sediments. *Geological Society of America*, Special Paper, 285, 21-40.

Mishra, S. (2013). *Effect of different bonding agents on sintering behaviour of Al_2O_3-SiO_2 based mortar*. (Masters' thesis). Department of Ceramic Engineering National Institute of Technology Rourkela.

Mishra, M., & Sen, S. (2012). Provenance, tectonic setting and source-area weathering of Mesoproterozoic Kaimur group, Vindhyan Super group, central India. *Geologica Acta*, *10*(3), 283-293.

Moore, D. M., & Reynolds, R. C. (1989). *X-ray Diffraction and the Identification and Analysis of Clay Minerals (378).* Oxford: Oxford university press.

Moufti, A. M. B. (2013). Mineralogy, geochemistry and possible provenance of desert sand dunes from western Rub' al Khali area, south eastern Saudi Arabia. *International Journal of Basic and Applied Sciences, 2 (4),* 399 - 407.

Muhs, D.R. (2004). Mineralogical maturity in dune fields of North America, Africa and Australia. *Geomorphology journal, 59,* 247–269. Doi: 10.1016/j. geomorph.2003.07.020.

Muhs, D.R., Reynolds, R.L., Been, J., & Skipp, G. (2003). Eolian sand transport pathways in the southwestern United States: importance of the Colorado River and local sources. *Quaternary Int., 104*, 3–18.

Nesbitt, H.W., & Young, G. M. (1982). Early Proterozoic climates and plate motions inferred from major element chemistry lutites. *Nature*, 299, 715-717

OECD SIDS. (2004). Soluble silicates. Retrieved from http://www.inchem.org/documents/sids/sids/SolubleSilicates.pdf

Otterstedt, J. E., & Brandreth, D. A. (2013). *Small particles technology*. Springer Science & Business Media.

Pachauri, T., Singla, V., Satsangi, A., Lakhani, A., & Kumari, K. M. (2013). SEM-EDX Characterization of Individual Coarse Particles in Agra, India. *Aerosol and Air Quality Research, 13*, 523–536.

Pandey, S., &Mishra, M.B. (2011). Sol–gel derived organic–inorganic hybrid materials: synthesis, characterizations and applications. *Journal of Sol-Gel Technology*, *59*, 73-94.

Puligilla, S. (2011). *Understanding the role of slag on geopolymer hardening and microstructural development*. (Master's thesis). University of Illinois at Urbana-Champaign.

Pye, K., Tsoar, H., 1990. Aeolian Sand and Sand Dunes. Unwin Hyman, London. 396 pp

PQ Europe. (2004) Sodium and Potassium Silicates; versatile products for your application, Product Brochure, pp. 1-16.

PQ Corporation. (2004). PQ Potassium silicates NL, Brochure, pp 1-16

Qureshi, M. N., & Ghosh, S. (2013). Effect of alkali content on strength and microstructure of

GGBFS paste. Global journal of researches in engineering civil and structural engineering, 13, (1) 2249-4596.

Rabbi, A. (2001). Sodium silicate glass as an inorganic binder in foundry industry. *Iranian Polymer Journal*, *10*, Retrieved from http://www.sid.ir/en/vewssid/j pdf/81320010403.pdf.

Rawlyk, D, & McDonald, M. (2001) Potassium silicate based drilling fluids: an environmentally friendly 788 drilling fluid providing higher rates of penetration, CADE/CAODC Drilling Conference, pp. 1-11.

Sdiri, A., Higashi, T., Bouaziz, S., & Benzina, M. (2014). Synthesis and characterization of silica gel from siliceous sands of southern Tunisia. *Arabian Journal of Chemistry*, *7*, 486-493.

Sharafat, A. (2009). *Preparation, characterization and properties of nitrogen rich glasses in alkaline Earth-Si-O-N systems*. (Doctoral thesis). Department of Physical, inorganic and structural chemistry, Stockholm University.

Simonsen, M. E., Sønderby, C., & Søgaard, E. G. (2009). Synthesis and Characterization of Silicate Polymers. *Journal of Sol-Gel Science and Technology, 50 (3),* 372-382. 10.1007/s10971-009-1907-4.

Skorina, T., & Tikhomirova, I. (2012). Alkali silicate binders: effect of SiO_2/Na_2O ratio and alkali metal ion type on the structure and mechanical properties. *Journal of Material Science, 47,* 5050-5059.

Sooksaen, P., Boonmee, J., Witpathomwong, C., & Likhitlert, S. (2010). Effect of K_2O/SiO_2 Ratio on the Crystallization of Leucite in Silicate-Based Glasses. *Journal of Metals, Materials, and Minerals*, *20* (1), 11-19.

Spencer, W.R., Reifsynder, R.H., & Falcone, J.C. (2013). Application of soluble silicates and derivative materials in the management of hazardous wastes. *Research gate.* The PQ Corporation, Lafayette Hill, Pennslyvania.

Strohbach, B. J., Strohbach, M., Kutuahuripa, J. T., & Mouton, H. D. (2008). A reconnaissance survey of the landscapes, soils and vegetation of the eastern communal areas (Otjozondjupa and Omaheke regions), Namibia. *National Botanical Research Institute and Agro-Ecological Survey Programme Directorate Agriculture Research and Training*. Ministry of agriculture, water, and forestry.

Sundararajan, M., Ramaswany, S. & Raghavan, P. (2009). Evaluation for the beneficiability of yellow silica sand from the overburden of lignite mine situated in Rajpardi District of Gujarate. *India Journal of Mineral and Material Characterization and Engineering*, *8* (7), 569-581.

Tambelli, C. E., Schneider, J. F., Hasparyk, N. P., & Monteiro, P. J. M. (2006). Study of the structure of alkali–silica reaction gel by high-resolution NMR spectroscopy. *Journal of Non-Crystalline Solids, 352,* 3429–3436. Thomas, D. S. G. (1986). Dune pattern statistics applied to the Kalahari Dune Desert, southern Africa. *Zeitschrift für Geomorphologie, NF*, 231-242.

Taylor, S.R., & McLennan, S. (1985). The Continental Crust: Its composition and Evolution. Oxford, Blackwell, 312pp.

Thomas, D.S.G. (1988). Analysis of linear dune sediment-form relationships in the Kalahari Dune Desert. *Earth Surface Processes and Landforms, 13,* 545 – 553.

Thomas, D. S. G., & Shaw, P. A. (1990). The deposition and development of the Kalahari Group sediments, Central Southern Africa. *Journal of African Earth Sciences (and the Middle East), 10*(1), 187-197.

Thompson, P. Q. (2012). Recent Developments in Soluble Silicate Based Binders and Coatings. *National silicates and PQ Corporation.*

Vail, J.G. (1975). Soluble Silicates. Reinhold Publishing Corporation, New York.

Vickers, L., van Riessen, A., & Rickard, W. D. (2015). *Fire-Resistant Geopolymers: Role of Fibres and Fillers to Enhance Thermal Properties*. Springer.

Wang, L., D'odorico, P., Ringrose, S., Coetzee, S., & Macko, S. A. (2007). Biogeochemistry of Kalahari sands. *Journal of Arid Environments*, *71*(3), 259-279.

Wills, J. H. (1982). A short history of manufacturing potassium silicate in United State. *Soluble silicates*, 3-15. DOI: 10.1021/bk-1982-0194.ch001.

Weiss, I. M. (2013). *Natural and mineral based binders for ecological building materials industries*. (Draft Proposal). Leibniz institute of new materials, Saarbrucken, Germany.

Yunsheng, Z., Wei, S., & Zingjin, L. (2008). Synthesis and microstructural characterization of fully-reacted potassium-poly (sialate-siloxo) geopolymeric cement matrix. *ACI materials journal*, *105*(2).

Zaclon. (2014). *Zaclon potassium silicate.* Zaclon LLC technical information. www.zaclon.com

Appendices

Appendix A Sand samples XRD pattern.

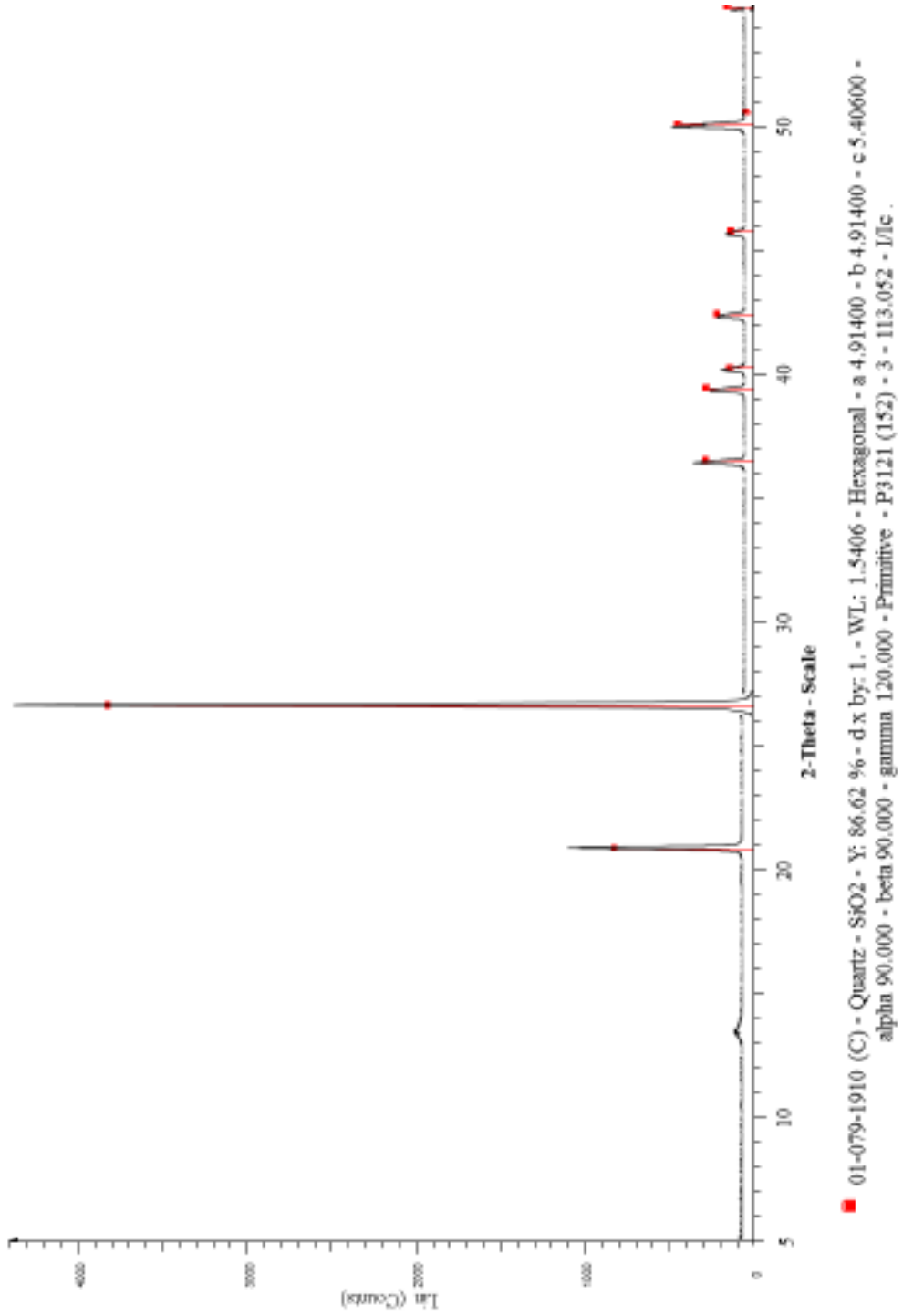

Appendix A1. XRD pattern for KS1.

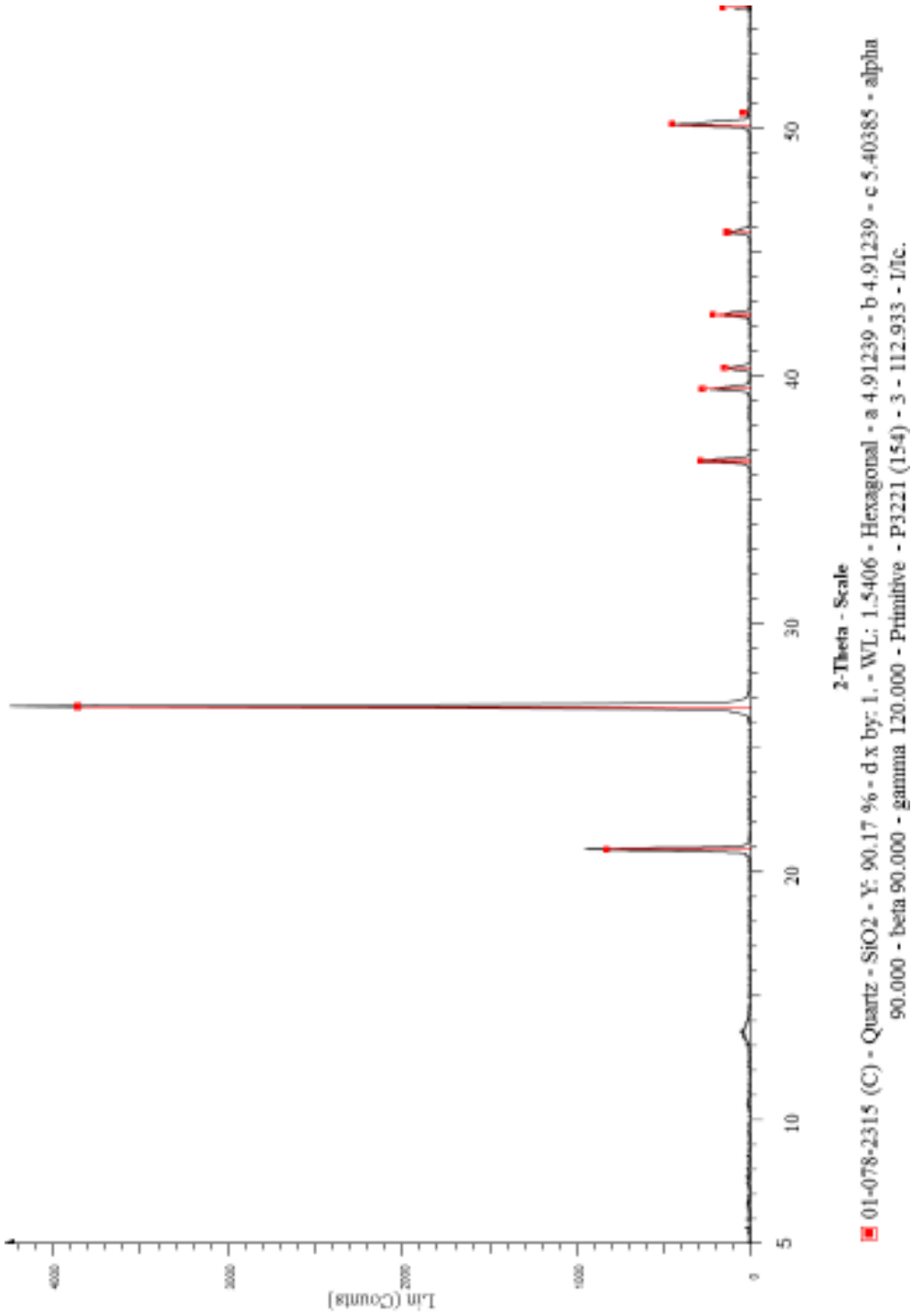

AppendixA_2.XRD pattern for KS2.

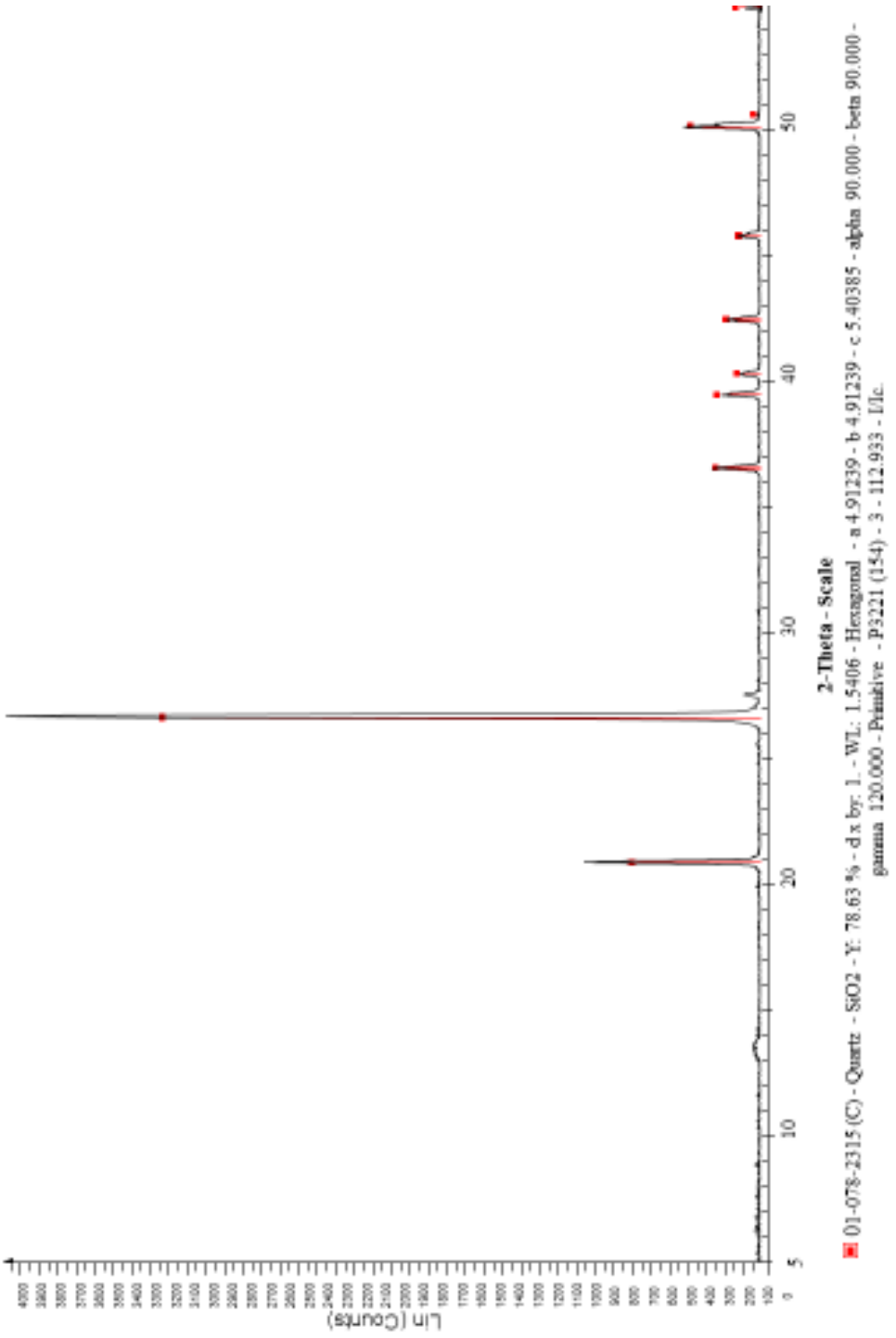

Appendix A$_3$. XRD pattern for KS3.

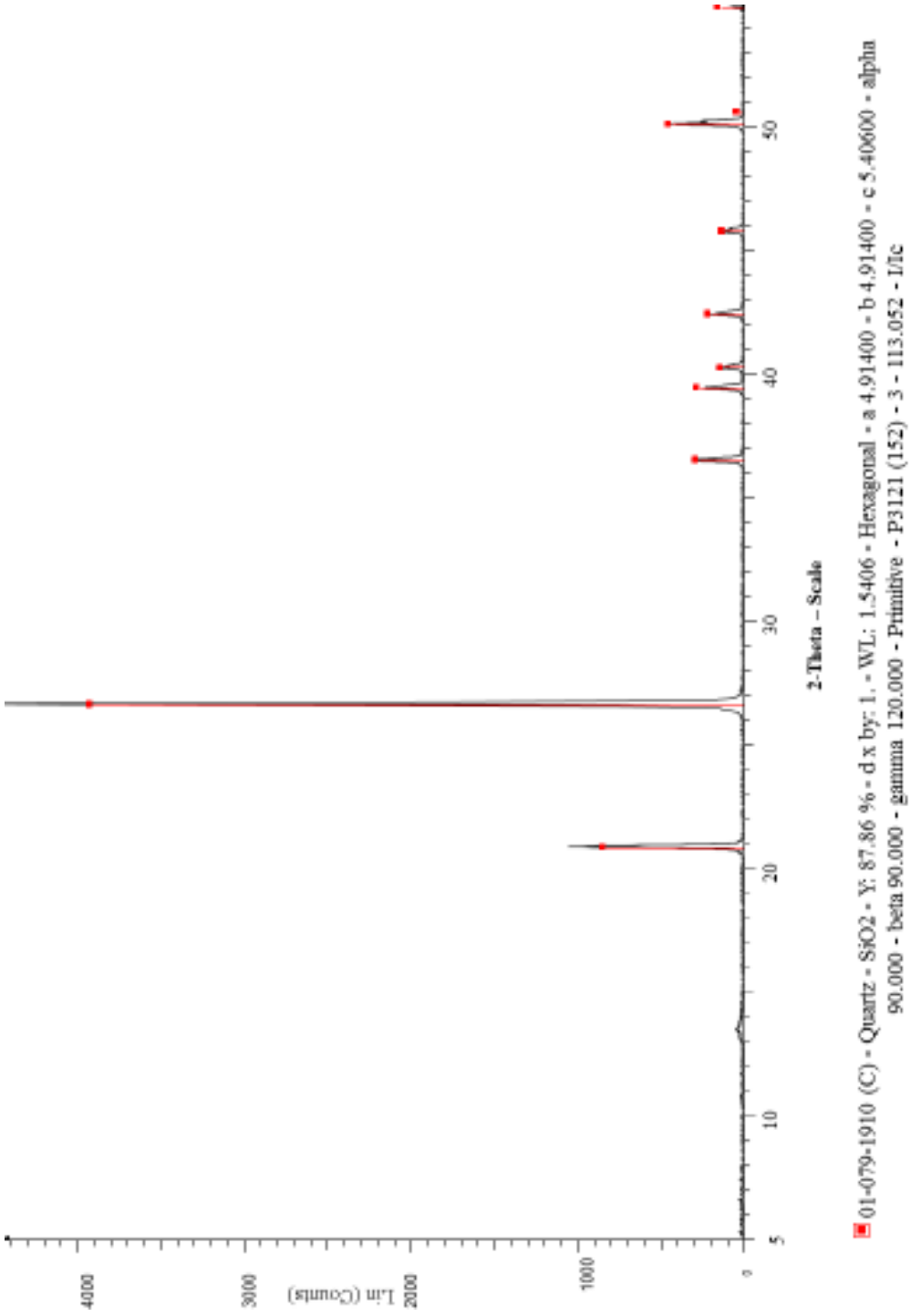

Appendix A4. XRD pattern for KS4.

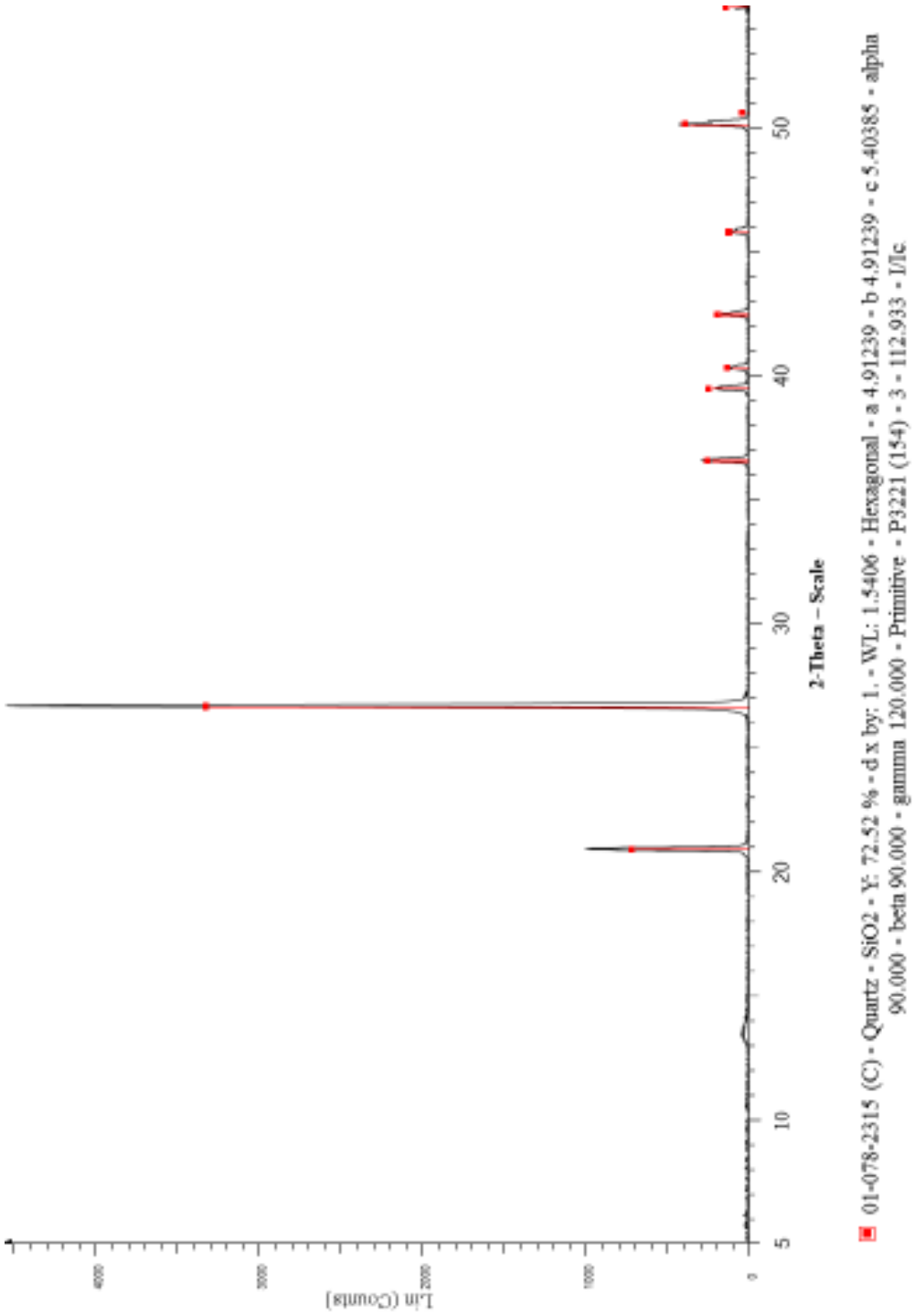

Appendix A$_5$. XRD pattern for KS5.

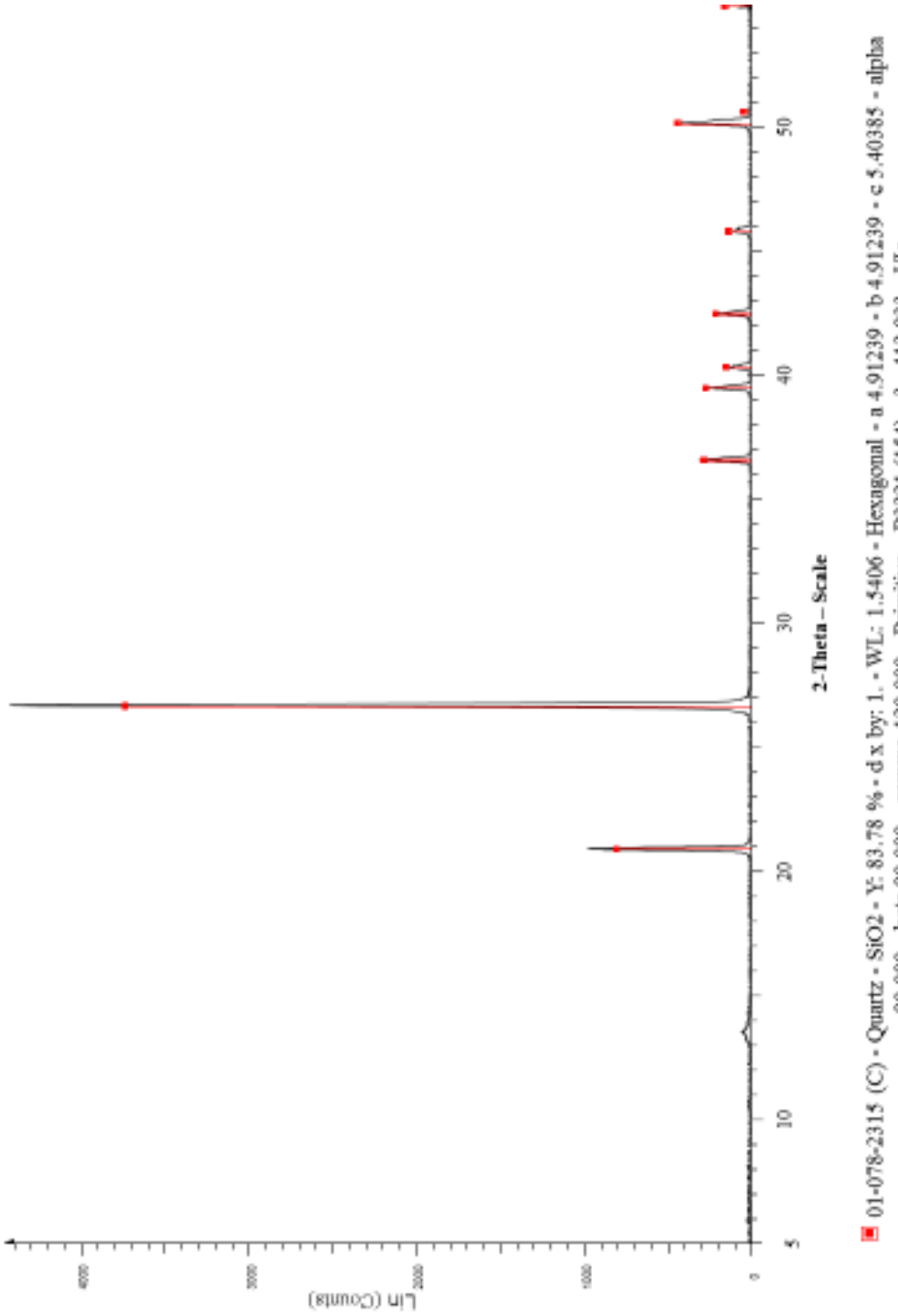

Appendix A7. XRD pattern for KS7.

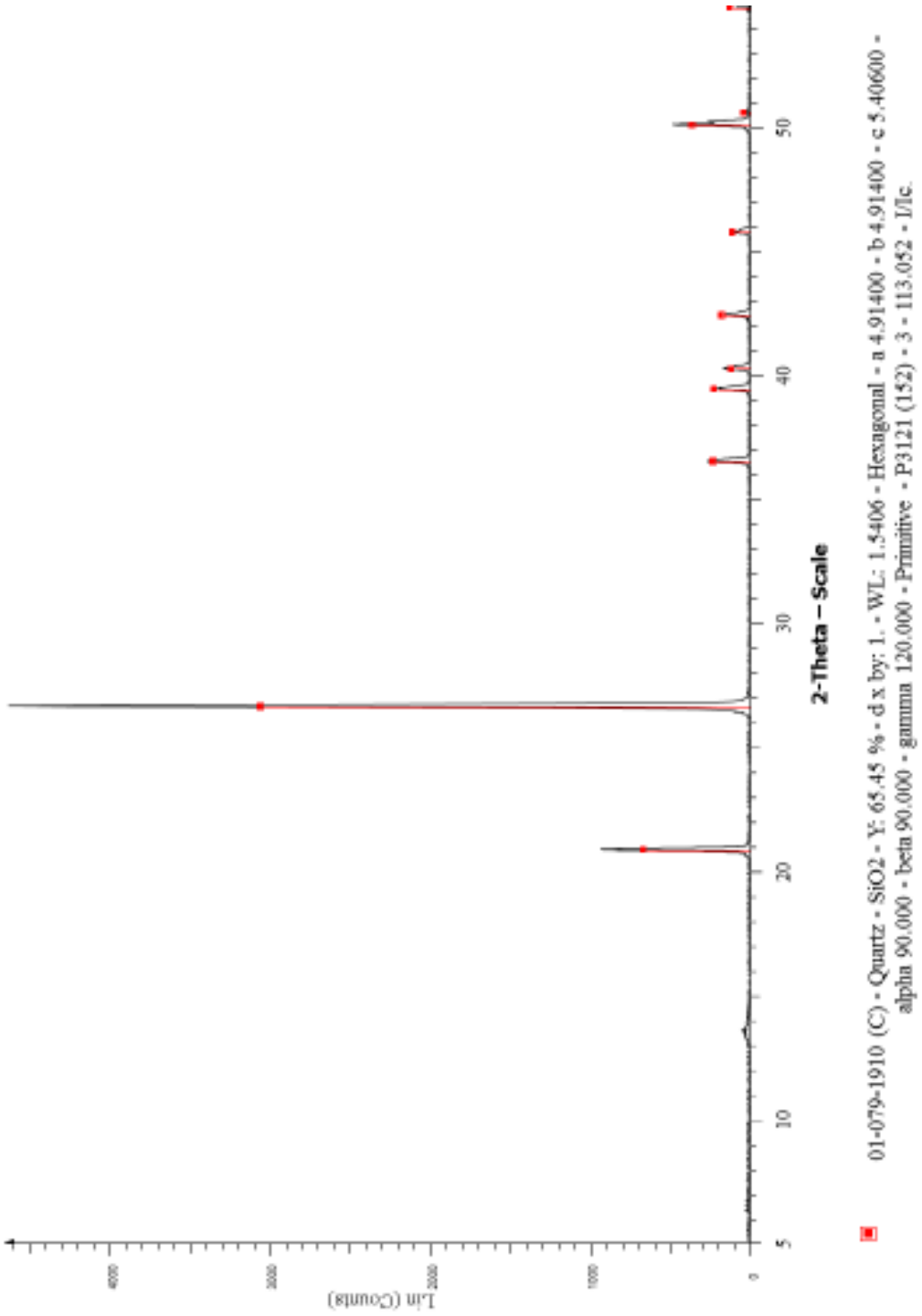

Appendix A₈. XRD pattern for KS8.

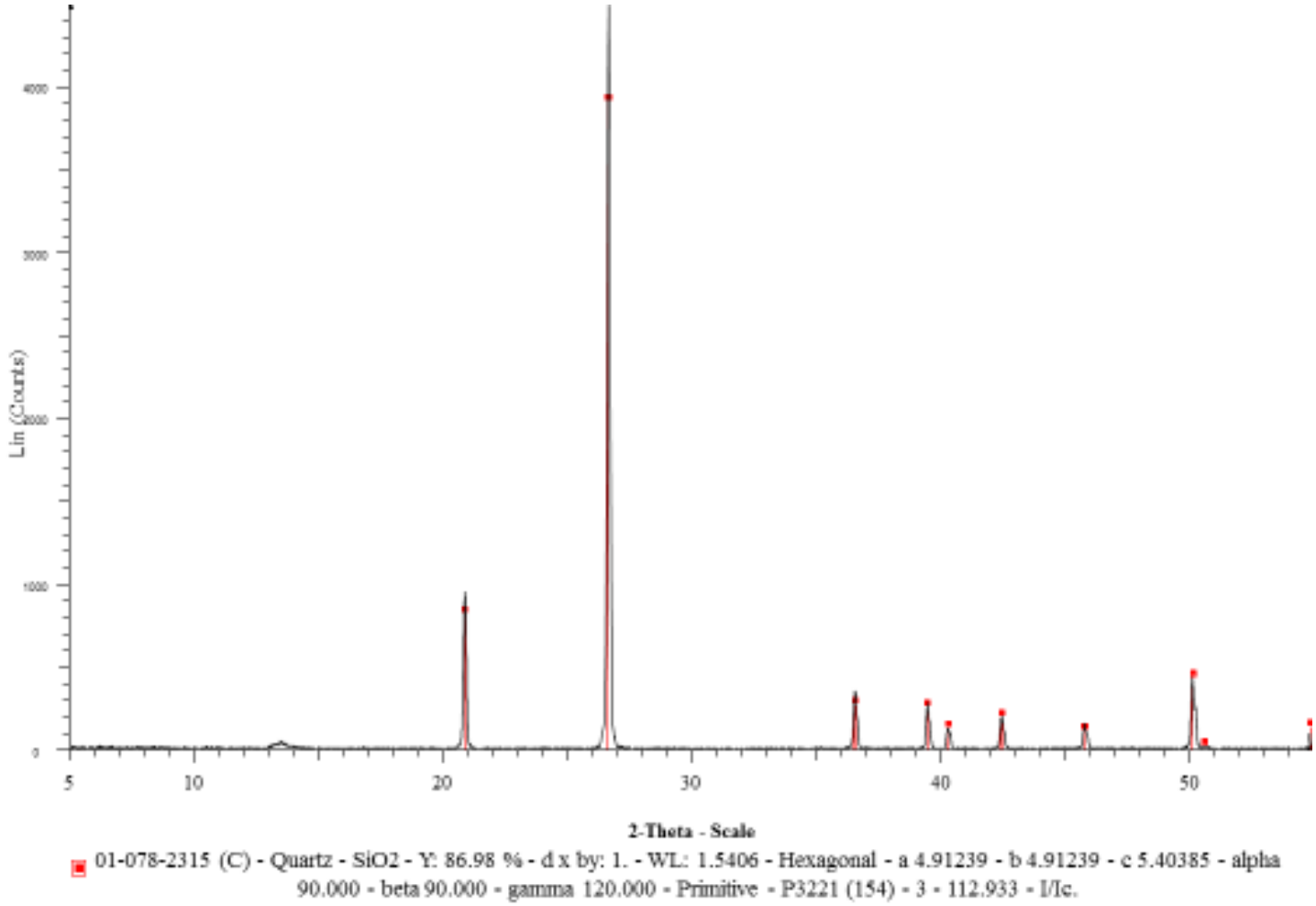
Lin (Counts)
4000
3000
2000
1000
0
5
10
20
30
40
50
2-Theta - Scale
01-078-2315 (C) - Quartz - SiO2 - Y: 86.98 % - d x by: 1. - WL: 1.5406 - Hexagonal - a 4.91239 - b 4.91239 - c 5.40385 - alpha 90.000 - beta 90.000 - gamma 120.000 - Primitive - P3221 (154) - 3 - 112.933 - I/Ic.

Appendix A9. XRD pattern for KS9.

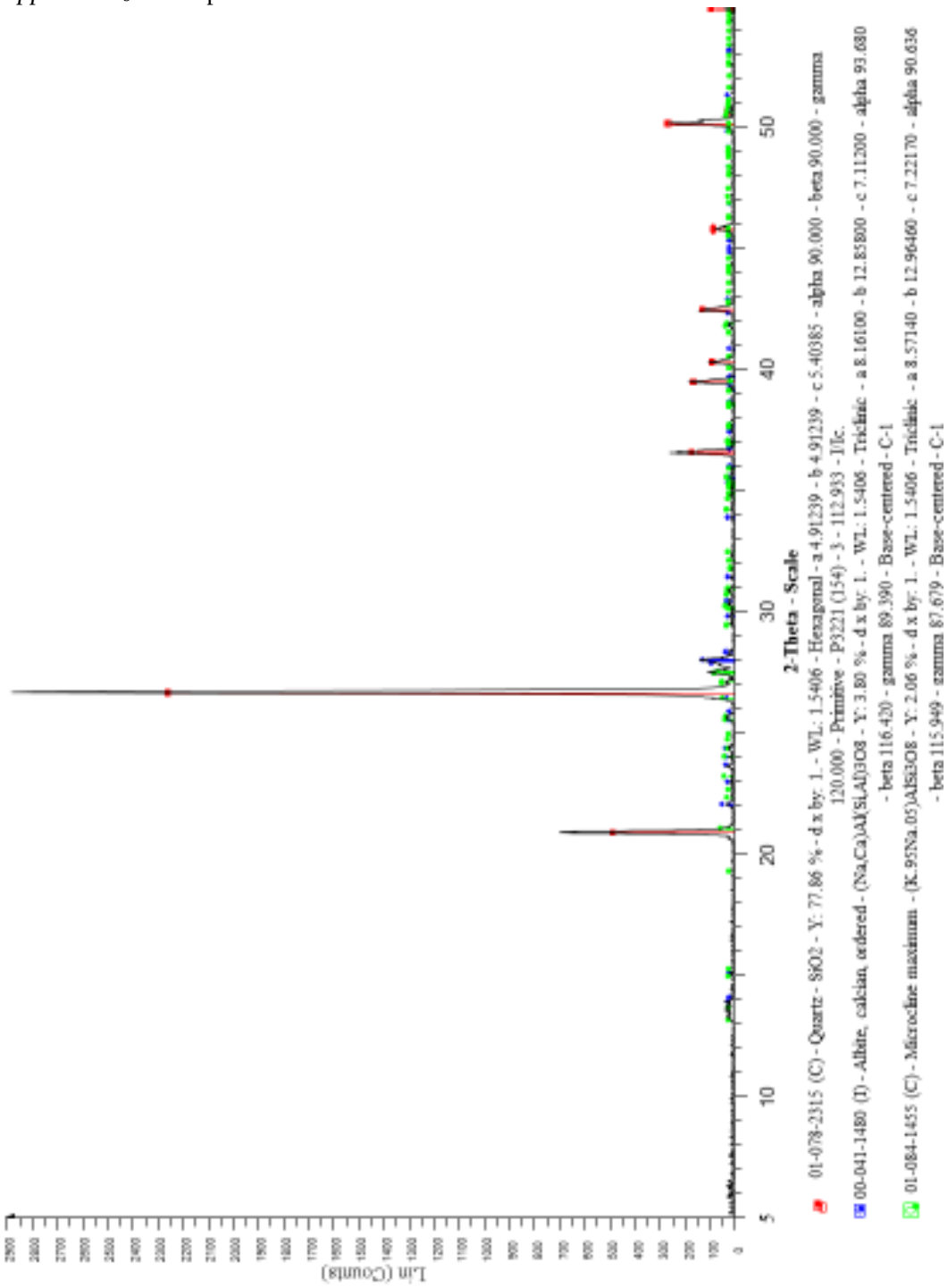

Appendix A10. XRD pattern for NS10.

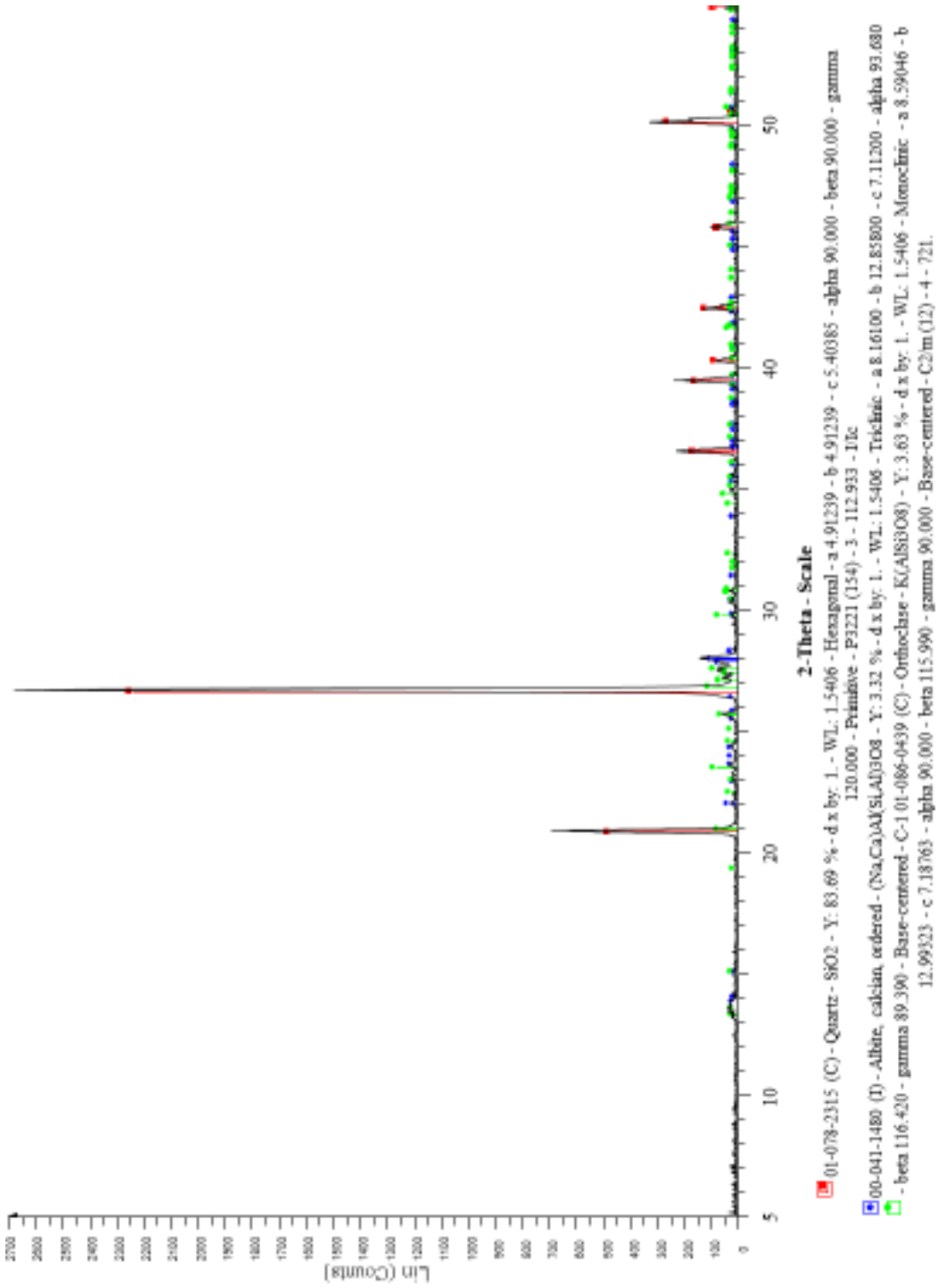

Appendix A$_{11.}$ XRD pattern for NS11.

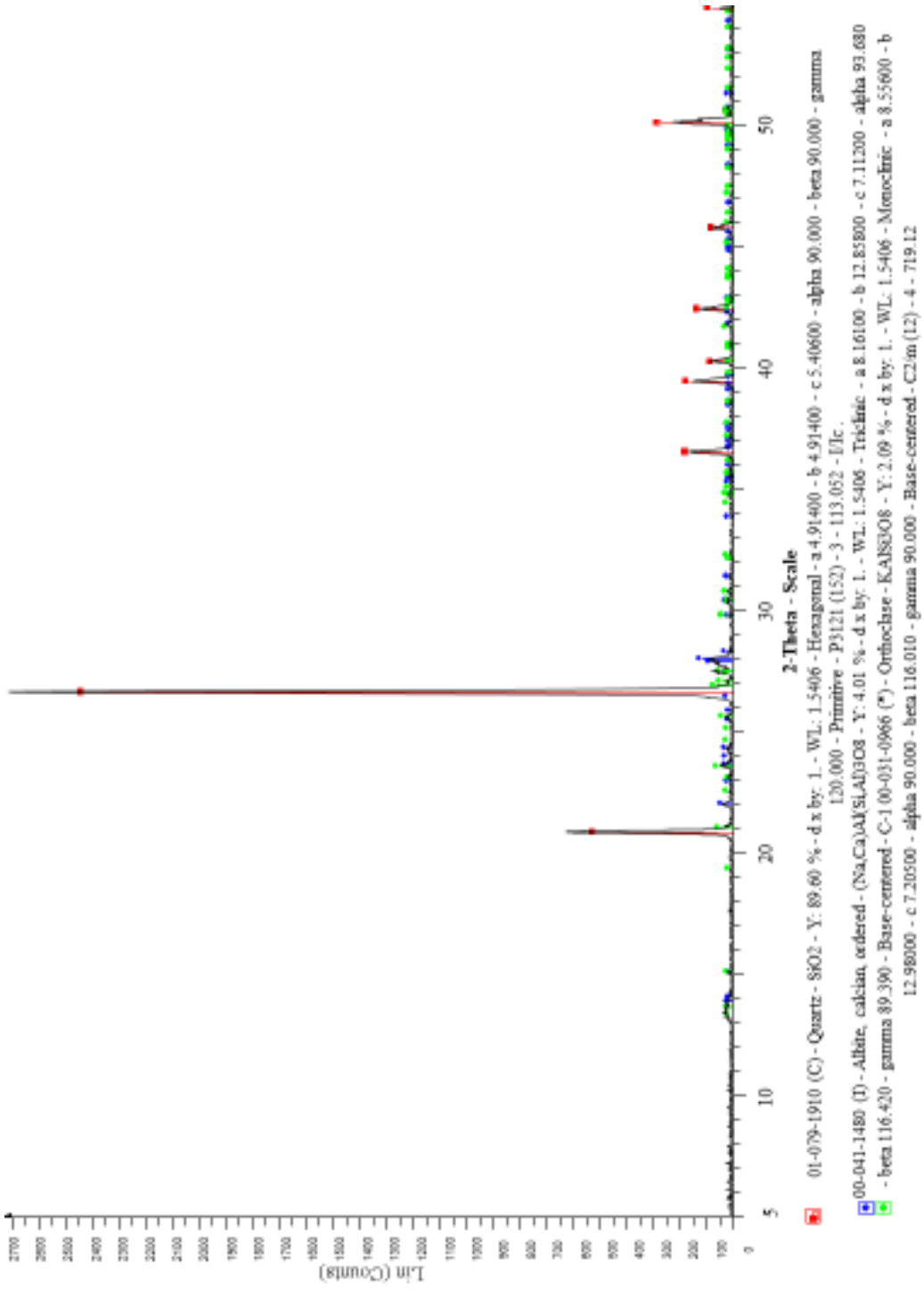

Appendix A$_{12}$. XRD pattern of NS 12.

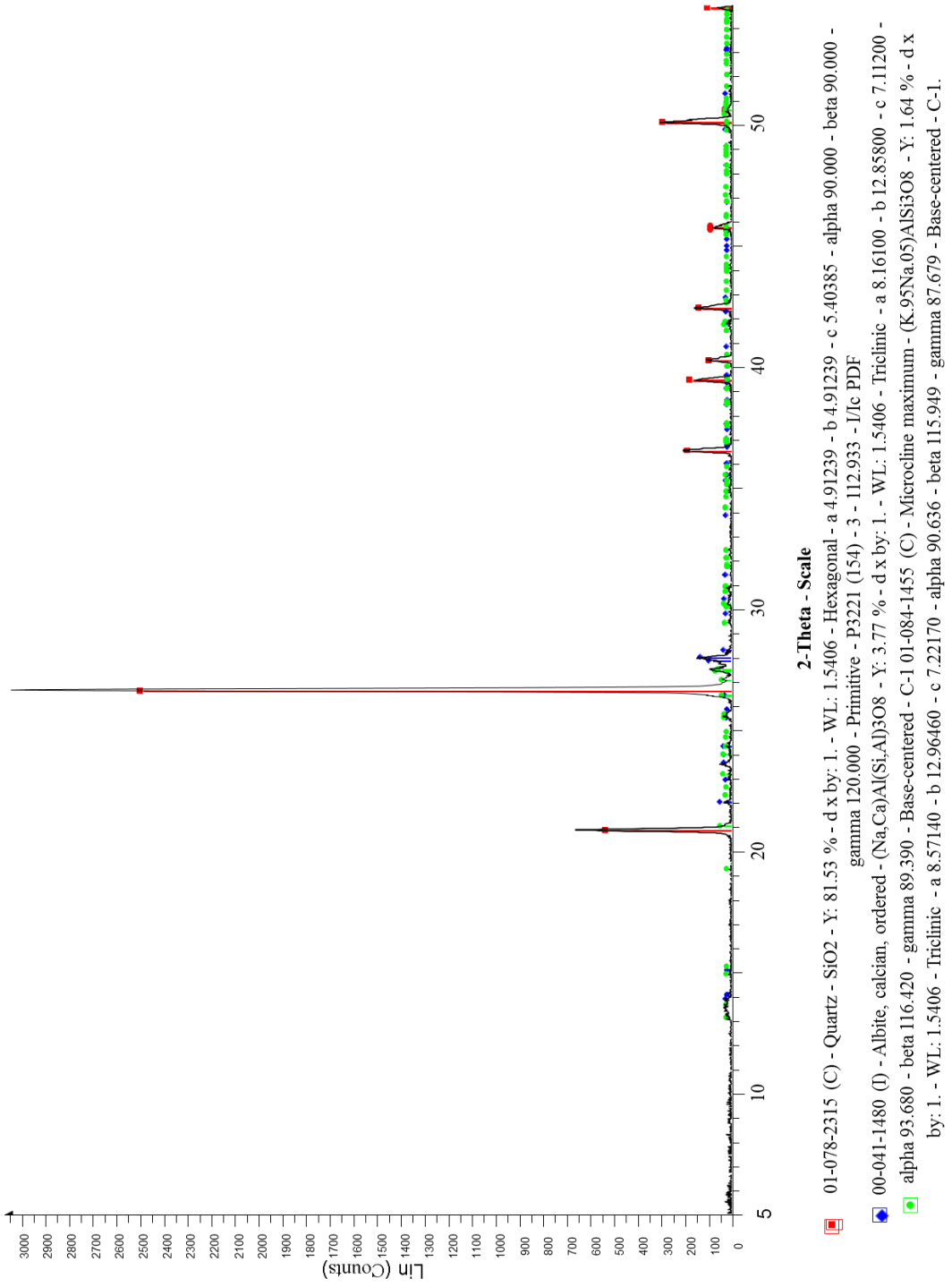

Appendix A₁₂. XRD pattern of NS 13.

Appendix B: Complete ICP-MS Trace and REE analysis (ppm) of the Kalahari dune sands (KS1-9) and Namib dune sands (NS 10-13).

Sample ID	KS1	KS2	KS3	KS4	KS5	KS6	KS7	KS8	KS9	NS10	NS11	NS12	NS13
Sc	1	< 1	1	< 1	< 1	< 1	< 1	< 1	< 1	4	7	7	4
Be	< 1	< 1	< 1	< 1	< 1	< 1	< 1	< 1	< 1	1	< 1	1	< 1
V	16	12	21	5	13	13	11	10	9	40	54	53	32
Ba	32	26	172	35	24	33	30	28	22	322	303	307	294
Sr	4	4	15	2	3	5	5	3	3	87	85	90	78
Y	7	8	10	7	9	9	9	10	7	16	18	21	15
Zr	121	79	119	149	114	109	89	109	76	96	179	138	69
Cr	< 20	< 20	30	< 20	< 20	< 20	< 20	< 20	< 20	50	70	90	30
Co	< 1	1	2	< 1	1	1	< 1	< 1	< 1	5	7	7	4
Ni	< 20	< 20	< 20	< 20	< 20	< 20	< 20	< 20	< 20	< 20	< 20	< 20	< 20
Cu	40	160	20	20	10	< 10	10	< 10	< 10	10	10	10	10
Zn	< 30	< 30	< 30	< 30	< 30	< 30	< 30	< 30	< 30	30	< 30	40	< 30
Ga	2	1	3	< 1	2	2	1	1	< 1	7	7	8	7
Ge	< 1	< 1	1	< 1	< 1	< 1	1	< 1	< 1	1	1	1	1
As	< 5	< 5	< 5	< 5	< 5	< 5	< 5	< 5	< 5	< 5	< 5	< 5	< 5
Rb	6	4	27	2	4	8	4	4	2	64	56	60	55
Nb	< 1	< 1	2	< 1	< 1	< 1	< 1	< 1	< 1	< 1	2	10	< 1
Mo	< 2	< 2	< 2	< 2	< 2	< 2	< 2	< 2	< 2	< 2	< 2	< 2	< 2
Ag	< 0.5	< 0.5	< 0.5	< 0.5	< 0.5	< 0.5	< 0.5	< 0.5	< 0.5	< 0.5	< 0.5	< 0.5	< 0.5
In	< 0.2	< 0.2	< 0.2	< 0.2	< 0.2	< 0.2	< 0.2	< 0.2	< 0.2	< 0.2	< 0.2	< 0.2	< 0.2
Sn	< 1	< 1	< 1	< 1	< 1	< 1	< 1	< 1	< 1	< 1	< 1	2	< 1
Sb	< 0.5	< 0.5	< 0.5	< 0.5	< 0.5	< 0.5	< 0.5	< 0.5	< 0.5	< 0.5	< 0.5	0,8	< 0.5
Cs	< 0.5	< 0.5	0,7	< 0.5	< 0.5	< 0.5	< 0.5	< 0.5	< 0.5	0,8	0,7	0,8	0,6
La	2,2	3	5,2	1,7	3,7	4,1	2,6	2,1	1,7	11,3	11,8	15,8	11,5
Ce	5	5,2	9,1	3,3	6,6	7,8	4,9	4,2	2,9	19,1	20,7	27	19,5
Pr	0,47	0,58	1,13	0,36	0,78	0,84	0,54	0,43	0,3	2,5	2,66	3,51	2,51
Nd	1,9	2,2	4,4	1,4	2,9	3	2	1,5	1,2	9,8	10,4	12,7	9,6
Sm	0,4	0,4	0,9	0,3	0,5	0,6	0,4	0,3	0,2	2	2,3	2,7	1,9
Eu	0,07	0,07	0,18	< 0.05	0,08	0,1	0,06	0,06	< 0.05	0,6	0,62	0,64	0,55
Gd	0,3	0,5	0,9	0,2	0,5	0,6	0,4	0,3	0,2	1,9	2,3	2,5	1,8
Tb	< 0.1	< 0.1	0,1	< 0.1	< 0.1	0,1	< 0.1	< 0.1	< 0.1	0,3	0,4	0,4	0,3
Dy	0,4	0,5	0,9	0,3	0,7	0,7	0,5	0,3	0,3	1,9	2,6	2,9	1,9
Ho	< 0.1	0,1	0,2	< 0.1	0,1	0,1	0,1	< 0.1	< 0.1	0,4	0,5	0,6	0,4
Er	0,3	0,3	0,6	0,2	0,4	0,4	0,4	0,2	0,2	1,1	1,7	1,9	1,2
Tm	< 0.05	0,06	0,1	< 0.05	0,07	0,07	0,06	< 0.05	< 0.05	0,17	0,26	0,32	0,16
Yb	0,3	0,4	0,7	0,2	0,5	0,5	0,4	0,2	0,2	1,1	1,8	2,1	1,1
Lu	0,06	0,06	0,11	0,04	0,08	0,09	0,06	0,05	< 0.04	0,18	0,29	0,32	0,18
Hf	2,7	1,8	2,9	3,4	2,5	2,4	1,9	2,4	1,7	2,5	4,1	4	1,5
Ta	0,2	0,2	0,4	0,1	0,1	0,2	0,2	0,1	< 0.1	0,2	0,3	0,8	0,2
W	< 1	< 1	1	< 1	4	1	< 1	2	< 1	< 1	1	< 1	< 1
Tl	< 0.1	< 0.1	< 0.1	< 0.1	< 0.1	< 0.1	< 0.1	< 0.1	< 0.1	0,2	0,2	< 0.1	0,1
Pb	< 5	< 5	< 5	< 5	< 5	< 5	< 5	< 5	< 5	10	10	14	9
Bi	< 0.4	< 0.4	< 0.4	< 0.4	< 0.4	< 0.4	< 0.4	< 0.4	< 0.4	< 0.4	< 0.4	< 0.4	< 0.4
Th	2	1,5	2,3	1,1	1,8	2	1,4	1,2	0,8	2,7	3,1	6	2,6
U	0,7	0,5	0,6	0,4	0,6	0,6	0,5	0,4	0,3	0,8	0,9	1,2	0,7
S	0,5	0,6	0,4	0,6	0,6	0,5	0,4	0,3	0,8	0,9	1,2	0,7	

Appendix C: Other ternary plots for Kalahari dune sands and Namib dune sands.

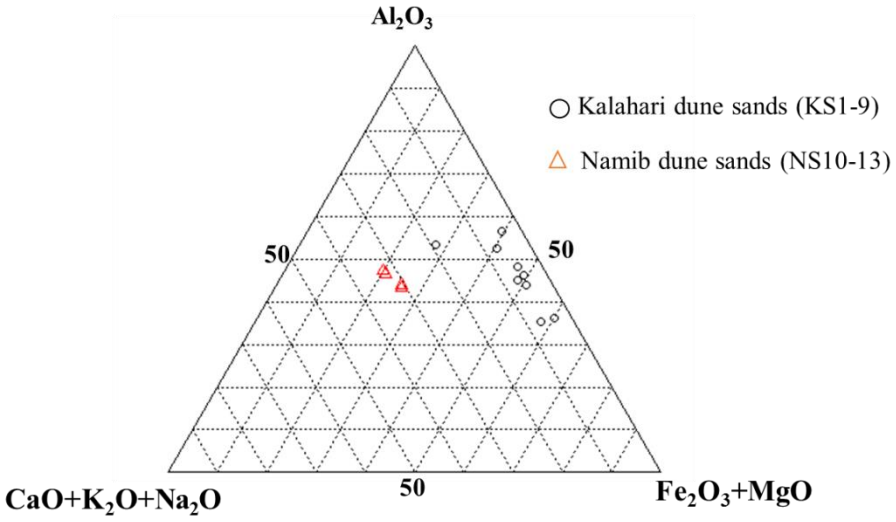

Appendix C_1: Al_2O_3- CaO+ K_2O+Na_2O-Fe_2O_3+ MgO ternary diagram for the Kalahari and Namib dune sands.

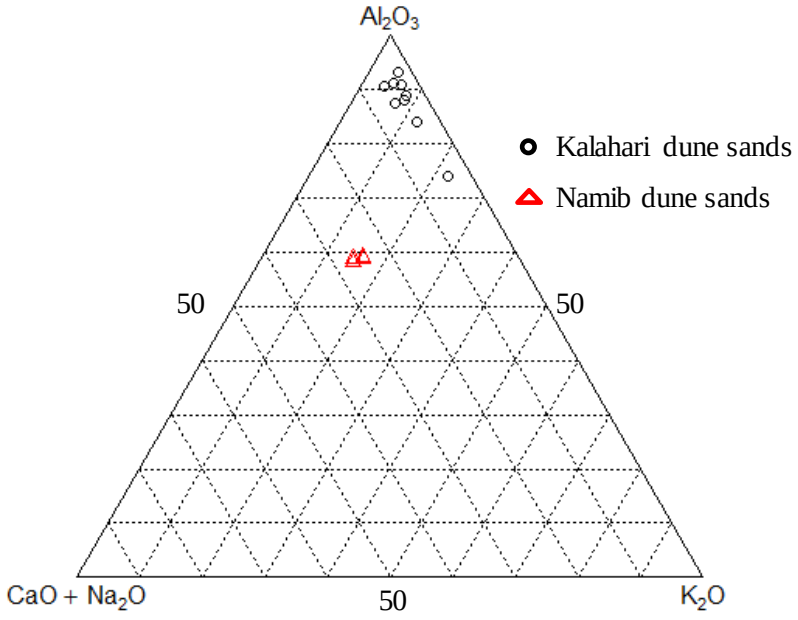

Appendix C_2: Al_2O_3- CaO+ Na_2O-K_2O ternary diagram for the Kalahari and Namib dune sands.

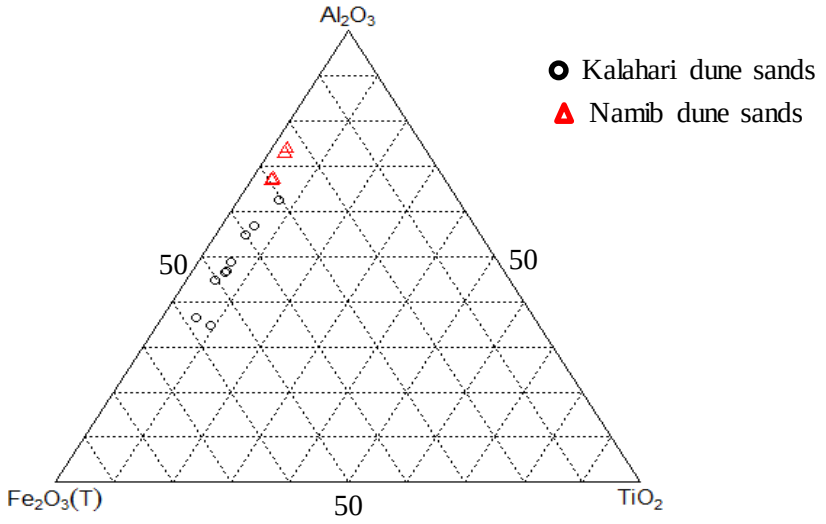

Appendix C_3: Al_2O_3- Fe_2O_3-TiO_2 ternary diagram for the Kalahari and Namib dune sands.

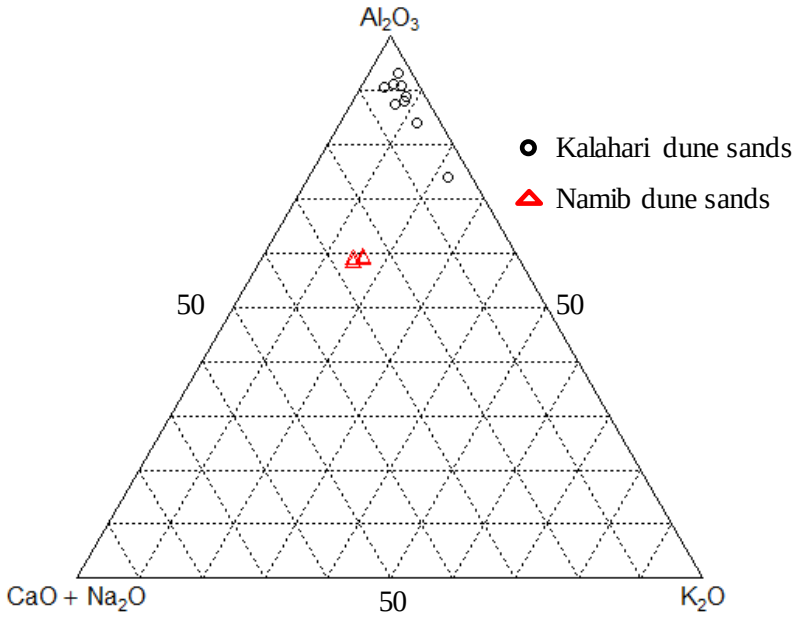

Appendix C_2: Al_2O_3- CaO+ Na_2O-K_2O ternary diagram for the Kalahari and Namib dune sands.